**ORIGINAL ARTICLE**

CrossMark

# Processing and tooling considerations in joining by forming technologies; part A—mechanical joining

Masoud Salamati[1] · Mahdi Soltanpour[1] · Ali Fazli[1] · Asghar Zajkani[1]

**Abstract**

Joining by plastic deformation, also called joining by forming techniques, has been developed as a powerful tool for joining a broad range of similar and dissimilar materials in an environmentally friendly manner. Generally, the joining by forming techniques fall into two distinctive categories, namely mechanical joining and solid state welding. In this paper, different methods of joining by forming are studied from processing and manufacturing points of view. The article is arranged in three parts. Mechanical joining processes will be discussed in this part A. Various processes in this category have been addressed individually. Principles of the processing, applicable materials, process variants, joint mechanical behavior including static and dynamic performance, and various optimization techniques including experimental, numerical, and analytical approaches are the fields of concentration in this study.

**Keywords** Joining · Plastic deformation · Dissimilar materials · Joint strength · Joining process

## 1 Introduction

Generally, a product is a result of assembling various parts and components. For example, a car or aircraft consists of thousands of different components. These elements are assembled by different joining techniques. Primary applications of a joint are load transformation from one part to another one and creating relative motion between two or more parts.

Joints are the most critical parts of a structure, and when loading, fracture usually occurs at the joining zones. However, usage of the joints cannot be eliminated. Manufacturing and transportation challenges are the main limitations of manufacturing integrated structures, which makes the application of joints inevitable. Because the joints are the most critical parts of the structure and, on the other hand, their use in the structure is unavoidable, obviously, there should be more attention on the joining methods. Mechanical joining by fasteners, adhesive bonding, and fusion welding are the most common joining techniques.

Mechanical fastening leads to property degradation due to stress concentration around the joining zone. The evolution of stresses around fastener holes, which induce strength degradation and eventually create corrosion-related problems, non-uniformly distributed loads which cause large local stresses, increased component weight, and special mechanical operations required by the method, such as drilling of holes, making screw threads, etc., prior to the joining process are some other limitations of the mechanical joining. Adhesive bonding requires long manufacturing time and is not applicable in some corrosive environments and when the structure is exposed to chemical compositions. Although the most durability and stability issues in engineering structures are fatigue related, but the environmental resistance plays a major role in durability issues of an adhesively bonded joint rather than fatigue loads. The environmental resistance of an adhesive bond is determined by the chemical bonds formed during cure of the adhesive and the resistance of the chemical bonds to environmental degradation. Most in-service failures of the engineering structures are caused by environmental degradation of the interface between the bonding surface and the adhesive. The temperature and moisture or environmental effects including humidity, solvents, corrosion, temperature extremes, thermal cycling, etc., strongly affect the adhesively bonded joints [1]. On the other hand, the degradation of the bondline mechanical properties due to either poor surface preparation or improper

✉ Mahdi Soltanpour
soltanpour@eng.ikiu.ac.ir

[1] Advanced Forming Technology and Materials Lab, Mechanical Engineering Department, Faculty of Engineering and Technology, Imam Khomeini International University, Qazvin, Iran

curing conditions is a major concern in adhesively bonded joints [2].

Fusion welding techniques are not capable of joining dissimilar materials, which is very important in hybrid structures and high-performance applications. Nowadays, to achieve different properties at different zones of the product, utilizing dissimilar materials become very common in automotive, aerospace, marine, and military industries. For example, a modern car body consists of steel, aluminum, magnesium, and composite materials to achieve high strength at the passenger compartment (also called safety cage) and large deformability as well as high energy absorption in the crumple zone. It ensures the best performance during a crash event. Figure 1 illustrates the crumple zones and passenger compartment (safety cage) for a car body and shows how a well-designed car body behaves during the crash. Another important reason to use dissimilar materials is weight reduction of the vehicles to meet energy saving purposes. Recently, even a hybrid car chassis is manufactured for some supercars such as Ferrari, Lamborghini, and McLaren and even is extended for some mass production cars such as BMW 7-series and Alfa Romeo 4C [4], whereas previously, the car chassis was manufactured only from steel by all automotive companies.

Joining this range of dissimilar materials by conventional abovementioned joining techniques (fusion welding, adhesive bonding, and mechanical fastening) is impossible or hard to apply. The large differences between the physical and mechanical properties of the dissimilar materials are a big challenge when applying fusion welding techniques. For example, the melting temperature of steel and aluminum differs about 800–900 °C; thus, at the time of reaching the melting point of the steel, aluminum has completely destroyed. The galvanic corrosion issues are another problem when joining dissimilar materials. Galvanic corrosion (also called bimetallic corrosion) is an electrochemical process in which one metal corrodes preferentially when it is in electrical contact (including physical contact) with another, in the presence of an electrolyte. The combination of corrosion issues and local stresses in a mechanically fastened joint is a highly destructive phenomenon leading to irreparable damages to the structure. Thus,

utilizing modern technologies should be considered for joining dissimilar materials.

The use of plastic deformation to join materials is a relatively new technology, which is developed in the last decades. In such processes, plastic deformation applied to one or more joining partner results in the partners to join together. This joining method has a lot of advantages. Due to the disuse of joining elements such as bolts, screws, rivets, and welding electrodes, weight and cost reduction purposes could be met. On the other hand, unlike to fusion welding, applying heat is not required thus a considerable saving on the energy sources can be achieved and subsequently the manufacturing cost can be further reduced. Another advantage of disusing heat sources is that thermal and residual stresses, as well as metallurgical complaints, can be avoided. As mentioned above, joints are the most critical parts of a structure, while in joining by forming, due to phenomenon like strain hardening, the strength of the joint can be increased considerably. In some techniques, the joint strength superior to parent materials can be achieved, which results in much more reliability of the joint compared to other joining technologies. No emission of fumes, sparks, and heat, as well as excellent capability in joining dissimilar materials are some other advantages of joining by forming.

As mentioned by Homberg et al. [5], a joint design must be developed taking into account holistic aspects to exclude suboptimal solutions. Furthermore, there are influencing, partially conflicting requirements in the field of material characteristics, design as well as production engineering which have to be considered. As a designated target for the joint design the according influencing factors, as well as their influencing intersections on the joint design, should lead to solutions considering the central aspects of joint quality, cost, and time. The joining by forming technologies can meet these requirements satisfactorily, because such technologies are generally high efficiency, inexpensive, and rapid methods for joint manufacturing.

Beside several advantages, joining by forming suffers some limitations. It is hard to apply to low-formability



Fig. 1 Different mechanical properties achieved on a car body resulted by using dissimilar materials: a safety cage and crumple zone, b the behavior of safety cage and crumple zone during the crash event [3]

Safety cage      Crumple zone

(a)                    (b)

materials. There are no standards for the processes [6], and implementation of the processes requires a high technical knowledge [7].

Joining by forming technologies are divided into two basic categories: mechanical joining and metallurgical joining [6]. Metallurgical joining is based on intermetallic bonds and is applicable for metallic parts only. The methods for obtaining metallurgical joints are known as *solid-state welding* technologies. Unlike the metallurgical joints, mechanical joining techniques can be applied to non-metallic elements too. These methods themselves are subdivided into two categories: form-fit joining and force-fit (interference-fit) joining. On form-fit joining, the joint is a result of plastic deformation of partners and creation of an interlock between them. While on force-fit joining, residual stresses produced by plastic deformation are the principal mechanism of joining. Mechanical clinching and joining two tubes by electromagnetic compression are examples of form-fit and force-fit joining, respectively. In some techniques, both the form-fit and force-fit mechanisms occur. The material combination, the surface, and the mechanical and thermal conditions influence the levels of activation of each mechanism [8].

There are two comprehensive reviews on joining by forming published in last years. Groche et al. [7] deeply focused on joining mechanisms and studied the mechanisms of joint formation in different joining by forming processes and categorized the methods based on these mechanisms. Mori et al. [6] focused on the operations from a manufacturing point of view. More recently Mori and Abe [9] published a review article concentrating on the mechanical joining of aluminum and high-strength steels (HSS). In the two former works, some of the methods are discussed too briefly. Basic knowledge of the process parameters is of extraordinary importance to obtain a sound joint made by plastic deformation, which is not so much focused on the prior reviews on joining by forming [6, 7]. On the other hand, the latter work is only focused on the clinching, self-pierce riveting (SPR), and hemming of aluminum and HSS sheets and does not investigate other technologies, materials, and material combinations. Because of the particular importance of joining by forming in modern high-performance applications, a large number of studies and researchers had been conducted within last 3 to 4 years, leading to further development and optimization of the processes.

Furthermore, successful employment of joining by forming technologies requires in-depth knowledge of the process principles and parameters influencing the processes. Therefore, in this paper, a more detailed study of the process principles is provided; several works containing publications of last 3 years are reviewed from a manufacturing point of view and methods of applying each process on different materials or material combinations are investigated. Also, the joint mechanical performance is an important field of concentration in this paper, including tensile, shear and fatigue strengths as well as elongation to failure, and the influence of process parameters on these properties. Although the main focus is on the processing and tooling conditions, process optimizations by various techniques including numerical approaches, finite element (FE) simulations, analytical approaches, and different designs of experiment methods like Taguchi method as well as experimental procedures are reviewed in this work, because of its importance on the accurate implementation of a process.

In the next section first, an overview is provided, and the mechanical joints are categorized as mechanical joints by fasteners, clinching, SPR, hemming, rolling, die-less hydroforming, joining by incremental forming, joining by electromagnetic forming (EMF), joining shaft-hub connections, and other techniques. Processing and tooling conditions, process variants, applicable materials, joint strength, and optimization techniques are investigated for each technology. There are extensive studies and material about some techniques, such as clinching and SPR. Thus, the sections addressing such techniques are subdivided into sub-sections. While less attention from both academia and industry has been paid to some techniques, such as rolling and there are a few studies related, thus, such techniques are discussed in a single section without any sub-section.

## 2 An overview on mechanical joints

Mechanical joints are categorized into two main groups: mechanical joining by fasteners and mechanical joining by forming. The first group uses additional joining elements, such as bolts, screws, and rivets. In joining of new materials, these methods are applicable for joining composite materials, which are hard to form due to their low elongation. In the case of metals, usually, other joining technologies are preferred. Due to the widespread use of mechanical fasteners in composite industries, there are many studies on the strength of these joints and the influence of different parameters on the joint strength. In an earlier work, joining of glass/polyester and carbon/polyester composites by mechanical fasteners were studied by Matthews et al. [10]. They categorized the influencing parameters in three groups: material parameters, design parameters, and fastener parameters. In this technique, a predrilled hole on the joining partners is required. Thus stress concentration takes place at the location of the hole [11]. It is suggested to use glass fiber strips around bolt holes to reduce stress concentration and subsequently increase the joint strength. Geometrical parameters, such as fastener diameter ($d$), the thickness of the composite laminate ($t$), the width of the workpiece ($w$), and edge distance ($e$), are another critical parameters influencing the joint strength [12].

The second group of mechanical joining is joining by forming which utilizes some plastic deformation for joining purposes. In such technologies, the joint is a result of

interfacial stresses or creation of an interlock between the joining partners. Unlike the metallurgical joints (see part B and part C of this review article), there is no metallurgical bonding at the interface of the workpieces. Thus, no surface preparation is required [6]. Force-fit joints usually are manufactured in tubular workpieces, two parts are aligned, and a forming force either compression or expansion is applied to the interface area. For example in compression force-fit joints, the forming force is applied on the outer surface of the outer part where the collision between two parts, compresses them together and increasing the forming force, leads to the plastic deformation of the outer portion and elastic deformation of the inner part. When the forming force is released, elastic recovery of both parts occurs. The plastically deformed workpiece (i.e., in this case, the outer part) prevents the complete elastic recovery of the other part (i.e., in this instance the inner part), and resultantly, interfacial stresses are created at the interface of two parts that cause a force-fit. An important matter which should be considered in this type of joints is that the plastic deformation of the second workpiece (i.e., in this case, the inner part) should be controlled and prevented because it negatively influences the joint strength due to lack of the interfacial stresses caused by the elastic recovery. Figure 2 shows the mechanism of joint formation in the force-fit joints. In this mechanism, the joint strength is a function of friction coefficient, interfacial stress, and contact area of the joint.

In form-fit joints, the joint is a result of interlocking between the joining partners. In this case, there are no interfacial stresses and the plastic deformation of the materials should be controlled in ways that a proper interlock can be created. Clinching is an example of such joints. In clinching which is explained in more detail later, the die cavity controls the plastic deformation. The cavity prevents the vertical flow of the material; thus, the material flows in a radial direction, and an interlock can be created. Figure 3 shows the mechanism of joint formation in form-fit joints. In this arrangement, the joint strength is a function of the amount of plastic deformation and interlock and the strength of the material at the joining zone.

In this paper, various techniques leading to force-fit and form-fit joining will be discussed individually. Table 1 summarizes the most important features of the methods investigated in this paper. First, the fundamentals of the process and applicable materials are explained; then the processing and tooling parameters and their influence on the joint strength and mechanical behavior are investigated; the joint strength and different optimization methods with the aim of improvement in the joint mechanical behavior are described. The particular variants of the processes (if any) are also discussed.

# 3 Clinching

## 3.1 Processing

Clinching is a joining process without additional or consumable joining elements, where only plastic deformation of both workpieces leads to the joining. In this process, two sheets either metallic or non-metallic, stack up, and experience a locally severe plastic deformation applied by clinching equipment. The pre-drilling step is not necessary on the sheets (however, in some process, variants such as hole clinching which will be discussed later, one of the sheets should be pre-drilled), expensive equipment, and additional joining elements, and any surface preparation process [16] is not necessary, all leading to considerable reduction in manufacturing
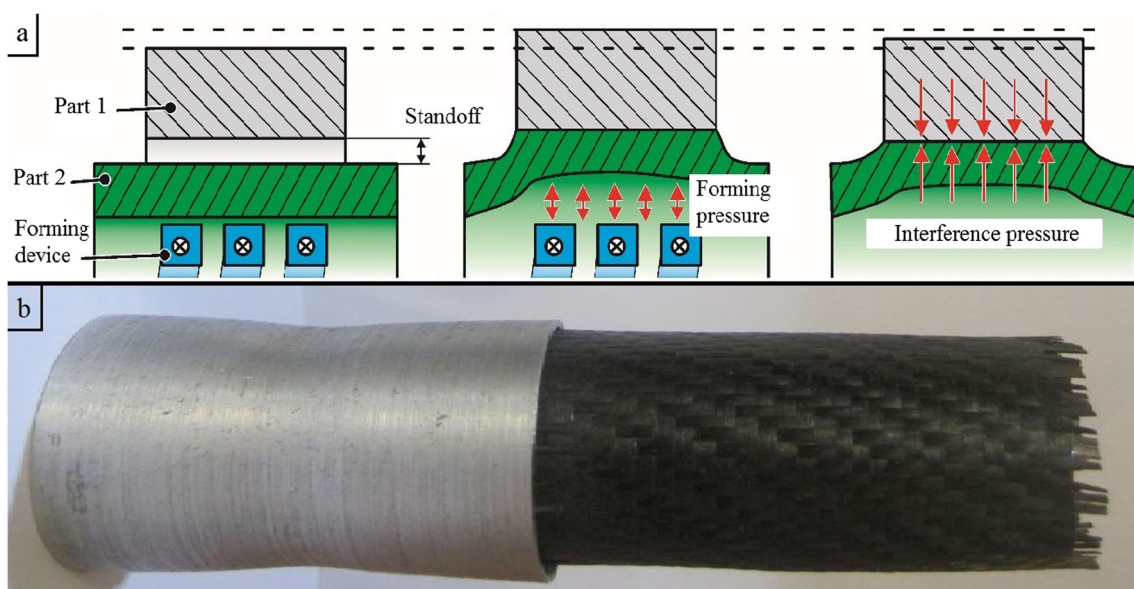


Fig. 2  **a** Mechanism of a force-fit joint [13]. **b** A force-fit joint of aluminum and carbon fiber reinforced plastic tubes manufactured by EMF [14]
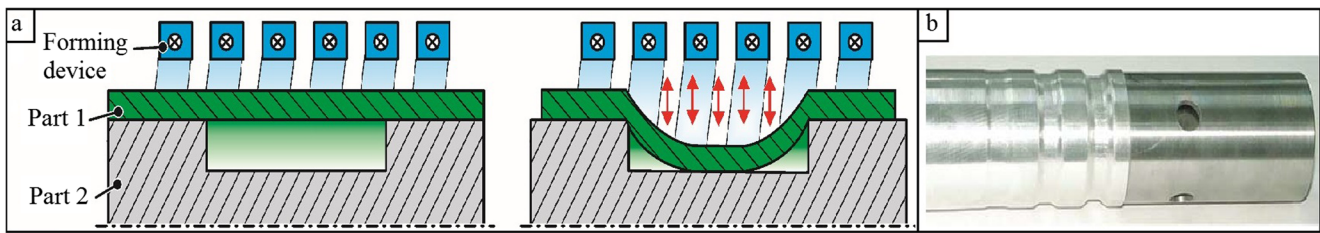
**Fig. 3** **a** Mechanism of a form-fit joint [13]. **b** A form-fit joint of aluminum to aluminum manufactured by EMF [15]

time and cost. The main drawbacks of the method are that it is applicable only to the materials of relatively high formability due to the locally severe plastic deformation of the work-pieces, which may lead to cracking of the workpieces of lower formability [17]. However, measures have been taken to im-plement the process on materials of low ductility. Rectangular (shear) clinching, preheating the workpieces, or increasing the hydrostatic pressure and/or strain rate during the process are among these measures, which will be discussed in the follow-ing sections in more detail. The process applies to different industries, such as automotive subassembly [18], building components [19], and electrical appliances [20].

The clinching method is illustrated schematically in Fig. 4. The clinching equipment has consisted of a punch and a die and in some cases a blank-holder. First two sheets are stacked up and placed on the die (step I), blank-holder, or any other type of clamps which are used to fix the layers and to prevent their relative motion or displacement on the die. Then, punch is moved towards the punch-sided sheet and after contact, the sheets start to deform plastically, and the material of both sheets begins to flow towards the die cavity (step II). The material of the lower sheet limits the vertical flow of the upper sheet. Thus, it flows in the radial direction (step III) resulting in a mechanical interlock between two layers (step IV). A typical clinching equipment is illustrated in Fig. 5.

The joints made by clinching have some geometrical fea-tures that primarily determine the joint quality, strength and other mechanical properties. These features are illustrated in Fig. 6 and are namely: neck thickness ($t_n$), undercut ($t_s$), and thickness of the clinched zone or joint bottom thickness ($X$).

Dies with different geometrical features can be used for the clinching process (Fig. 7). Fixed flat dies (Fig. 7c) and exten-sible dies (Fig. 7a) are the most common ones [23]. Flat dies are divided into two categories: simple and grooved dies. Abe et al. [20] and Neugebauer et al. [24] utilized flat dies and Lambiase and Ko [4], Lambiase [25], Lambiase and Di Ilio [22], and Lambiase [26] used extensible dies for clinching various materials. Other types of the dies are rectangular (shear) dies (Fig. 7d) [27], which has lower applications com-pared to other types. This type of die is generally utilized to clinch materials of lower formability. Clinching with rectan-gular dies is illustrated schematically in Fig. 8. In the rectan-gular shear clinching process, the sheets are joined with partial separation in the upper sheet. The sheets are joined by inter-lock between the upper and lower sheets with upper sheet separation in the short sides of a rectangle, whereas fracture is prevented in the long sides of a rectangle. To obtain a certain joint strength, both modulate interlock and minimum wall thickness are required [28]. Lambiase et al. [29] investigated the effect of die geometry on the quality of aluminum (Al)/ glass fiber reinforced plastic (GFRP) joint made by clinching. They stated that round grooved dies are not proper for this combination of materials because the GFRP crumbles fill the die groove and the removal of crumbles from the die is time-

**Table 1** The most important features of the mechanical joining techniques

| Joining technique | Form-fit | Force-fit | Spot joining | Continuous joining | Direct joining | Indirect joining | Contact joining | Non-contact joining | Sheet joining | Tube/profile joining |
|---|---|---|---|---|---|---|---|---|---|---|
| Mechanical fastening | × | × | ✓ | × | × | ✓ | ✓ | | ✓ | ✓ |
| Adhesive bonding | × | × | ✓ | ✓ | × | ✓ | × | ✓ | ✓ | ✓ |
| Clinching | ✓ | * | ✓ | × | ✓ | × | ✓ | × | ✓ | × |
| SPR | ✓ | * | ✓ | × | × | ✓ | ✓ | × | ✓ | ✓ |
| Hemming | ✓ | × | × | ✓ | ✓ | × | ✓ | × | ✓ | × |
| Rolling | ✓ | ✓ | × | ✓ | ✓ | × | × | ✓ | × | ✓ |
| Die-less hydroforming | ✓ | ✓ | × | ✓ | ✓ | × | × | ✓ | * | ✓ |
| Incremental forming | ✓ | * | × | ✓ | * | * | * | * | ✓ | ✓ |
| Hydraulic/mechanical crimping | ✓ | * | × | ✓ | * | * | × | ✓ | × | ✓ |
| EMF | ✓ | ✓ | * | ✓ | ✓ | × | * | ✓ | ✓ | ✓ |
| Lateral extrusion | ✓ | * | × | ✓ | ✓ | × | ✓ | | × | ✓ |

✓: utilized ×: not utilized *: partially utilized
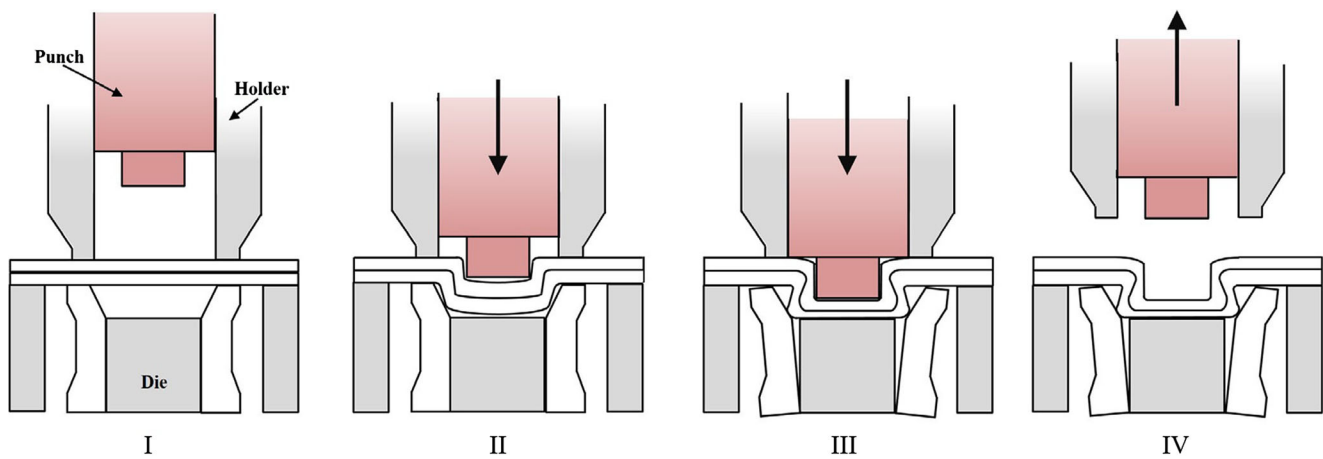
**Fig. 4** Schematics of the clinching process [21]

consuming. When using flat, due to higher hydrostatic stress, a smaller undercut is created leading to joints of lower strength. The best joint strength was achieved using extensible dies, and shear dies created joints of intermediate strengths.

The toolset geometry and joining force (the force applied to the workpieces by the punch) are the most critical factors affecting the lock formation in clinching. The toolset geometry directly controls the material flow by generating different stress states during the process. Also, the amount of undercut and neck thickness is directly influenced by the joining force. Generally, a higher joining force leads to a higher undercut [30]. The effect of joining force differs in different toolsets. For instance, Lambiase [31] found that when manufacturing a hybrid metal/polymer joint, rectangular clinching tools require lower joining forces as compared to round clinching tools. Actually, other than depending on the materials flow stress and thickness of the sheets, the joining force threshold (below which the interlock is not formed) is highly influenced by the clinching tools configuration and mainly by the developing hydrostatic stress [32]. Generally, in shear clinching, the lower joining forces can lead to a desirable undercut, but in other

toolsets, some higher joining forces are required to obtain a sound undercut. In fact, with rectangular tools of the shear clinching, a lower hydrostatic stress develops owing to the shearing effect on the workpieces [31]. Ismail and Buang [33] investigated the effect of punch speed and joining force on the joint geometrical features, including undercut, neck thickness, and bulge thickness, as well as the joint strength. They concluded that increasing the joining force increases the undercut and decreases the neck thickness and bulge thickness. This increase led to an increase in joint strength in all the samples. On the other hand, the increase in punch speed until a certain point leads to an increase in the undercut and joint strength, but the further increase will lead to a decrease in joint strength. However, Zajkani and Salamati [34] obtained superior joint strength utilizing an ultra-high-speed punch. The reason is that using such an ultra-high-speed punch leads to great strain hardening resulted by high strain rate values, which in turn, leads to a superior joint strength.

The joining force and toolset geometrical features also affect the material characteristics in the processing zone. Krztoń et al. [35] used the X-ray micro-diffraction technique to study the effect of joining force and forming conditions on the changes in austenite content of a dual-phase DP600 steel processed by clinching tools. They found that the austenite contents in every deformed part decrease significantly depending on the forming conditions. The amount of decrease in the
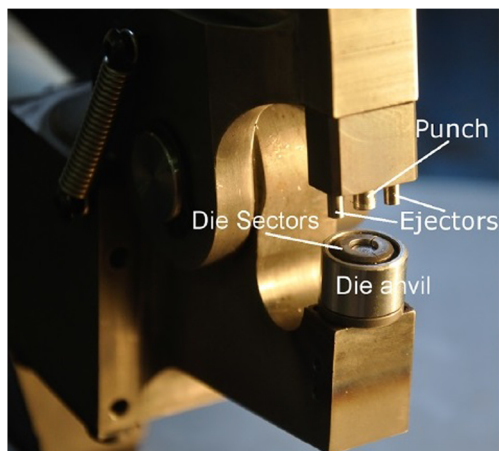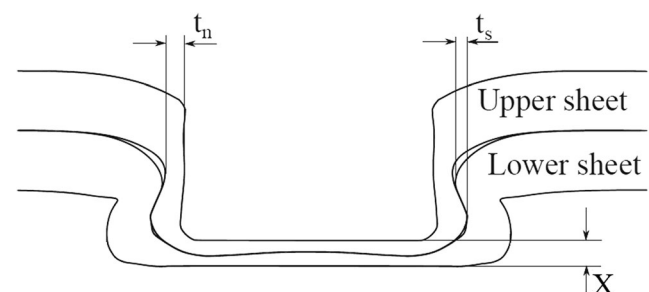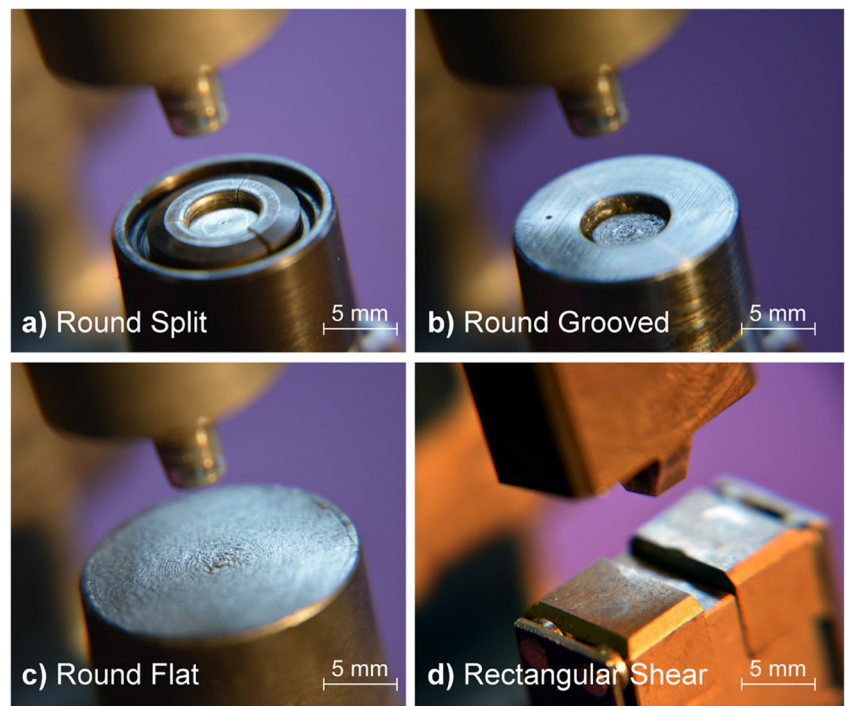


**Fig. 5** A typical clinching machine [22]



**Fig. 6** Interlocking conditions of a clinched joint [16]

**Fig. 7** The most common clinching tools [22]



a) Round Split    5 mm
b) Round Grooved    5 mm
c) Round Flat    5 mm
d) Rectangular Shear    5 mm

austenite content was observed to be higher in the die-sided sheet for all the samples. On the other hand, the reduction of the punch diameter lowers the austenite content in the necking zone and the bulge zone as well. Lambiase et al. [17] stated that the high deformation on the processing zone of the clinched joints results in a drastic hardness increase stem from material strain-hardening. However, this increase is dependent on the work hardening characteristics of the processed material. They studied the effect of forming temperature on the micro-hardness distribution of AA 6082-T6. The highest increase in micro-hardness was shown at the bottom protrusion, regardless of the joining temperature, due to the severe plastic flow. Comparing the micro-hardness distribution of specimens produced at different temperatures, it was proved that the micro-hardness of the punch-sided sheet zones reduces with the joining temperature. This could be ascribed to a higher strain-hardening of the material when joined at room temperature and partial recovery annealing arising at higher temperatures. On the other hand, the die-sided sheet seems to be only marginally influenced by the joining temperature. Indeed, because of the heating flux is directed towards the punch-sided sheet, the die-sided sheet experiences a lower temperature increase, which could explain the lower sensitivity to the joining temperature.

Different stress states can be produced on the workpieces when utilizing different clinching toolsets. When round split tools are used, the adoption of deeper dies involves a reduction in the hydrostatic stress during upsetting (since the reduced material flow), which leads to lower restricting action on the material flow [32] and consequently, larger undercuts. Besides, joints characterized by deeper bulges undergo to lower bearing stress acting on the die-sided sheet [31]. Nevertheless, deeper dies involve higher thinning on the punch-sided sheet, which may also affect the mechanical
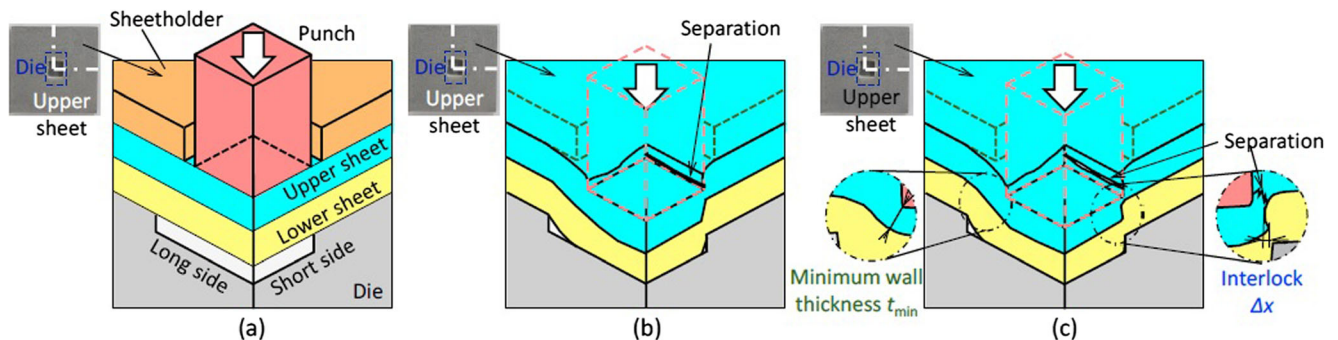


**Fig. 8** Process sequence of rectangular (shear clinching): **a** initial positions, **b** separation in log side, **c** formation of interlock [28]

behavior of the joints. Indeed, excessively deep dies may result in bulge fracture [29]. The flat dies can be regarded as round tools with anvil depth of $h = 0$ mm. In this case, the offsetting phase is negligible; thus, the neck thinning is reduced as compared to split dies with a certain height. The flat dies promote high hydrostatic stresses during joining, which restrain the material flow, and consequently, the undercut dimension. There is more compressive stress in flat clinching, whereas tensile stress can be observed when clinching with the contoured dies at the beginning of the process, which increases the danger of crack formation in the hard to form materials [24]. So, this is evident that the clinching toolset should be selected considering the workpiece materials and contributed flow stresses, the joining force available for the process.

## 3.2 Materials

Clinching is a powerful technique for joining a broad range of similar and dissimilar materials including metallic and nonmetallic parts. But, it is required to control the plastic deformation carefully especially in materials of low formability or to consider some special treatments to enhance the material formability, such us increasing the hydrostatic stress [20] and pre-heating the workpieces [24]. Using these techniques, clinching is successfully applied for joining low formability materials, such as titanium alloys [36], aluminum alloys [17], magnesium alloys [24, 37], and copper alloys [38]. Clinching can also be applied to high-strength materials, such as steel. Lee et al. [39] utilized the clinching process for joining aluminum alloy AA5052 and DP780 steel, and Varis [40] joined two high-strength structural steel sheets and introduced the clinching as a suitable process for joining structural steels. Abe et al. [41] joined the zinc-coated steel sheets, which are of great importance in the automotive industry. They optimized the shapes of punch and die by controlling the plastic deformation of the sheets using the FE simulations to increase the layer thickness of the coating of the joined sheets.

Clinching is a well-suitable process for joining any combination of dissimilar materials. During the clinching process, the coating or paint layer of sheets will also plastically flow with the plate plastic deformation without causing tearing damage; therefore, the clinching process does not affect the anti-corrosion performance of the sheets; so, it is a proper method to join even materials of corrosion risk such as HSS and aluminum [42].

It is essential to consider the arrangement of the materials on the die when joining dissimilar materials by clinching. For example, when joining Al/HSS, placing the steel sheet at the punch side will lead to fracture of the steel sheet around the punching zone due to low formability of HSS and placing it at the die side will cause tensile stresses at the bulging region of the other sheet leading to cracking on the steel sheet [20].

Prevention of these fractures can be achieved by optimization of process tools including punch and die shape. Zhou et al. [42] also investigated the configuration of the aluminum and steel sheets and stated that placing the aluminum on the punch side will lead to a more quality joint. Values of undercut and neck thickness achieved by two configurations are listed in Table 2. In this table, the HSS-Al means that HSS is the punch-sided sheet and Al-HSS means that Al is the punch-sided sheet.

It can be seen that when aluminum is punch-sided, neck thickness is a little lower than the other configuration, but the undercut is 2.5 times higher that leads to a considerable increase in the strength. Usually, this is true for most material combinations, to use the lower strength material at the punch side. The fracture during the implementation of the process is generally caused by the concentration of deformation around the corner of the punch, or due to the tensile stress generated in the bulged bottom into the groove of the die [20]. The former one can be prevented using a lower strength punch-sided sheet. Since deformation of the punch-sided sheet during the clinching concentrates, the fracture occurs due to the small ductility when using high-strength materials on the punch side. On the other hand, the die-sided sheet generally experiences a higher hydrostatic pressure generated by the clamping device which facilitates the forming process and can overcome the poor formability of the higher strength material. Thus, it is recommended to use the higher strength material on the die side. Another reason to use the lower strength material on the punch side is due to the fact that the clinching tool should be made of a harder material compared to the workpieces. Kaščák et al. [43] numerically (employing FEM simulation) and experimentally evaluated and monitored the wear of a CrN coated clinching toolset when joining two sheets of dual-phase DP600 steels. They found that the wear of the clinching die is less pronounced as compared to the punch. FEM analysis showed a maximum von Misses stress of 2991 MPa in the punch corner radius and cracks were detected in the punch corner radius vicinity using an SEM, while all other critical zones exhibited only minor wear in the form of removed spheroidal particles. Considering the fact that the punch suffers higher wear compared to die reveals that it is desirable to use the lower strength material on the punch side. The effect of different coating materials on the wear of clinching toolset was studied by Kaščák et al. [44]. Three types of PVD coatings CrN, TiCN MP, and ZrN were

**Table 2** Neck thickness and undercut values for two configurations of HSS/Al joint

| Configuration | Neck thickness $t_n$ (mm) | Undercut $t_s$ (mm) |
|---|---|---|
| HSS-Al | 0.389 | 0.032 |
| Al-HSS | 0.345 | 0.079 |

deposited on the surface of rigid dies for round mechanical clinching and experimentally tested by joining of two H220PD + Z steel sheets. The total number of 300 mechanically clinched joints was produced by each pair of tools (punch and die) and by each coating deposited. The samples with 900 mechanically clinched joints were prepared. Surfaces of die cavities were divided into five regions illustrated in Fig. 9 and scanned by SEM. Some galling was detected in the RVD area of die cavity covered with the CrN and ZrN coatings. This area remained intact in the case of TiCN MP coating. The EDX qualitative analysis confirmed the presence of zinc and iron in the RVD area of CrN and ZrN coatings. Relatively, planar VD and OD areas were worn only slightly. Small spherical particles were removed from the surface by the material flow, or they were plastically deformed by the action of the normal and contact stresses. Compressive forces or stresses are the main driving factor for galling and adhesion. Levels of normal stress (in the Y direction) and material flow along with the location of the contact pressure maximum were evaluated by the FEA calculations. Tools (die and punch) were modeled as deformable solid bodies without coating. High levels of normal stress were evaluated in the areas where the galling wear was observed, which was ROD especially. Another highly loaded areas were RVD and VD. Maximum levels of contact pressure were detected in the areas of VD, RVD, and ROD. The material flow at each stage of mechanical clinching, such as drawing, compression, and interlocking, showed the direction of material flows and loading curvature of the die cavity.

Clinching can be used to join non-metallic parts. Lüder et al. [45] joined wood and aluminum by this process. By increasing application of the polymeric materials and polymer matrix composites (PMC) in various industries, applying clinching on these elements becomes a field of interest. Lambiase and Di Ilio [22] joined polystyrene (PS) and aluminum alloy AA5053 by clinching. To increase the formability of the polymeric sheet, the pre-heating process was used.
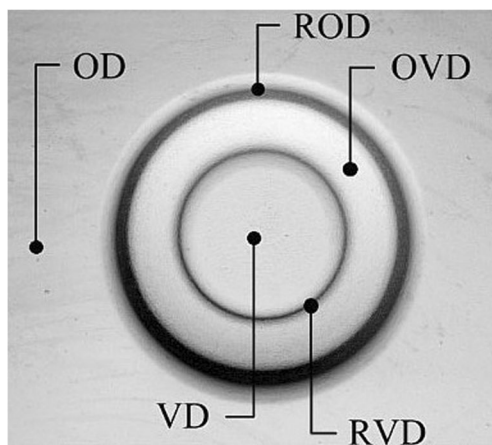


**Fig. 9** Different regions on the die cavity to be scanned by SEM [44]

Influence of clinching force and pre-heating time on the neck thickness undercut, and shear strength is investigated. Lambiase [26] stated that polymers, which have high toughness at the room temperature such as polycarbonate (PC), could be easily joined by clinching because these polymers are not fractured under joining conditions even without pre-heating. Polymers with low toughness and high yield strength, such as polymethyl methacrylate (PMMA), are joinable by pre-heating in proper time, and polymers with both little toughness and yield strength, such as PS, are hard to join by clinching.

Lambiase et al. [29] investigated the effect of the clinching tools and workpiece thickness on the joinability of aluminum and GFRP. GFRP sheet has minimal elongation (2.4%); thus, it cannot be used on the punch side. Joining CFRP and aluminum by clinching is also investigated [4]. The CFRP used was the thermosetting type, which cannot be pre-heated and has very poor formability; it was used as a die-sided sheet, and an extensible die was utilized for the experiments. Figure 10 shows the material flow during the process by applying the punch force on the sheets; CFRP sheet delaminates under the aluminum bulge. By increasing the punch stroke, the CFRP is upset against the underlying die and fractures. Thus, a hole in the CFRP sheet is formed, since there is a complete cut of the carbon fibers surrounding the aluminum bulge, by a further increase in the punch stroke the aluminum bulging is upset between the punch and the CFRP and spreads radially, compacting the walls of the CFRP hole resulting in the undercut. It is suggested that a decrease in the punch taper angle and increase in the punch diameter lead to more significant material flow and subsequently a larger undercut.

### 3.3 Process variants

Applying the clinching on the high-strength materials, such as advanced high-strength steels (AHSS) and CFRP, faces some limitations due to the low formability of these materials. The low formability of materials, in turn, leads to some consequential problems, such as reduced undercut, cracking in the necking zone, and incomplete or defective clinch bulge. However, some considerations had been done by some researchers, but generally, conventional clinching is not the best way to join such materials. Figure 11 shows some problems of joining AHSS and aluminum by conventional clinching. As shown in Fig. 11a, the high strength of the steel makes it difficult to achieve geometrical interlocking with a punch or rivet. Figure 11b illustrates the necking of the high-strength, low-ductility steel upper sheet that occurs during clinching. Figure 11c shows a split that the top sheet causes in the lower sheet owing to the difference in strengths of the two materials. To address such limitations, some special modifications are applied
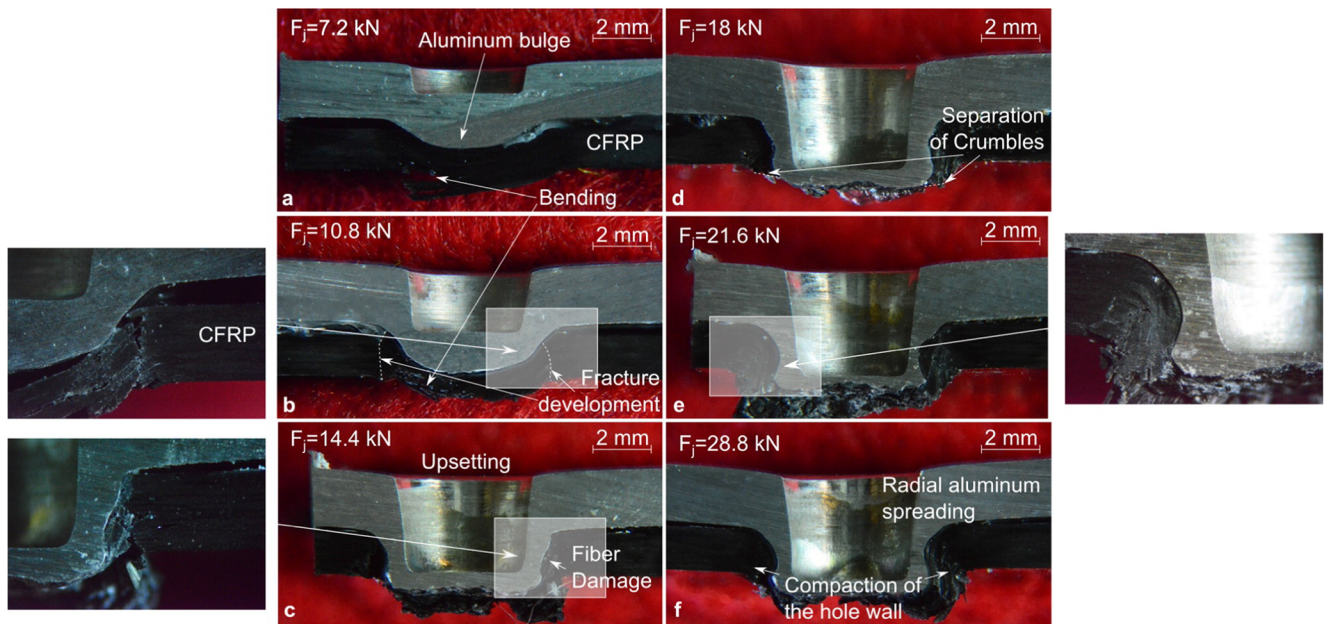
**Fig. 10** Material flow in clinching aluminum and CFRP in different punch strokes [4]

to the conventional clinching, each of which leads to develop a unique process variant, with the aim to minimize a particular limitation of the process.

A particular variation of the process was developed to join high-strength materials, so-called hole-clinching. In this process, a hole is predrilled on the high-strength material, and then it is used as the die-sided sheet, after punching, the material of the formable sheet bulges onto the predrilled hole, and the die cavity helps to the creation of the interlock. The

schematics of the process is shown in Fig. 12. Lee et al. [46] used hole clinching to join aluminum alloy AA6061-T4 to DP780 HSS, hot pressed 22MnB5, and CFRP. Aluminum is used as a deformable material, and a numerical and analytical approach was used to design the tools of the process. Lee et al. [47] numerically and experimentally investigated the hole-clinching of SPRC440 and CFRP. Influence of geometrical features of the clinching tools including punch diameter and punch corner radius on the joint strength was investigated.

**Fig. 11** Typical problems in mechanical clinching of AHSS and aluminum [46]
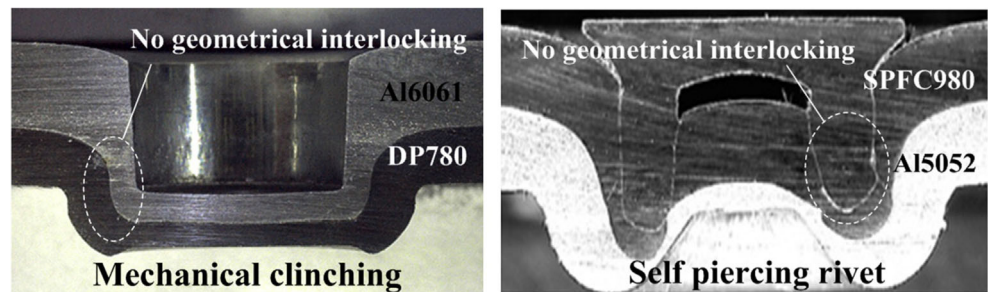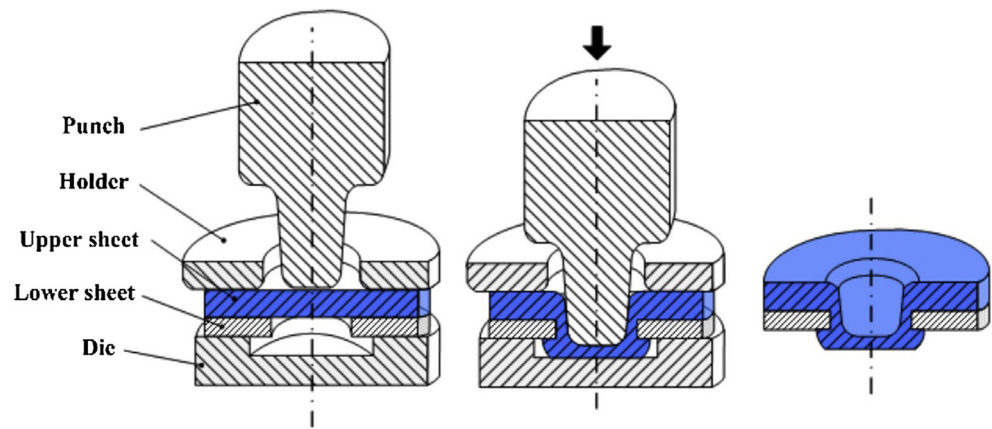


(a) no geometrical interlocking
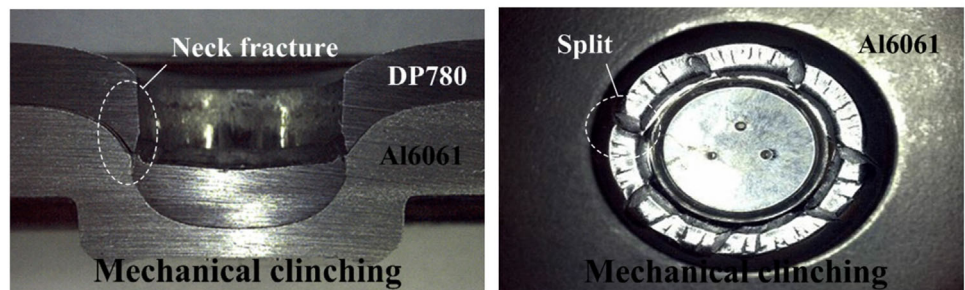
(b) necking of upper sheet          (c) splitting of lower sheet

**Fig. 12** Schematic of the hole-clinching process [46]



They obtained a maximum shear strength of about 3.5 kN that is a considerable value.

Zajkani and Salamati [34] introduced an electromagnetically assisted hole-clinching of the aluminum and CFRP. An actuator disk made of aluminum is attached to the punch that translates the magnetic field to the punch. As a result, the punch strokes the aluminum sheet with a high velocity. Therefore, the strain rate of the process is so high leading to high strain hardening at the clinched zone as compared to the conventional clinching. This results in greater strength of the clinched region and subsequently a higher strength joint.

An important design parameter of the hole-clinching is that the hole of the high-strength material and the punch should be aligned coaxially that needs high precision. Otherwise, the material of the high-strength sheet around the hole would prevent complete bulging of the deformable sheet, resulting in a defective joint. One other significant limitation of the process is high manufacturing time due to the need for the predrilling process. Busse et al. [48] developed a modified clinching equipment to meet this challenge. In this method, a ductile material and a very brittle material can be joined together in a one-step continuous process without the need to predrilling. The material with high formability lies on the punch side and the high-strength material on the die side. Then punching of the die-sided high-strength material is performed by indirect shear-cutting and subsequent forming of the deformable material into this hole, see Fig. 13. The use of the punch set consisting of outer and inner punch realizes the indirect shear-cutting operation of the die-sided material. During the process, a fixed die anvil causes the radial material flow of the punch side ductile material. The lateral extrusion process is controlled by the opening of the die lamellae, and the resulting interlock between the joined materials creates a form-fitting, non-positive connection [49]. This process is so-called shear clinching that is a hybrid process combining the shear-cutting and clinching and prevents high manufacturing times. Han et al. [50] investigated the influence of the punch geometry on the deformation of specimens and occurring tool loads in shear-clinching processes. They found that both, using a blank holder with chamfer and reducing the outer diameter of the outer punch lead to a decrease of the bending of the joint sample. However, while the slim outer punch results in a lower force during joining, the force increases for the variation with the added chamfer. By combining both geometrical adaptions, a distinct decrease in the bending of the joint sample is achieved. Moreover, the maximum process force is reduced, too.

Hörhold et al. [51] introduced shear-clinching and hole-clinching as the solutions to clinch hard to form materials such as ultra-high-strength steels (UHSS). As a case study, they used these two processes to clinch AA 6016-T4 to 22MnB5. The aluminum alloy is used as the punch-sided material and the steel as die-sided one. They compared the mechanical performance of the joints manufactured by two techniques under tensile and shear loading. It should be mentioned that the effect of pre-drilled hole geometry on the load-bearing capacity of the joint manufactured by hole-clinching is also investigated. A cylindrical and a tapered hole geometry is considered for the investigations. Based on the results, under shear load, the cylindrical pre-hole bears 3.51 kN. The tapered pre-hole bears the maximum shear load of 4.11 kN. Under tensile load, the results of maximum force and displacement are not significantly different. The cylindrical pre-hole withstands 1.99 kN, the tapered pre-hole reaches a maximum tensile strength of 2.16 kN on average. While, under shear load, the shear-clinched specimens bear about 3.83 kN on average. Under tensile load, the maximum load decreases to 1.76 kN. Notably, the displacement until the break is significantly lower. Due to the formation of the lower and upper neck thickness, the aluminum is more highly deformed, and the lower neck thickness is thinner (0.54 mm) than the neck thickness of the tapered pre-hole (0.87 mm). The neck fracture occurs earlier, but still, both tests show a high level of load capacity.

Other particular variants of the clinching process are introduced in some literature, each of which is suitable for a unique application. Abibe et al. [52] proposed injection clinching

Positioning        Pushing,        Upsetting,        Retraction
                   Punching        Extrusion
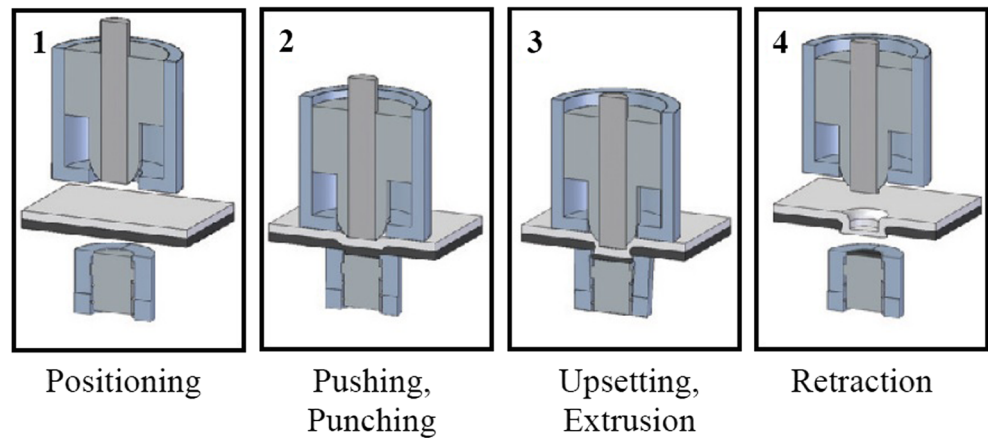
joining (ICJ) as a method for joining polymeric materials to metallic ones. The process is based on staking, injection molding, and mechanical fastening. This is a staking joining technology for multi-material structures, which can join polymers or PMC to other materials including metals, ceramics, or other polymeric materials. Schematics of the process is shown in Fig. 14. A polymeric part with a protruding stud is pre-assembled with a pre-drilled joining partner so that the stud fits in the hole. A hot case contains the polymeric stud and then reaches the pre-assembled parts with the punch-piston. The stud is heated at a certain temperature for a pre-determined joining time, after which, the punch-piston pushes the molten or softened polymer into the hole. Then the system is cooled under pressure to reduce the polymer thermal degradation, and the joint is consolidated. Abibe et al. [53] investigated the strength and failure modes of AA2024-T351/short glass fiber reinforced polyamide 6.6 (PA66-GF) joints made by injection clinching. A shear stress of 60 MPa was achieved for the joints.

Neugebauer et al. [54] utilized the pressure of a high-pressure fluid, as the driving force of the clinching process.

In this case, the fluid works as a punch replacement. Figure 15 shows the process sequence; first joining partners (3 and 4) are brought into contact with the hydroforming tool (2) by the fluid (5). During calibration, the hydroformed sheet (4) is pressed through a hole in the part to be attached (3). The punch (1) is withdrawn, to avoid bursting and to ensure a higher forming level at the produced bulb. Subsequently, the punch is set towards the high-pressure fluid. Because the high-pressure fluid prevents the back forming, the material that has been pressed through the hole is spread and develops an interlock.

Another variant of the process is dieless clinching, where two parts to be joined are lying partially overlapped on a flat anvil (see Fig. 16). Clamp and the punch are moved together towards the parts to be joined. First, the clamp gets into contact with the upper sheet, and a limited pressure is applied to the sheets, without deforming them. Then the punch is pressed directly into the parts, with high force. The material of the parts is displaced partially and flows in the opposite direction to the movement of the punch. Thereby, pushing the clamp upwards. Thus, an elevation is formed on the downside of the
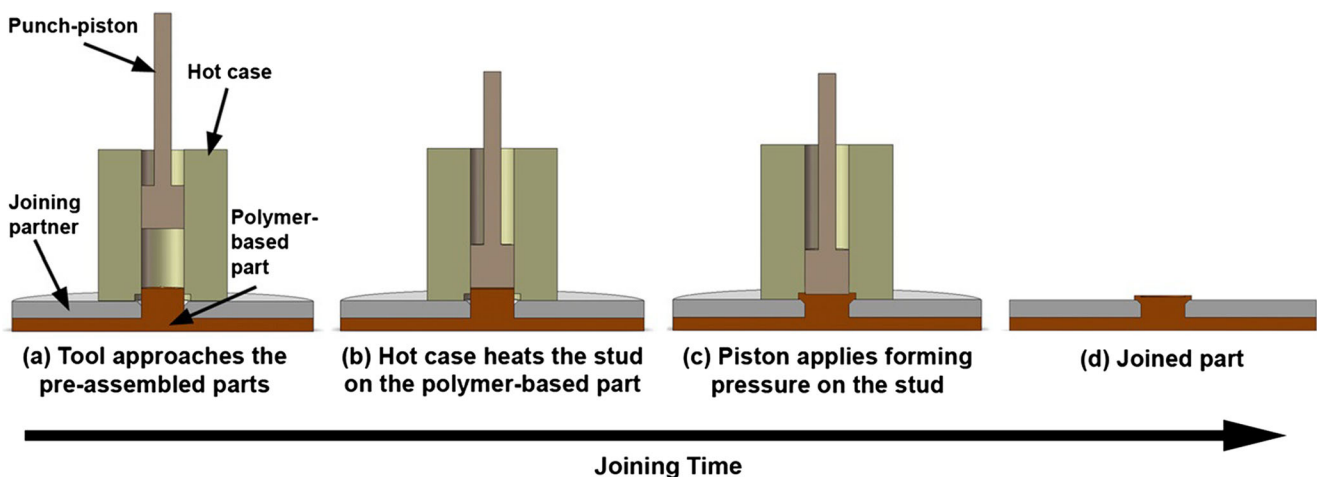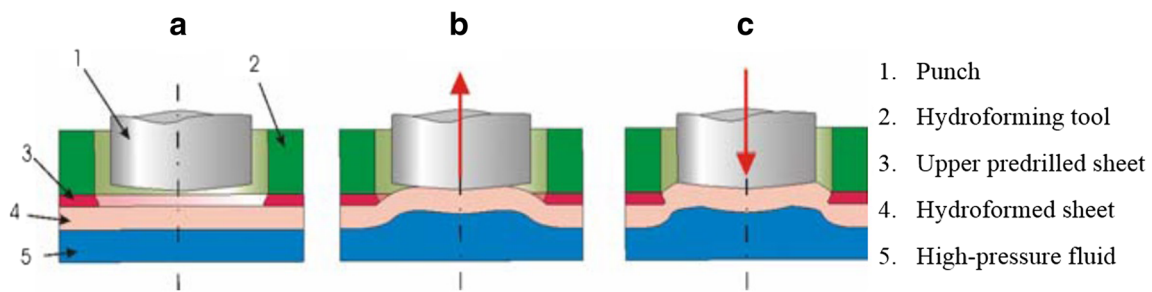


**Fig. 14** Steps of injection clinching [52]

Fig. 15 Operational sequence of hydro clinching [54]

1. Punch
2. Hydroforming tool
3. Upper predrilled sheet
4. Hydroformed sheet
5. High-pressure fluid

bottom sheet. The size of this elevation is increasing the further the punch is pressed into the sheets. As soon as the material of the upper sheet has come into contact with the shoulder of the punch, the material flow against the movement of the punch is stopped. When the punch is pressed even further into the sheets, the elevation at the downside of the bottom sheet is flattened, and the material displaced by the punch is forced to flow in a radial direction, thus forming an interlock between the parts [37].

Chen et al. [55] introduced a two-step clinching process that lowers the protrusion height of the joint that can be applied in the visible areas of a structure where a lower protrusion height is required to meet esthetic requirements. Furthermore, it is proved that both the tensile and shear strengths of the joints manufactured by this process are higher than those of conventional clinching. The first stage of the process is precisely the traditional clinching by extensible dies, subsequently followed by an upsetting process in the protrusion extending out of the clinched zone, using a pair of flat upsetting dies and a clinch-rivet. The clinch-rivet which was embedded in the pit of the joint was applied to control the material flow in the second stage.

A hybrid clinching riveting technique so-called ClinchRiveting is one other process variant. The ClinchRiveting is a cold process for joining two or more sheets by directly piercing the sheets with a special rivet. Since the ClinchRiveting process does not require a pre-

drilled hole unlike the conventional riveting, the joining speed is the same level as that of the spot resistance welding, and the equipment is similar. As depicted in Fig. 17, the joint is formed by a rivet, the punch, under pressure conveyed by a hydraulic power device, pushes the rivet to penetrate into the top plate, and the die shape causes the rivet to flare within the lower sheet to form a mechanical interlock [57]. This process, therefore, requires access to both sides of the joint. It is similar to the clinching process, which is used without any additional elements. Like the conventional clinching, the main advantage of ClinchRiveting technology is low running costs, since the processed components need not be heated. Only a die and a punch are used to press the sheet components to finish the whole joining process. The incomparable advantages of CR in practical production are as follows: no joining hot-stress has been produced, no poisonous gas has been given off, there is little noise in the process, the energy consumption is low, and this process leads to no damage to surface coating and does not require any predrilling of holes to the joined materials [57]. Compared with the conventional clinching, the main advantage of ClinchRiveting is to increase the joint strength [56] because of the existence of a solid rivet in the clinched hole. The rivet in the clinched hole increases stiffness; thus the ClinchRiveted joints feature higher load-carrying ability [58]. Mucha and Witkowski [56] found the maximum shear strength of ClinchRiveted joint of steel sheets 45% higher than conventional clinched joints of the same materials. Also, the
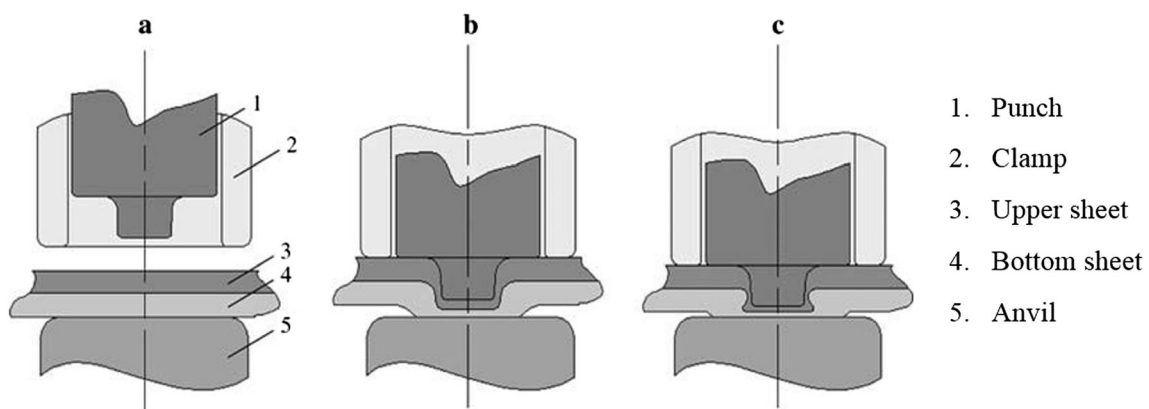


Fig. 16 Operational sequence of dieless clinching [37]

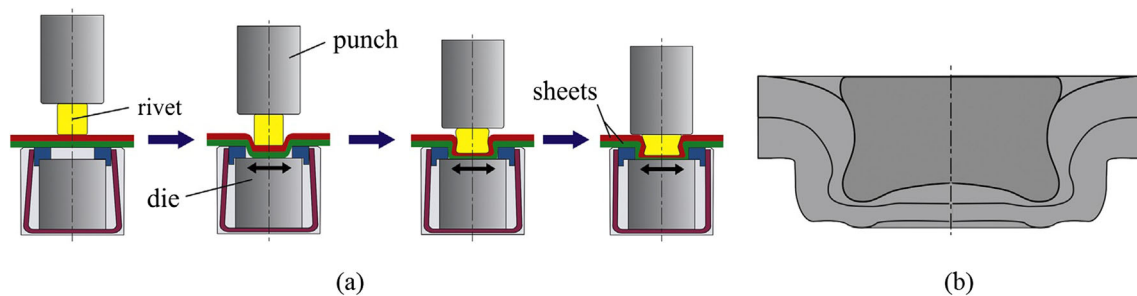1. Punch
2. Clamp
3. Upper sheet
4. Bottom sheet
5. Anvil

Fig. 17 **a** Process sequence of ClinchRiveting. **b** Schematic representation of a ClinchRiveted joint [56]

destruction energy for ClinchRiveted joint was more than twice as that for the conventional clinched joint. The main drawbacks are to increase the forming force required for the process and to increase the weight of the structure because of the existence of steel rivets. Mostly, steel rivets are used in the ClinchRiveting process. The ClinchRiveting using aluminum rivets is indeed a challenging task, since the strength of aluminum alloys is much weaker than that of steels. The aluminum rivet can be easily deformed when compressed into the plates, and hence, no interlock is formed [57]. On the other hand, the forming force is higher than that in conventional clinching. Using the rivets increases the energy required for its deformation and creating the interlock [56].

Zhang et al. [59] proposed a new hybrid technology called resistance spot clinching (RSC) and implemented the process to join two sheets of AA 5052. The process sequence of RSC is similar to conventional clinching, which includes an additional current passing phase. One cycle of the RSC process consists of four phases (i.e., initial, forging, melting, and detachment phases). These stages are described as follows: (1) in the initial phase, the workpieces are clamped together between the punch and the die; a thin processing tape is also inserted between the toolset and the AA 5052 sheets. (2) A period of low-level current passes through the metal sheets during forging when the punch is driven down towards the die. In this phase, a dent is formed locally in the joining zone. (3) During the melting phase, the joining zone of AA 5052 is melted by the heat generated by a period of high-level current. (4) After the workpieces are joined, the punch moves back to its initial position, and the processing tape is removed from the joining spot. Compared with the traditional resistance spot welding (RSW) process, the RSC technique is energy-efficient and yields joints with a superior tensile property. Furthermore, owing to its low electrical and thermal conductivity, the processing tape acts as an additional heat source and barrier to heat dissipation during the process. A large fusion zone is realized, even if the energy input is low. Zhang et al. [60] utilized the RSC process to join AA 5754 and DQSK steel. In this material configuration, the liquid aluminum alloy reacted with the solid steel to form a layer of Al–Fe intermetallic compounds, which joined the two metal sheets together. The Al–Fe intermetallic compounds layer at the Al/steel

interface in the clinched–welded joint was thinner and smoother than that in the spot-welded joint, leading to increased joint strength and toughness. On the other hand, digital image correlation analysis of the Al/steel dissimilar joints revealed that during the tensile–shear testing of the clinched–welded joint, the main strain region avoided the Al–Fe intermetallic compounds layer (the weak point of the joint). This structural merit coupled with metallurgical factors substantially increased the joint toughness. With adequate heat input, the energy absorption ability of the Al/steel clinched–welded joint was nearly three times that of the Al/steel spot-welded joint.

Wang et al. [61] proposed a novel clinching technique for ultra-thin metallic foils using a laser shock wave. The basic schematic diagram of micro-clinching with cutting by laser shock forming is shown in Fig. 18. Metal foils can be joined using this specific joining device, which includes the blank holder, confinement layer, ablative layer, soft punch, metal foils, mold sliders, spacer, mold substrate, and die anvil. When a high energy laser beam is focused onto the ablative layer through the transparent confinement layer, one part of the ablative layer is vaporized instantaneously into a high-temperature and high-pressure plasma after absorbing a large amount of laser energy. The plasma continues to absorb the laser energy, and the rapid deposition of laser energy ignites the plasma and changes into a laser-supported detonation wave. Under the constraints of the confinement layer and blank holder, the induced shock wave can only propagate downwards and generate tremendous impact on the soft punch. As the soft punch is incompressible and hyper-elastic, the shock wave will load on the metal foils after propagating in the soft punch. Under the combined action of the impact load and the micro-mold, the metal foils are subjected to a considerable shear stress at the fillet of the mold and a series of physical processes—such as elastic deformation, plastic deformation, and fracture—are completed. Subsequently, the lower foil is cut off, and the material of the upper foil flows into the mold. A certain interlock is generated by the material flow, which can hook the upper and lower metal foils together. Eventually, the metal foils under the micro-scale are clinched with cutting by laser shock forming. The necessary condition for the process of micro-clinching with cutting by laser shock forming is the generation of interlock without fracture of
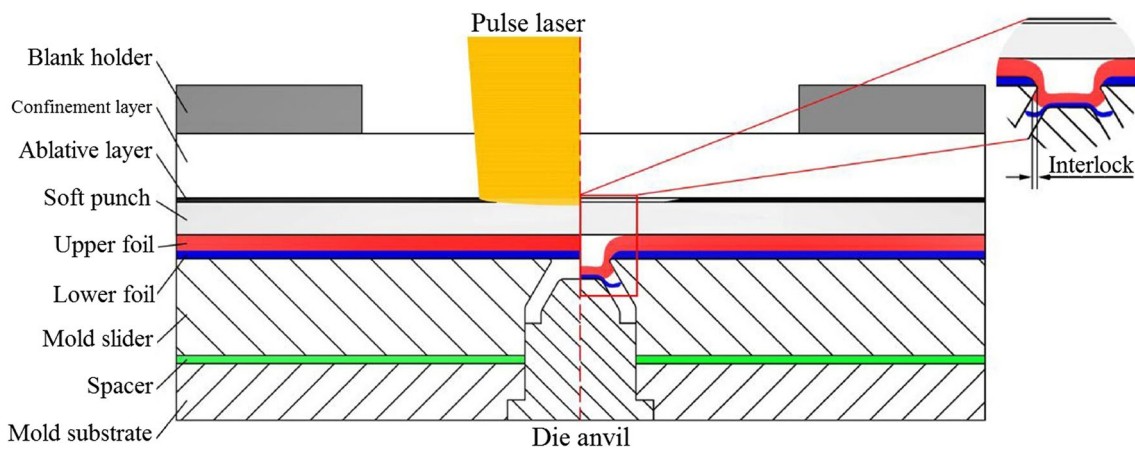
**Fig. 18** Schematic representation of clinching by laser shock forming [61]

upper foils. The interlock between metal foils ensures the appropriate joining strength. However, the fracture of upper foils destroys the air tightness and water tightness of the joints and accelerates the corrosion of the joints.

In the work of Wang et al. [61], PMMA was used as the confinement layer. Given the increase in laser energy, the confinement layer (PMMA) constantly broke along the laser path after a single laser shock, which blocked the following laser. To address this problem, Wang et al. [62] employed a waterfall as a confinement layer instead of PMMA in the experiment system. Meanwhile, aluminum foil was used as the ablative layer in almost all of the industrial applications, because of its excellent toughness and easy maneuverability. Thus, they also adopted aluminum foil as the ablative layer. Compared with aluminum foil, black paint might be partly brushed away by the waterfall and could not be instantly complemented to suit several laser shocks. The rest of the process is similar to the abovementioned work of Wang et al. [61].

### 3.3.1 Heat assisted clinching

Many materials of poor formability have been successfully joined just by means of heating. Osten et al. [63] remark that in order to realize the clinching of high-strength materials, such as HSS, the sheet can be heated locally at the joint, to improve ductility. There are various heat-assisted techniques for clinching the brittle materials. Either a simple setup consisted of a heating gun (inductive heating or convective heating) or some more complex techniques such as laser heating, resistance assisted heating, ultrasonic assisted heating and friction-assisted heating can be used to preheat the workpieces. Lambiase [64] used a system consisted of a heater gun to manufacture AA6082-T6 joints and investigated the effect of preheating position (whether the heating gun is placed towards the punch-sided or die-sided sheet). They claimed that the employment of preheating represents a viable solution to control the material flow in the clinching process other than

increasing the formability of the sheets. Indeed, when the airflow is directed towards the punch-sided sheet, the development of cracks at the neck can be prevented by improving material formability. On the other hand, if the heating airflow is directed towards the die-sided sheet, thicker necks can be produced since the die-sided sheet exerts a minor restraining effect during the offsetting phase. Besides these advantages, they remarked that the main drawback in the adoption of preheating on heat treatable alloys, other than increasing the complexity of the machines also resulting in higher costs, could be represented by decreasing the local hardness of the material because of increase in grain and precipitates dimensions.

The ultrasonic assisted clinching is another way to reduce the forming force required to clinch the materials and to apply the process for the high-strength and hard to form materials. The ultrasonic vibration can induce softening effect to metals. The ultrasonic softening effect is affected by not only the ultrasonic vibration amplitude but also the vibration frequency. The mechanism of ultrasonic softening effect lies in the fact that the ultrasonic vibration acts like high frequency impacting to the samples, refines the grain size in the sample, and leads to localized plastic deformation, which causes an unload phenomenon [65]. When the clinching process is superimposed by an ultrasonic oscillation, the uniform motion of the punch is overlayed with a high-frequency vibration. The punch oscillates with a certain frequency and amplitude during down-stroke and up-stroke. Superimposing a clinching process with ultrasonic excitation induces higher temperatures in the sheets. Thermo-mechanical tests show a correlation between the increased temperatures and the reduced forming force [66]. It should be mentioned that the residual effect caused by ultrasonic vibration is quite material sensitive. For example, residual hardening occurs for aluminum and residual softening for titanium. The residual yield stress and strain hardening rate is also sensitive to the vibration amplitude, frequency, as well as the vibration duration [65]. Since in the

clinching the joint is a part of sheet metal, the strain hardening rate and residual yield stress at the joining zone are such important issues to be considered to achieve a high-strength joint. Mizushima et al. [67] applied ultrasonic vibrations during a clinching process for aluminum sheets in two types of ultrasonic vibration modes: the maximum-displacement–amplitude mode and the maximum-stress–amplitude mode. The application of ultrasonic vibrations in the maximum-displacement–amplitude mode improved the joint strength slightly; however, the amplitude of the applied ultrasonic vibrations was restricted because of crack generation. On the other hand, the application of ultrasonic vibrations in the maximum-stress–amplitude mode generated a vortex flow, and this vortex flow led to a stirring effect. Because of this stirring effect, the joint interfaces vanished, thereby; leading to the metallic adhesion and 60% improvement in the joint strength was obtained. This stirring effect promises to produce more advanced joining methods and grain refinement methods.

Laser-assisted clinching is the most complex heat-assisted clinching technique and probably, the most expensive one. Utilizing a laser beam to heat up the workpieces in clinching process was first patented by Beyer et al. [68] and was applied to clinch middle strength steels. With this new method, the overlap section is heated locally by a laser during the clinching process. As long as the heating is confined to the joint area, the properties of the material away from the joint should be unchanged by the joining process [69]. Reich et al. [70] aimed to apply the process for HSS 22MnB5. Figure 19 shows the cross-sectional image of laser-assisted clinched joint of 1.3-mm thick 22MnB5 (as the punch-sided sheet) and 1.5-mm thick HC500LA (as the die-sided sheet). Reich et al. thermomechanically analyzed the deformation behavior of 22MnB5 steel under laser-assisted clinching process. They found that the flow stress of the 22MnB5 decreases from

about 1400 MPA at 300 °C to about 200 MPa at 650 °C, thus preheating using a laser beam significantly facilitates the forming process. Therefore, the 22MnB5 martensitic steel could be clinched for the very first time by laser assistance. The authors also determined the phase transformations during short time heating using calorimetry and dilatometry and obtained good agreement between the numerical and experimental results.

Chen et al. [71] proposed an innovative hybrid technology combining the hot stamping and clinching processes to clinch UHSS. The mechanical clinching of UHSS sheets is difficult because UHSS have low ductility so that fractures can occur in the joint area. To avoid this defect and improve the joint strength for the clinching of UHSS, hot stamping technology is used for the clinching process. Chen et al. [71] improved the joint strength of mechanical clinching by using hot stamping technology. The results show that the interlock value is 15% greater than the value when there is no heating process. The neck thickness is 5% less than the value for cold stamping clinching. The static strength of the joined sheets is 27% greater than that for cold stamping clinching. The preheating process also increases the ability of the material to flow. The stamping load decreases by 77%, compared to the cold clinching process. Compared to traditional cold clinching, the number of production processes and the cycle time are increased, and the equipment is more costly. Most of the sheet parts that are to be connected are also large and complex, so they cannot be sent to a furnace for the heating process. Therefore, the traditional hot stamping process is unrealistic to combine the clinching process to joint general sheets. Thus Chen and Cai [72] developed a new tool to complete this task. They integrated a forming system, a heating system, and a cooling system and designed a hot stamping clinching tool in a single setup. They replaced the traditional heating furnace by resistance heating technology to achieve in-die heating. The hot stamping clinching tool is illustrated in Fig. 20, and its operational sequence is controlled by a PLC system. The initial position is that the upper setting is fixed on a moving bed, and the lower setting is fastened on a fixed bed. During the operating sequence is, the upper setting moves down but stops moving as soon as the electrodes clamp the sheets. The power for the heating system is then turned on to enable resistance heating until the sheet temperature in the central region reaches 900 °C. At this moment, the upper setting continues to move down. When the blank holder touches the plate, the forming and quenching process is starting. The upper dies then remains stationary for a few seconds, until the temperature of the sheets cools to room temperature. Finally, the upper setting is moved up to the original position and the process finishes. The material flows better at high temperatures, and a promising tensile strength was obtained for the joint samples. The tensile strength at the processing zone is increased up to about 2500 MPa that is a considerable value
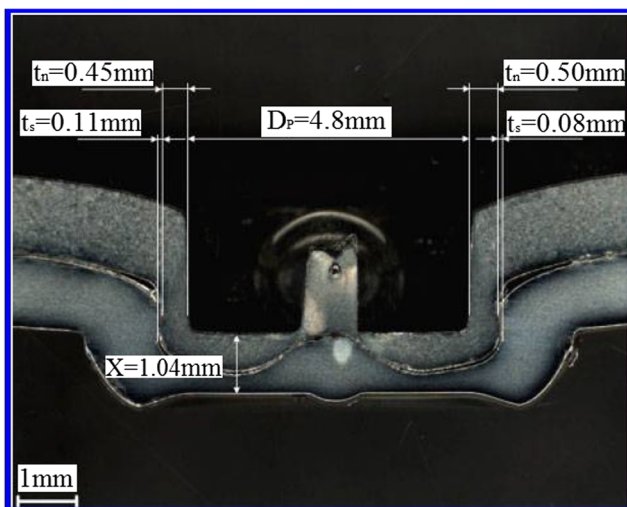


**Fig. 19** Cross-section of laser-assisted clinching joint ($t_n$: neck thickness, $t_s$: undercut, DP = punch diameter, $X$: thickness of the clinched button)
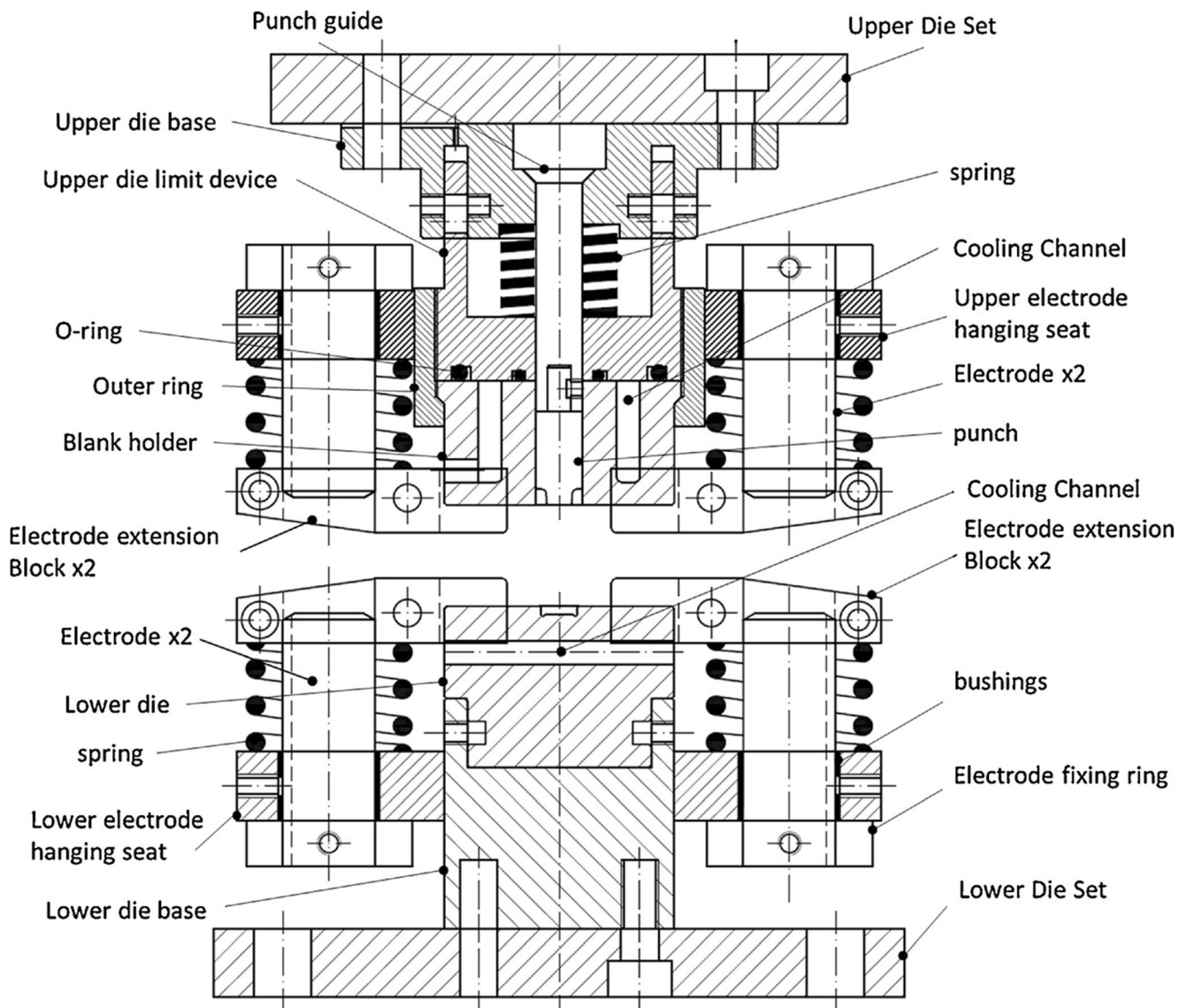
**Fig. 20** Schematic representation of the hot stamping clinching toolset [72]

compared to the tensile strength of the base material (665 MPa). In this process, the cooling rate is a critical factor in the final microstructure of the processed material. Thus, it is essential to control the cooling rate carefully to get better joint characteristics.

Although the heat-assisted clinching methods allowed to improve the material formability, they introduce further concerns including efficiency of energy consumption (convective heating), difficulty to integrate the system directly on the clinching press (flame heating), production of thermal distortions (as expected by flame heating), relatively high cost of the heating system (laser and induction systems), and safety issues for the operator (laser-assisted clinching) [73]. Thus, a more effective way to heat up the workpieces is to use a rotational tool. The adoption of the rotating tool enables to significantly increase the aluminum temperature (up to

300 °C) that comes with higher formability [74]. The adoption of the rotating tool enables to achieve sound joints without cracks at the necking zone, and the great increase in the material formability enables using very sharp tools (with a fillet radius up to 0 mm) that comes with the higher material flow and consequently larger undercuts. Another advantage of friction-assisted clinching (FAC) is to reduce the joining force significantly. Lambiase and Paoletti [74] joined 2.0-mm thick AA6061 and CFRP sheets with a joining force of almost 300 N that is decidedly smaller as compared to that usually involved in conventional clinching that typically ranges between 10 and 20 kN.

FAC is a promising technique to manufacture hybrid metal/polymer joints. In the FAC of metallic to polymeric parts, the heat is conducted towards the metal-polymer interface. As a result, physical, chemical, and either mechanical joining can

be achieved between the substrates depending on the chemical affinity and roughness of the materials. In this case, the polymer exceeds the glass transition temperature ($T_g$) and softens, enabling the formation of the joint with the metal part [75]. The mechanical joining mechanism created in this case leads to the friction-assisted clinched joints, while the process is called friction-assisted joining (FAJ) when the physical and chemical bonds are responsible for the joining mechanism. The joint mechanism and morphology are different in FAC and FAJ. A similar process to the FAC utilizing a rotational tool to clinch two metallic sheets by metallurgical bonds is called friction stir clinching (FSC) and will be covered in part B of this review study. Table 3 provides a summarized representation of clinching process variants and the problems they enabled to overcome.

## 3.4 Joint strength and optimizations

The strength of a joint can be studied from two aspects: static strength and dynamic strength. Clinching is a spot joint, and thus, its strength usually is compared to other spot joining techniques, such as SPR (see Sect. 4) and RSW. It is crucial to avoid the fractured zones around the clinching zone, because these fractures, however, to be small, would decrease the static and dynamic strength of the joint drastically [29]. Mota and Costa [76] compared the strength of the clinched joints and spot welds and obtained that the strength of the clinched joints is 50–70% weaker than the spot welding. Mucha [77] investigated the effect of sheet thickness on the mechanical behavior of the clinched joints for automotive applications. They stated that a considerable increase in the joint strength can be achieved when the thicker sheet is placed on the punch side and the thinner one at the die side. They also find that by increasing the clinched zone diameter or increasing the number of clinched zones, the joint strength can be increased considerably. Zajkani and Salamati [34] also achieved a considerable increase in joint strength by increasing the thickness of the workpieces. The reason is that at thinner workpieces, the neck thickness becomes very small that negatively influences the joint strength. The mechanical behavior of the clinched joints and hybrid adhesive-clinching joints is investigated by He et al. [78]. Using the adhesive layer between two sheets would increase the shear strength and energy absorption of the clinched joints. However, the increase in shear strength is not considerable (only 2%), but the energy absorption had been increased by 32%, which is an outstanding value.

Tensile, shear, and fatigue tests were carried out on the clinched joints by Carboni et al. [18]. The location of crack formation in the fatigue test of steel sheets joined by the clinching corresponds to that at the concentration of stress calculated from FE simulation. The fatigue strength is strongly dependent on the stress distribution during repeated loading of

the joint. It was proved that the fatigue limit is 50% of the ultimate strength: a value significantly higher than that of spot welding.

In general, three failure modes can be observed when a clinched joint is loaded. Figure 21 shows two of them. In mode A, there is insufficient material in the necking zone, which means less neck thickness and leads to failure in the neck. On the other hand, in the mode B, the sheets are deformed and the joint subsequently open. Typically, insufficient deformation leads to minor interlocking of the sheets and then lower undercut which results in this failure mode. Finally, the third failure mode is a combination of modes A and B. As a general rule, larger neck thickness and undercut value indicated in Fig. 6 means the clinched joint can bear greater tensile strength and shear force [42].

Damage criterion and crack evolution during clinching of lower ductility materials were studied numerically. Lambiase and Di Ilio [79] concluded from their simulation and experiments that circumferential cracks might be produced during the offsetting phase on both the upper and lower sheets. These may completely shear the punch-sided sheet as a result of in-plane tensile stress. During the subsequent steps including upsetting and flow pressing, radial cracks can be produced as a result of high hoop stress developing on both the sheets.

Regarding the absence of certain standards for the clinching process [80] and the fact that the joint strength and mechanical properties strongly depends on the process parameters, thus process optimization and increasing the joint quality by different analytical, numerical, and experimental approaches as well as various methods for design of experiments (DoEs), such as Taguchi method is of particular importance. Mucha [30] numerically investigated the effect of geometrical features of the clinching tools on the joint formation. They found that the die impression geometry, especially the groove, significantly influences the lock shape and parameters. Lambiase [25] investigated the effect of geometrical features of the clinching tools on the strength and mechanical properties of clinched joints made by extensible dies. The undercut is increased by reducing the extensible die diameter and by using tools with sharper corner radii, by increasing the punch diameter or by increasing the die depth, and the neck thickness increases with a more considerable punch and die, smoother corner radii, and shallow dies. Roux and Bouchard [81] conducted an FE simulation considering ductile damage theory for the real behavior to optimize the process conditions [81]. The optimized parameters induced 13.5% increase in the tensile strength and 46.5% growth in shear strength of the clinched structure. Wang et al. [82] listed the eight geometrical parameters as the most critical parameters influencing the joint characteristics. These parameters are shown in Fig. 22 and are including: punch face draft angle (A), die cavity face draft angle (B), width of die cavity groove (C), hump of the die cavity side (D), punch radius (E), die anvil corner radius (F),

**Table 3** Clinching process variants

| Process variant | Schematic | Limitation(s) enabled to overcome |
|---|---|---|
| Hole-clinching |  | Overcomes the low formability of high strength materials by clinching the material into a pre-drilled hole |
| Electromagnetic clinching |  | Overcomes the low formability of materials by using high strain rate values, improvement in joint strength |
| Injection clinching |  | Polymer to metal hybrid clinching, overcomes the brittleness of polymeric material by direct curing the material during the process |
| Hydro clinching |  | Overcomes the low formability of materials by using a high pressure fluid |
| Die-less (flat) clinching |  | Overcomes the low formability of materials by increasing the hydrostatic pressure |
| Two-steps clinching |  | Lower button height overcomes the aesthetic related problems, increase in undercut and improvement in joint tensile and shear strength |
| ClinchRiveting |  | The existence of solid steel rivet increases the stiffness, strength, and destruction energy of the joint |

**Table 3** (continued)

| | | |
|---|---|---|
| Resistance spot clinching (RSC) |  | The hybridization of metallurgical bonds and form-fit connections results in a higher tensile and shear strength for the joints. |
| Hot stamping clinching |  | Better material flow due to the high temperatures, superior strength at the processing zone |
| Laser shock clinching |  | Suitable for ultra-thin metallic foils |
| Induction/convection assisted clinching |  | Overcomes the low formability of materials by pre-heating the material |
| Ultrasonic assisted clinching |  | Overcomes the low formability of materials by using ultrasonic vibrations to heat up the materials |
| Laser assisted clinching |  | Overcomes the low formability of materials by using a laser beam to heat up the materials |
| Friction assisted clinching |  | Overcomes the low formability of materials by using frictional work to heat up and plasticize the materials, considerably reduces the required joining force |

(a)                                        (b)
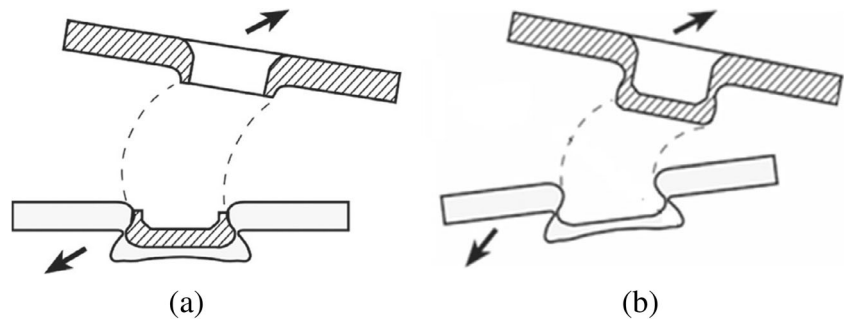
corner radius of the hump (G), and depth of die cavity (H). They stated that these eight parameters are more significant and sensitive for neck thickness, interlock forming, and tensile force, which should be introduced in modeling and optimization tasks.

Kaščák et al. [83] numerically investigated a three-layer clinching of steel sheets (DC06, DX53D, and H220PD). The 2D axisymmetric conditions were used to simulate the joining process, and the isotropic material model of joined sheets was applied. The comparative analysis of geometries showed that specific areas of mechanically clinched joints (such as the individual sheet thicknesses in bottom and neck area, the shape of the interlocking area, filling of the die groove by the bottom sheet) calculated by FEA and experimental tests are in very good agreement. Only minor differences were found in the case of the mechanically clinched joint of DX53D steel. The most considerable difference in the neck thickness was observed in the case of DC06 steel. The evolution and distribution of plastic strains in the deformed sheets were similar for all observed materials. The plastic strain was found to initiate in the contact zones between sheets and tools

or between the adjoining sheets and then to progress towards the thickness of individual sheets. The peak values of plastic strain were attained in the critical (neck) zone of mechanically clinched joints. This critical zone corresponded to the location with the largest thinning of the upper sheet. The development of reaction forces in the punch during the joining process coincided with the curve shape observed during joining of two sheets. The characteristic joint forming phases could be identified by the shape variation of the individual force reaction curves. The calculated and experimental values of force reactions differed only slightly. One more parameter investigated in this study was the material flow during drawing, compression and interlocking phases of joining. The so-called backward extrusion phenomenon which occurs when the die cavity is wholly filled [46] was observed in the case of DX53D steel sheets, which could be attributed to the increased thickness of joined sheets, in contrast to the other materials under study. This state causes the backward material flow of the upper and middle sheets in the opposite direction to the die cavity. At the interlocking phase of joining, thicker sheets filled the volume of the die cavity before reaching the preset punch stroke. At this point, the middle and upper sheets tended to flow out of the die cavity. This deficiency can be bypassed by the tool geometry modification. Since the upper sheet undergoes large plastic deformation and excessive thinning during the joining process, the upper sheet model should be replaced with a more advanced one capable of simulating the material separation or cracking.

During the simulation of the metal forming processes using the FEM, significant distortion of the elements in the mesh may appear especially when a severe plastic deformation occurs. To compute an accurate simulation, one wishes to ensure a sufficient geometrical quality to the mesh by use of remeshing techniques. Thus, an FE simulation of the clinching process with automatic remeshing was conducted by Hamel et al. [23]. By the FE simulation, the influence of changes in the clinching die and punch geometry on the material flow and consequent neck thickness and undercut of clinched joints was investigated by De Paula et al. [84]. It is shown that introduction of protrusions at the punch corner, associated with a slightly conical die and a reduced groove depth, as well as
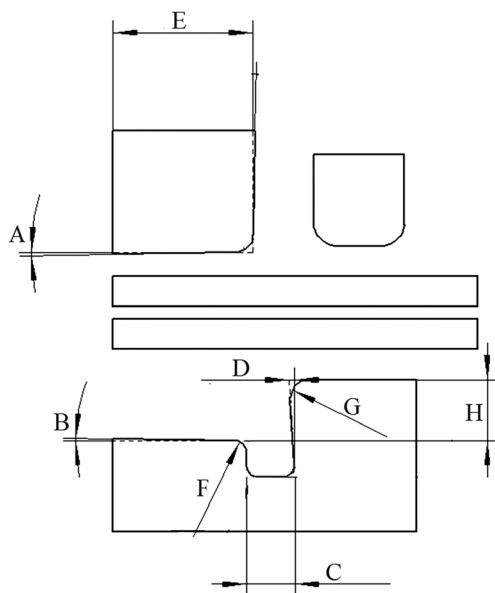


Fig. 22 Schematic representation of the most important geometrical parameters in clinching [82]

with restrictions on the upward movement of the sheets, led to enhanced undercuts of a clinched joint.

The effect of die cavity geometrical parameters including hole depth and cavity diameter on the metal flow of the sheets was investigated by Abe et al. [85]. Decreasing the die depth relieves the concentration of deformation around the punch corner, resulting prevention of fracture of the punch-sided sheet, an excessive reduction in die depth leads to insufficient interlock. In case of die diameter, the amount of interlocking is inadequate for excessively small and large diameters. Thus, an optimum value should be considered.

Taguchi's DoEs are reliable tool to investigate the effect of parameters and selecting the optimum setting especially when a large number of parameters exists. This approach was used by Oudjene and Ben-Ayed [80] to determine the impact of tools geometrical parameters on the joint quality. By optimization of the geometrical parameters, the tensile strength of clinched joints of AA5754 was increased by 18%. In another work, a further 10% increase was achieved for maximum tensile strength by using the response surface methodology with moving least-square approximation [86]. Lambiase and Di Ilio [16] developed a flexible tool for the optimization of the tool selection, with extensible dies. FE simulations assessed the effect of the process parameters on the joint strength. An artificial neural network (ANN) was developed to predict the critical features of the clinched joints under different processing conditions.

Lee et al. [87] developed a design method of clinching tools with analytical models of joint strength for neck fracture mode and button separation mode. The analytical models of joint strength are defined as the geometrical functions of neck thickness and undercut; these geometry functions were determined by using the Box-Behnken method [88]. Dean et al. [89] remarked the necessity of the utilization of a finite strain elastoplastic material model for the FE analysis of hybrid metal-composite clinching joints. They developed an invariant-based transversely isotropic elastoplastic material model for short fiber reinforced plastics and implemented the model in clinching process simulation. The adaption of the proposed model and considering re-meshing techniques led to more realistic numerical predictions. A tensorial-based transversely-orthotropic material model was used to simulate the clinching process of a metallic sheet and short GFRP. The formulation accommodates the anisotropy of the material by using a structural-tensor representation. Two main approaches were used for performing the homogenization of the structural tensors: first, an averaged fiber distribution over the whole sheet thickness and second, a domain-based procedure that takes into consideration the corresponding fiber orientation of each of the layers that compose the specimen. It is proved that the second methodology provides a closer representation.

# 4 Self-pierce riveting
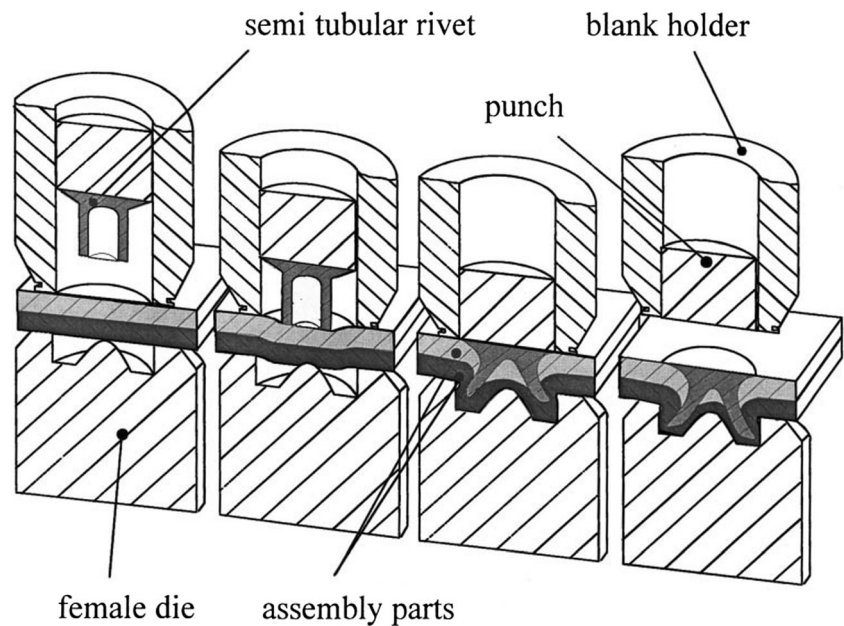
## 4.1 Processing

SPR is another spot joining by a forming technique, which creates a form-fit joint. The main difference between SPR and clinching is that SPR uses additional joining elements, which are self-piercing rivets. SPR is essentially a cold forming process in which a semi-tubular rivet, pressed by a plunger, pierces through the thickness of the upper sheet, and flares in the bottom sheet under the guidance of a suitable die, forming a mechanical interlock between the two sheets. The SPR joint can be set flush on one side if a countersunk rivet is used. Oval head rivets can also be used if non-flush on both sides is acceptable [90]. Since the SPR does not require a pre-drilled hole unlike the conventional riveting, the joining speed is the same level as that of the RSW, and the equipment is similar. In the SPR, the difference between the melting points of dissimilar sheet metals is not a problem because of plastic joining [91].

As the process relies on a mechanical interlock rather than fusion, it can be used on similar as well as a wide range of dissimilar materials. Examples are zinc-coated, organic-coated, or pre-painted steels, a combination of steel to aluminum alloys and some plastic to metals [92]. A fundamental advantage of SPR is that various materials of different-coated may join, from painted and galvanized sheet metal to plastic ones [93]. The process can be applied to form multi-layer joints that may also include interlayer sealants or adhesives. In comparison to spot welding, the process is environmentally friendly due to the low energy requirement, little noise, and absence of particulate and fume emissions, and it does not introduce heat into the components [94]. It maintains or improves the joint quality without many of the RSW risks, such as expensive maintenance, toxic fumes, and sparks [95].

The two distinct phases of piercing and flaring in SPR can be done through the following four steps: (1) clamping: the rivet is forced by a low punch perpendicularly to the top sheet surface and presses the sheets against the die; (2) piercing: the punch pushes the rivet through the top sheet and into the bottom sheet; (3) flaring: the material of the lower sheet flows into the die, and the rivet shank is flared, thus forming a mechanical interlock between the substrates; and (4) releasing: the punch stops and retracts when it reaches the predetermined value of force or stroke [92]. The process is schematically illustrated in Fig. 23. SPR involves extensive and highly localized plastic deformation that can lead to cracking, especially in the materials used as the bottom sheet in the design of the joint [97].

SPR was initially designed for the construction industry and was subsequently used in domestic products including machines and ventilation systems [98]. Furthermore, SPR joints gain a significant share in the thin-walled structure

**Fig. 23** Schematics of the SPR process [96]



assembly process in the metal industry, especially in the automotive industry [99]. Audi A8, the first generation of the aluminum space-frame vehicle, first adopted this joining technique in its assembly followed by other automotive companies including Mackenzie, Jaguar, and Volvo [98].

### 4.2 Materials

As mentioned above, SPR applies to join a broad range of similar and dissimilar materials. The joinability of aluminum alloy and mild steel sheets using a self-piercing rivet is evaluated by Abe et al. [100]. The possibility of joining aluminum alloy blanks and fiberglass composite panels by SPR operation was investigated by Fratini and Ruisi [101]. Experimental tests were carried out on different thicknesses of joining partners and the influence of the most relevant process parameters for each of which considered case studies were obtained. The joining of sandwich panels of the polymeric core and aluminum alloy skin was investigated [93] that are used widely in the automotive, aerospace and railway industry. Durandet et al. [97] studied the laser-assisted SPR of AZ31 magnesium alloy strips. The effect of laser absorption and heat transfer between the top and bottom sheets was investigated using a combination of joining experiments, thermal modeling, metallurgical analysis, and mechanical testing.

Coatings are used to prevent corrosion in hybrid structures made of dissimilar materials. Han and Chrysanthou [90] studied the effect of coatings on the quality, and mechanical behavior of SPR joints in aluminum alloy sheets joined with high-strength low alloy steels (HSLA), which have been coated with E-coat or Zn-plate. It is shown that the use of coatings and type of the coatings on the sheets affected the quality and

strength of SPR joints. The extent of this effect differed significantly according to the kind of coating used.

The SPR process currently utilizes HSS rivets. The combination of steel rivets with an aluminum car body not only makes recycling time to consume and is costly but also leads to galvanic corrosion. Galvanic corrosion occurs when dissimilar, conductive materials are joined, and the ingress of water forms an electrolytic cell. In this type of corrosion, the material is uniformly corroded as the anodic and cathodic regions move and reverse from time to time [92]. To prevent the corrosion and overcome recycling challenges, Hoang et al. [102] replaced steel rivets with aluminum ones. Two sheets of aluminum alloy AA6060 with a 2.0-mm thickness which were selected at three different temperatures were joined by the rivets made of three different alloys. The results are illustrated in Fig. 24. It can be seen from the Fig. 24 that the rivet material did not affect the initial stiffness of the mechanical force-
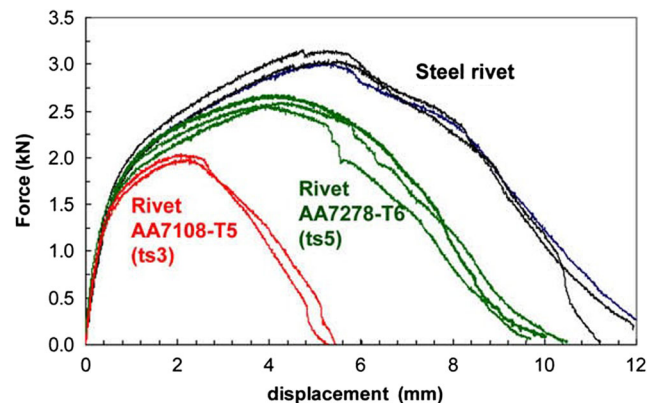


**Fig. 24** Comparison of load-displacement curves for aluminum and steel rivets [102]

displacement curves, but only the maximum force as well as the movement at the maximum loading.

SPR can join more than two layers of sheet materials. The cross-section of a multi-layer SPR joint is indicated in Fig. 25. Han et al. [94] examined the effect of different specimen configurations on the mechanical response and loading characteristics of SPR multi-layer joints. Abe et al. [104] investigated the joinability of the SPR process of three HSS and aluminum alloy sheets. Upper and middle sheets were HSS, and the lower sheet was aluminum. The effect of the tensile strength of the steel sheets on the amount of interlock obtained from the experiments is illustrated in Fig. 26.

Meschut et al. [105] investigated the damage to the carbon fiber composites in a hybrid composite/metal joint manufactured by SPR. They observed surface cracks which are assumed to be caused by tangential strains arising from the piercing with the punch. This press fit results in a strong elastic stretch of the fiber composite in the hole edge region in the tangential direction. Due to the low ultimate elongation of the carbon fibers, radial fibers breaks occur in areas where the fibers are arranged tangentially to the hole, while the areas with a radial orientation of the fibers to the hole remain undamaged. This effect can be explained by the punching behavior of FRPs. Since in SPR the composite material is always arranged as the top layer, the material is shear-cut on the upper side directly at the sharp cutting edge of the rivet. However, on the underside, a trough is formed in the metallic joining partner, so that a local biaxial bending of the composite occurs. Since there are no defined cutting conditions, the material is not cut but breaks off. In such areas, the composite is severely damaged, and further delamination can be induced at these points. Thus SPR may easily cause damage such as delamination at the points of piercing on the CFRP, so some modifications were considered in the process by Ueda et al. [106] to join two CFRP laminates. Two flat washers were used on the joining zone, and the pressure was applied to the washers using two supporting dies to prevent the dragging and subsequent delamination of the laminates. The modified SPR joints showed greater joint stiffness and strength than bolted joints. The maximum load was retained for a period for the revised SPR joint although the load was suddenly dropped for the bolted joint. Di Franco et al. [107] also used SPR to join AA2024-T6 and a thermosetting CFRP laminate. They used
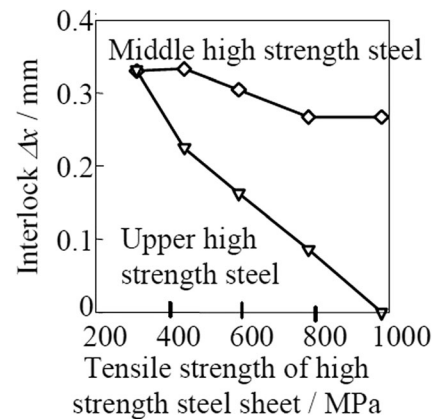


**Fig. 26** Effect of tensile strength of sheet on the amount of interlock obtained from experiments [104]

an epoxy resin adhesive same type as the matrix of the CFRP laminate and manufactured a hybrid adhesive-SPR joint.

## 4.3 Joint strength and optimizations

Since SPR is a spot joining technique, its static and dynamic behavior usually is compared with other spot joining methods, such as clinching, RSW, and spot friction joining (SFJ). Briskham et al. [108] conducted a comparative study on the static response of SPR, RSW, and SFJ of aluminum alloy sheets. SPR showed the best performance on both the T-peel tensile test and lap shear tensile test while SFJ showed the worst performance in both cases (Figs. 27 and 28). Han et al. [109] made a back-to-back comparison on the aluminum alloy sheets joined by SPR and RSW. Static behavior of different joint samples by various thicknesses under different loading conditions was compared. It is stated that in small layer thicknesses, the static strength of RSW joints is more than SPR joints, but by increasing the sheet thickness, the strength of SPR joints increases and finally reaches a value more than RSW. For T-peel joints, the strength of SPR joints is more than RSW for all sheet thicknesses. Lennon et al. [110] compared initial displacement and plastic shear behavior of joints made by four different techniques: rectangular mechanical clinching, SPR, pop-riveting, and screw connections, for two layers of galvanized mild steels of 1.0-, 1.2-, 1.6-, and 2.0-mm thickness. SPR showed maximum static strength in all cases. Lee et al. [87] obtained the load-displacement curve of impact test for SPR and clinching. The resulted curves for the two techniques were quite close to each other (Fig. 29). Mori et al. [111] compared the static behaviors of aluminum alloy sheets joined by mechanical clinching, SPR, and RSW. The results are illustrated in Fig. 30; it can be seen that when using SPR, failure occurs under large plastic deformation. Mucha and Witkowski [112] compared the static strength of riveted joints using different rivets including SPR. They found
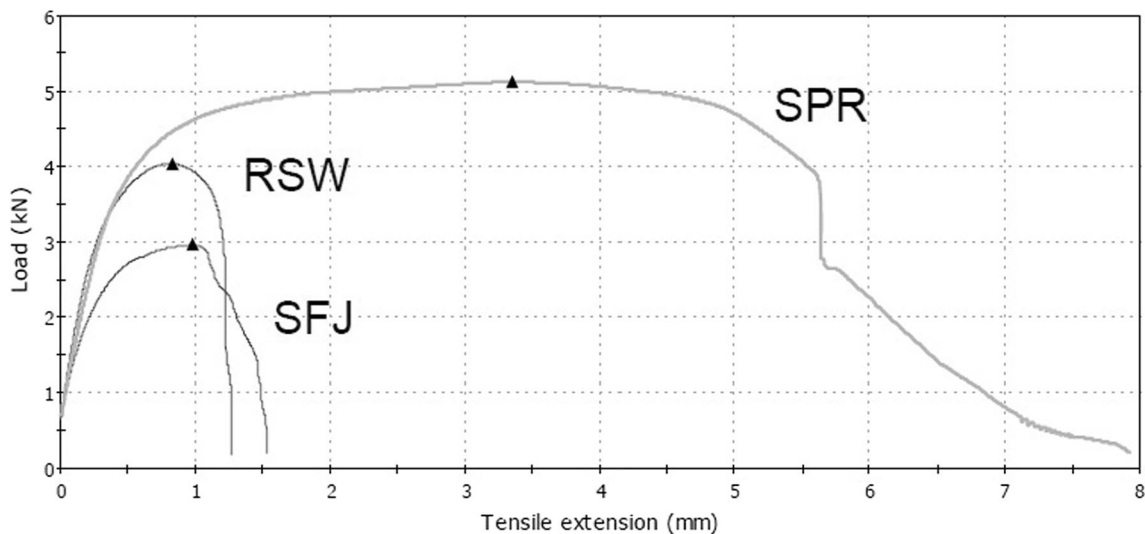


**Fig. 25** Cross-sectional shape of the rivet and workpiece plates in multi-layer SPR joining [103]

**Fig. 27** Typical lap-shear tensile test results for SPR, RSW, and SFJ in joining AA5754 of 2.0-mm thickness [108]

that for joints with conventional rivets, the same level joint strength is reached, regardless of the joint sheet materials. The fastener strength corresponds to the maximum load-bearing capacity of the joints. While for the SPR joints, the joint strength depends on the mechanical properties of the joined sheets. It is highest for steel sheets and lowest for the aluminum alloy sheets. It should be noted that the shear strength of SPRed joints was obtained considerably higher than the tensile strength (almost three times higher). Thus, the SPRed joints like the clinched joints are more suitable for applications with shear or tensile-shear loading. Joining force also plays an essential role on the joint strength. Mucha [113] obtained a 36% increase in maximum shearing strength by increasing the joining force from 14 to 32 kN (by 128%). However, it should be noted that this affects the tool durability adversely and increases the residual stress in the rivet. Too high forming force may result in serious residual stress values in the rivet,

especially around the rivet head. The rivet head becomes a potential fracture location when loading the joint. Too low forming force results in disappointing notch filling and clinching the rivet in the joined sheet metal. The effect of lower pressing force results in smaller material dent around the rivet and smaller joint strength [114].

Dynamic and fatigue behavior of SPR joints are of high importance, and several studies are conducted for this purpose. It is found that the fatigue strength of the SPR joints is considerably superior to that of the RSW [115] and the fatigue strength of mechanical clinching and RSW are at same level and substantially lower than SPR [111]. Li and Fatemi [116] studied and compared the fatigue behavior of T-peel joints made by pop rivet and SPR. The effect of the joining method, plate thickness combination, and geometry deformation resulting in a monotonic deformation and fatigue behaviors was studied. Fu and Mallick [117] examined the fatigue
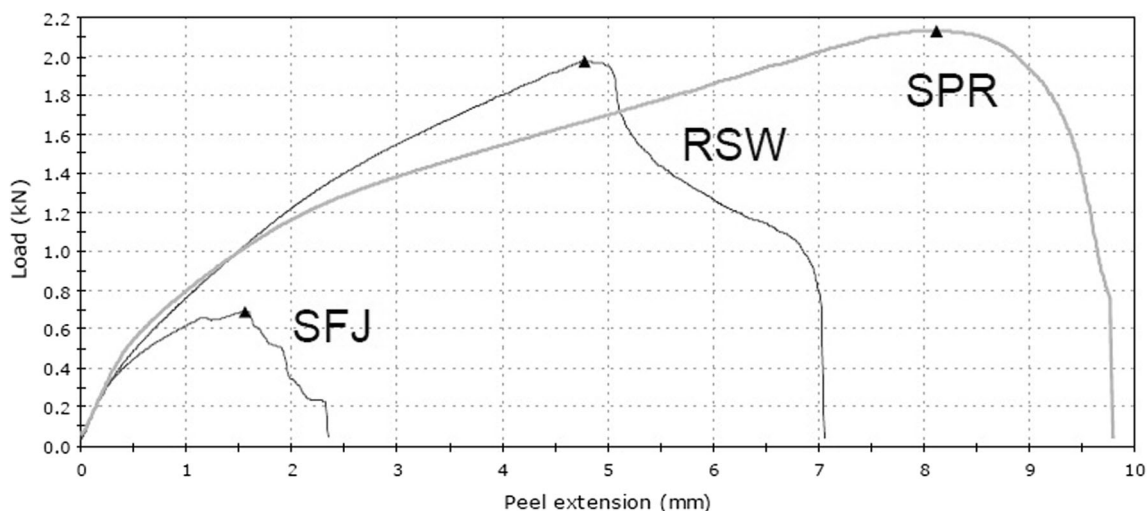


**Fig. 28** Typical T-peel tensile test results for SPR, RSW, and SFJ in joining AA5754 of 2.0-mm thickness [108]
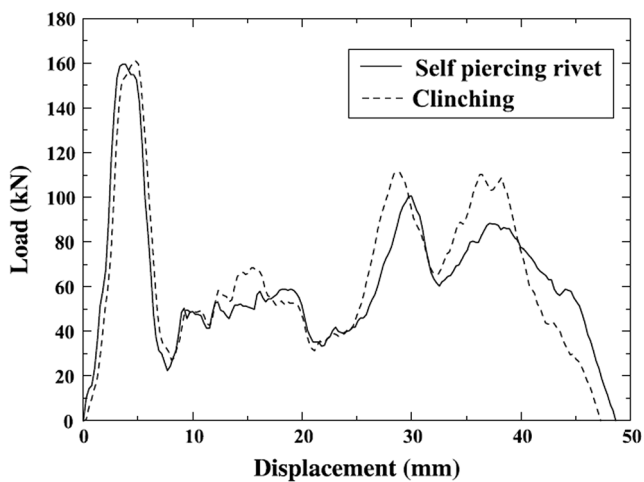
**Fig. 29** Load-displacement curves of impact test for clinching and SPR [87]

behavior of SPR joints in aluminum alloy AA6111-T4. They found that fatigue pre-cycling up to 75% of the fatigue life tends to deteriorate the joint strength gradually, but above 90% of the fatigue life there is a sudden decrease in joint strength.

Fretting wear damage is inevitable when SPR joints are subjected to cyclic loading [118]. Fretting wear at the interface between the joined sheets takes place for two-body fretting and three-body fretting. The fretting behavior between two aluminum alloy sheets joined by SPR was studied, and the influence of lubricant and polytetrafluoroethylene (PTFE) insert between metallic layers on the fretting behavior was investigated [98]. The presence of an oil lubricant could delay the onset of fretting damage on the alloy surface leading to extended fatigue life, and the application of a PTFE insert at the interface between the riveted sheets eliminated fretting at the lower fatigue loads. The effect of heat treatment on fatigue performances of SPR joints in titanium, aluminum, and copper alloys was investigated [119]. Relief annealing significantly reduced the fatigue strength of Ti/Ti SPRed joints in the long life range but enhanced it in the short-life range.

The crashworthiness of second hat-shaped section members made by SPR and adhesive bonding was evaluated by
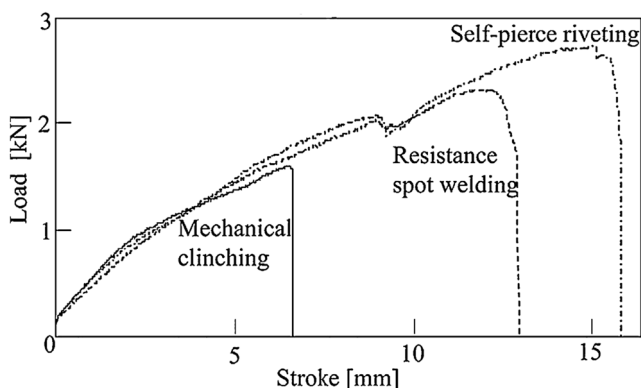


**Fig. 30** Static behavior of joints made by clinching, SPR, and RSW [111]

Lee et al. [120]. They found that however, the mean crush load and maximum crush load of the SPR joined structure were lower than that of the spot-welded structure, but SPR joining method could use in a vehicle composed of dissimilar materials as a substitute for spot welding. Porcaro et al. [121] present a study on identification and modeling of SPR connections in aluminum alloy. The behavior of a single-rivet specimen under combined pull-out and shear static loading conditions was investigated. All the pull-out tests showed the same failure mode, i.e., bending of the sheets and pull-out of the rivet from the bottom plate.

Pressing and stamping are certain processes in the fabrication of a body composed of sheet materials, resulting in additional straining, gauge thinning and work hardening of the sheet materials. The effect of sheet pre-straining on the quality and the mechanical behavior of the SPRed aluminum alloy joints was investigated [122]. It was found that increasing the pre-straining levels led to SPR joint of higher lap-shear strength and fatigue life. The interlocking condition is the most critical parameter in characterizing the quality and mechanical performance of the SPR connections. This feature is usually measured by destructive testing which is time and cost consuming. Johnson et al. [123] developed an online monitoring method of the SPR process to provide non-destructive testing of the mechanical interlock which prevents material and time wastage.

The performance of cold-formed steel (CFS) shear walls with SPR under monotonic and cyclic loading was studied by Xie et al. [124]. The effects of loading methods, rivet spacing at the sheet edges, rivet number at CFS framed joints, axial compression ratio, and the types of sheathing on mechanical properties and failure modes were analyzed. Based on the results, the primary failure modes for a SPRed CFS wall were listed as pull-over of the sheet from rivet head, sheet buckling, end stud buckling, and track tearing. Rivet spacing at the sheet edges was a key influencing factor on failure mode of shear walls. With the increase of rivet spacing, the damage level of pull-over of the sheet from rivet head was intensified, but the failure level of sheet buckling, end stud buckling, and track tearing reduced. In the design of the shear wall, sheet buckling and end stud distortional buckling should be considered in particular when rivet spacing of sheet edges was less than 100 mm. Pull-over of the sheet from rivet head should be considered especially when rivet spacing greater than 100 mm. Shear strength and ultimate deformation for CFS shear walls with SPR decrease linearly with the increase of rivet spacing. They concluded that using double rivet in CFS framing joints cannot only dramatically enhance stiffness and deformability but also effectively reduce deformation of the wall and enhance the frame effect in the process of installation for walls. The increase of axial compression ratio can efficiently increase initial stiffness and ductility of shear walls under monotonic loading. Finally, comparing to traditional

self-drilling screw, CFS shear walls with SPR have improved in strength and stiffness, but reduced deformability and ductility.

In the SPR process, the complex joint geometry and its three-dimensional nature combine to increase the difficulty of obtaining an overall system of governing equations for predicting the properties of joints [125]. Thus, FE simulation gains an important share on the optimization of the process. An SPR process for joining UHSS and aluminum alloy sheets was developed, and to attain better joining quality, the die shape was optimized using the FE simulation without changing mechanical properties of the rivet [126]. Authors reported that the joint strength is greatly influenced by not only the strength of the sheets and rivets but also by the ratio of the thickness of the lower sheet to the total thickness. The effects of flow stress of the HSS sheets and the combination of the sheets on the joinability were investigated by FE simulation and an experiment by Abe et al. [91]. They found that as the tensile strength of the HSS sheet increases, the interlock for the high upper strength steel sheet increases due to the increase in flaring during driving through the upper sheet, whereas that for the lower HSS sheet decreases. Furthermore, Abe et al. [100] stated that when joining aluminum to mild steel using SPR, due to the significant difference of flow stress between two workpieces, the joinability deteriorates and thus, the optimization of joining conditions is desirable. Thus a dynamic explicit FE method was used to optimize the process, and defects for the SPR process were categorized to obtain optimum joining conditions. To improve the joinability with the HSS sheets, Abe et al. [104] optimized the shape of the die by controlling the deforming behaviors of the sheets and rivet using the FE simulation. Mucha [127] numerically simulated the SPR process to evaluate the effect of different process conditions on the joint quality. It is proved that one of the significant factors affecting the finished joint form is the die impression geometry and proper selection of corresponding rivet material features, i.e., its yield point and strain hardening, enables a significant change of the sheet joining process and specific joint parameters. Porcaro et al. [128] studied how to perform numerical simulation of SPR joint using LS-Dyna, and a study was made to suggest the optimum values of process parameters like friction and adaptive interval.

Due to a combination of piercing and flaring, the SPR process requires large forces (30–100 kN), which can cause severe local distortion, called joint distortion. This joint (local) distortion can, in turn, transmit its stresses and strains to the whole structure and induce global distortions. Cai et al. [129] established math-based models to predict assembly dimensions for SPR applications. They remarked that the joint distortion due to SPR is about two or four times the magnitude of that for RSW, and the inclusion of SPR joint distortion is

needed for accurate global assembly predictions. Furthermore, since reducing the forming force of the SPR process is a particular challenge, the force characteristics of the SPR process were studied, and it was found that the maximum punching force decreased dramatically with the increase of the workpiece temperature. Even more, other information such as metal flow and details of die fill and distribution of strains in the material obtained from the simulation [130]. The behavior of the SPR connection under quasi-static loading conditions was investigated experimentally and numerically [131]. A 3D numerical model of different types of riveted connections subjected to various loading conditions was developed based on the numerical simulation of the riveting process. FE simulation of crash testing of SPR joints, peel specimen was conducted [132]. The simulations were performed with the FE software ABAQUS/explicit and involved dynamic inertia effect. The results show that the load-displacement curves are quite similar to the spot welded and SPR cases, except for the oscillating amplitudes as the SPR is larger. Since SPR is a rapid process both the highly localized plastic deformation and friction contacts generate adiabatic heating, thus, using the material data obtained by uniaxial tensile tests at room temperature leads to wrong predictions. Therefore, Carandente et al. [133] considered the effects of thermal softening and strain hardening to achieve a precise prediction of the SPR process. By these considerations, they obtained excellent agreement between numerical and experimental results.

## 4.4 Process variants

Friction self-pierce riveting (FSPR) is a variation of SPR introduced by Li et al. [134] during which the rivet is rotating while being punched into the workpiece. They found that the joints manufactured by FSPR have shear strength twice as much as that of an SPR joint of same materials. In fact, the combination of force-fit and solid state joining mechanisms improves the joint strength significantly. Ma et al. [135] optimized the FSPR process, they optimized the rivet from commercial SPR rivets regarding hardness and geometrical features, but due to the slow reduction of rotating speed at the end of the process, a considerable amount of cracks were observed in the joints. Livatyali et al. [136] used an especially designed machine which its high-speed rotating spindle can achieve a sudden stop motion within 0.3 s. This helps the residual spinning of the rivet as the punch starts to retract from the workpiece. Ma et al. [137] proposed an improved FSPR process, aiming at joining different multi-material stack-ups using the same equipment with just changing rivets, dies and process parameters. They used a pip die for low ductility materials. For stack-ups that need single-sided joining, a die with a large through hole is used. For stack-ups with lightweight material on top and HSS on the bottom, a flat die is used. They used

this new process for joining three typical stack-ups (including aluminum alloy to magnesium alloy, aluminum alloys of different gages that needs single-sided joining, and aluminum alloy to HSS) to validate its effectiveness on different dissimilar materials.

An SPR process using a fluid pressure was introduced by Neugebauer et al. [54]. This process is called hydro-self-pierce riveting. The forming fluid is used as a die replacement (Fig. 31). First, the hydroformed sheet (5) and the part to be attached (4) are brought into contact with the hydroforming tool (2) by the fluid (6). The punch (1) presses the spreading rivet (3) into the sheets. The high-pressure fluid (6) is preventing too sharp bending of the hydroformed sheet. To the axial movement of the punch, a wobble movement can be overlaid to decrease the necessary joining force and thus limit the necessary pressure of the fluid.

An SPR process using solid rivets is introduced by Mucha [138]. This technique is called solid self-pierce riveting (SSPR). Using the solid rivet in SPR technology allows achieving a flat and quite a smooth surface on one side of joint. In some cases, this improves the finished product's look. When making the joint (Fig. 32), the rivet acts as a cutting punch. The hole in the sheets joined is cut when the punch presses the rivet head (phases I, II, III). The scrap is expelled by the opening in the lower die. The used die has the edge around the opening, and its inner edge acts as the cutting edge. In phase IV, the joined sheets are pressed in a way that the bottom sheet material fills in the groove on the rivet perimeter. Finally, this locks the rivet, and the joint is made. The additional movement may be made by the bottom die or the clamping device with the punch. This technology enables the joining of various materials. These are not only metal sheets but also their combinations with cast alloys, the plastics, and various intermediate layers: gluing and sealing ones. This technology is used in the production of the thin-walled car body elements using materials of improved mechanical properties.

The solid rivets used for this process have grooves on the body. Mucha [113] states that while forming the joint with the solid rivet, there are some difficulties with filling in all the grooves with the joined sheet material. The number of grooves and their location in relation to the lower sheet are crucial factors for the filling amount. While selecting the number and layout of rivet grooves, the stress distribution in the rivet must be accounted for. The largest stress concentrator is a groove located at the rivet head base. Using three grooves enables moving the groove out of the rivet head base. Using a numerical analysis, they showed that moving the groove out of the rivet head base makes sense in order to improve the groove filling with the lower sheet material. Switching the tool movement order significantly affects the rivet's groove filling. It is possible to reduce the maximum axial stress in the rivet by changing the edge pressing method. However, this requires design changes of the tools and the press. Using the smaller edge height allows to fill the grooves and reduce the maximum axial stress in the rivet.

When joining materials with a significant difference between the mechanical properties (such as UHSS and aluminum) by SSPR, the high difference between the material strength and stiffness can result in the large (or excessive) deformations of the lower strength alloy. In fact, the high joining force required to punch the higher strength material results in an excessive material flow in the lower strength material. Figure 33 shows an example of this effect. Hybridization of adhesive bonding and SSPR cannot address this problem. The adhesive modifies the tribological system between the sheet layers. As the friction between the sheet surfaces is reduced, the sheets can easily slide on each other. Hahn et al. [139] introduced a hybrid adhesive/SSPR joining using an optimized SSPR toolset to address this challenge. They used a standard contour of the die emboss ring in combination with an additional outer reservoir ring. The contour of the outer ring prevents a free flow of material and thus reduces the deformation. On the other hand, the effect of "breathing" can be reduced and so inclusions of air can be minimized in the formation of the adhesive layer. Figure 34 shows the specimen joined by this optimized toolset.

Finally, a summary of SPR process variants and the limitations they enabled to overcome is provided in Table 4.



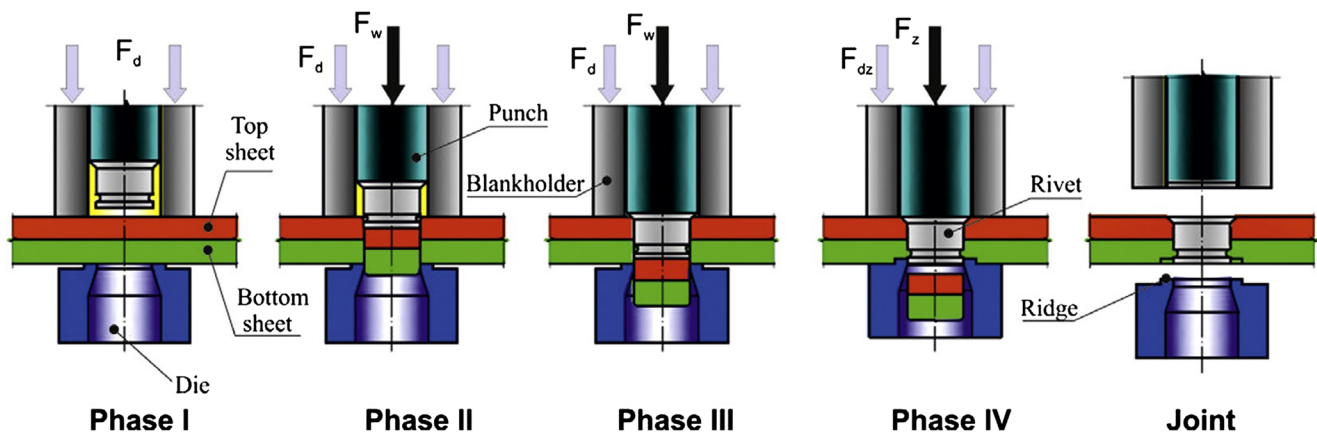Fig. 31 Schematics of the hydro-self-pierce riveting [54]
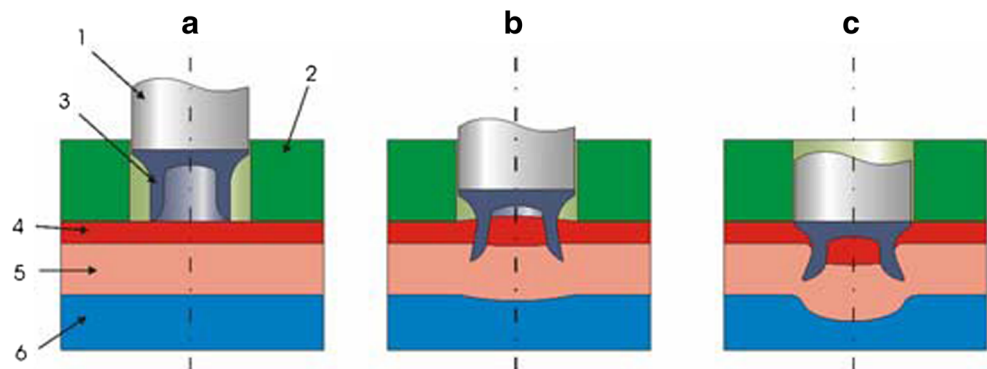
**Fig. 32** Process sequence of self-pierce riveting using a solid rivet [138]

In the end, the most important features of the different spot joining techniques including clinching, SPR and RSW are compared in Table 5.

## 5 Hemming

### 5.1 Processing

Clinching and SPR are only locally spotted, but if there is a need to connect mating parts in a large area, e.g., to achieve sealing, hemming should be considered [7]. Hemming is a method used to join two pieces of sheet metal by the plastic strain, which consists in bending the edge of one sheet, called the outer part, over the edge of another, called inner part [141]. Hemming is performed in two steps. In the first step so-called pre-hemming, the flange of the outer panel is bent down to an angle of approximately 45° to the outer surface, and in the second step, the flange of the outer part is bent down to the final position (Fig. 35). The advantage of hemming is that it gives a neat and a compact joint, while the disadvantage is that it is less strong than a welded joint [142]. Hemming is widely used in the automotive industry for example to connect the inner and outer panels of automobile doors, hood, or deck lids. It is also used to create a smooth edge on a sheet metal component by folding the edge of the sheet metal onto itself for appearance and safety considerations [143]. Furthermore, hemming can be used to increase the part stiffness [144].
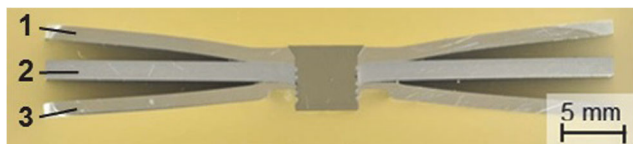
Regarding the geometry considerations, hemming can be categorized into different groups. These categories are listed in Table 6. Because hemming is the final stage of production operations, the defects introduced cannot be eliminated in subsequent operations and therefore the hemming quality significantly influences the overall quality of a product [145]. The most common hemming defects are shown in Fig. 36. Roll-in (creep) and roll-out (grow) are the inward and outward shift of the hem edge (Fig. 36a). Recoil is the out-of-plane displacement of the outer panel after final hemming (Fig. 36b), and warp is the indentation in the outside of the outer panel after final hemming (Fig. 36c) [146]. Recoil and warp are surface defects that generally appear after final hemming spring-back [145]. Wind is outward and localized waviness on the outer panel edge on the panel plane (Fig. 36d). Hem-out is a localized and exaggerated combination of recoil and grows, where the flange is subjected to excessive compression, exhibits instability, and bends in the opposite direction (Fig. 36e) Other defects such as wrinkling and splitting may cause failure of hemming (Fig. 36f). Also, spring-back is a problem in this process, such as all other sheet metal operations, and in the hemming, spring-back can lead to other defects such as recoil and warp [143]. Furthermore, fitting defects such as inappropriate clearance and the level mismatch can negatively influence the appearance considerations of the final product. The hemming defects are categorized in Table 7.

Livatyali and Larris [147] investigated the effects of contour radius, flange length, and final hemming force on the occurrence and elimination of final hem defects including roll-in, roll-out, warp, and coil. Livatyali et al. [141] studied
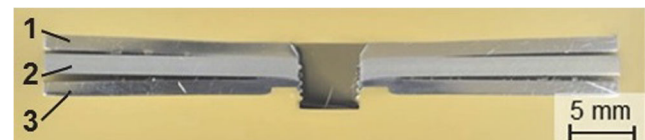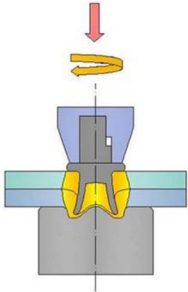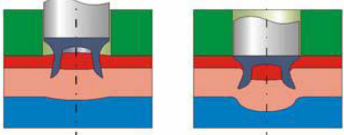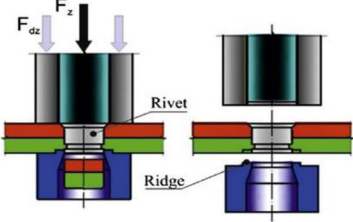


**Fig. 33** Large deformation of aluminum alloy while joining to UHSS using SSPR process (workpieces 1 and 3 are AA 6014 and workpiece 2 is 22MnB5) [139]



**Fig. 34** The specimen shown in Fig. 33 joined by the optimized toolset [139]

**Table 4** SPR process variants

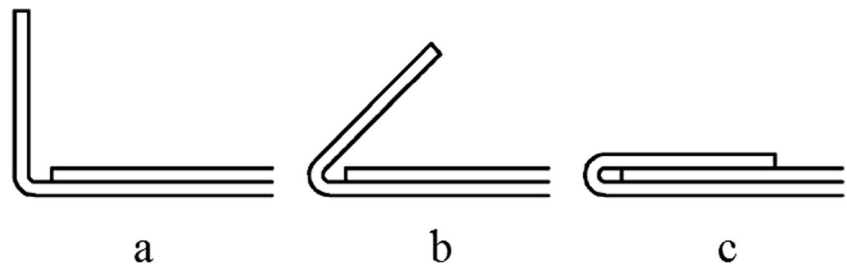| Process variant | Schematic | Limitation(s) enabled to overcome |
|---|---|---|
| Friction self-pierce riveting (FSPR) |  | The rotating rivet penetrates the harder materials much easier, Due to joint action of the mechanical joining mechanism and solid-state joining mechanism, a higher strength joint can be manufactured compared to conventional SPR [140]. |
| Hydro-SPR |  | Overcomes the low formability of materials by using a high pressure fluid, much lower joining force is required compared to conventional SPR |
| Solid self-pierce riveting (SSPR) |  | Improved joint look, improved mechanical performance, ability to join a wide range of dissimilar materials |

deeply on the pre-hemming step and stated that by carefully designing the pre-hemming operation, most forming defects including roll-in/out, recoil, and warp can be eliminated, minimized, or controlled. Wanintradul et al. [148] stated that roll-in could be prevented by reducing undesirable bending

moment, they applied a reaction force using an angled stopper to counteract the undesirable bending moment. The process is schematically illustrated in Fig. 37. In this process, the external force is introduced by the concept of a stopper as shown in the figure. The stopper angle should provide the necessary

**Table 5** Comparison of clinching, SPR, and RSW [96]

| Criteria for application | Clinching | SPR | RSW |
|---|---|---|---|
| Kind of connection | Mechanical, no heat transfer, connecting by shape, no joining elements required | Mechanical, no heat transfer, joining by form and force | Melting, heat transfer, connecting by material |
| Dissimilar materials | Possible | Possible | Only with bimetal |
| Non-metallic material | Possible | Possible | Impossible |
| Coated material | Possible | Possible | In general impossible |
| Optical view | Inconvenient | Inconvenient | Better |
| Thickness of material | St = 5.0 mm (total) Al = 8.0 mm (total) | St = 6.0 mm (total) Al = 11.0 mm (total) | With 60 kA up to 4.0 mm |
| Static strength | Less | Medium | Higher |
| Fatigue strength | Medium | Higher | Less |
| Lifetime of dies | 100,000–200,000 joining | 100,000–200,000 joining | 2500 points |
| Joints per min | 40–80 | 20–60 | 20–40 |
| Installation | Hydraulic Pneumatic | Hydraulic Pneumatic | Compressed air + current + water |
| Consumption of energy | Very low | Very low | High |
| Demand for area | Less | Less | More |
| Cost of investment | Low | Low | Higher |

conditions such that the flange will fold in the desired direction. The edge of the flange is released from the stopper after the flange touches the inner panel, and section AB (shown in Fig. 37a) will be folded down after the flange angle reaches 90°. With the optimum stopper geometry, the edge of the flange will be released from the stopper when the midsection of the flange touches the inner panel as illustrated in Fig. 37c. At the moment when the outer panel touches the inner panel, a new hinge is introduced. From this point, the rotation occurs around the point of contact of the outer panel and the inner panel, as shown in Fig. 37d and e. The hemming tool continues downward until the process is completed as shown in Fig. 37f. Using this modification on the process principles can lead to prevent roll-in and retain sharp radius from two-step flanging process.

## 5.2 Simulations and optimizations

Usually, hemming process control is experience-oriented and die design is based on trial and error. Therefore, understanding the hemming process from the mechanistic point of view, developing predictive modeling capability, and realizing process optimization are important goals in the quest for better design and quality [143], and a significant amount of both time and money could be saved if the defects could be predicted with high accuracy [142]. Svensson and Mattiasson [149] performed a two dimensional FE simulation using both shell as well as solid elements on the hemming process. Some effects cannot be predicted by 2D FE simulation of the process. For instance, in the 2D model, the material is prevented from moving in the direction perpendicular to the plane of the model. This difference between the 2D and 3D models will sometimes influence the amount of roll-in and make it necessary to perform 3D simulations when the impact on the roll-in of the shape of the parts should be determined. Thus Svensson

and Mattiasson [142] performed a 3D simulation of the hemming process. The overall accuracy of the simulation results was judged to be good enough to motivate the use of numerical simulations as an efficient industrial tool for predicting roll-in at the hemming of real production parts. Le Maoût et al. [150] conducted a numerical study on the hemming process of complex geometries. The use of an anisotropic yield criterion gave better predictions than the anisotropic yield criterion. Mechanisms of recoil and warp were studied using FE simulation and experimental methods on the flat [141] and the curved surface with straight edge geometry [143]. Zhang et al. [145] used FE simulations and statistical computer empirical design method to optimize the process. Huang [151] used an incremental updated Lagrangian elastoplastic FE method to analyze stretch flanging of circular plates with a predetermined smaller hole at the center of the sheet metal [151].

## 5.3 Materials

Due to very localized and severe plastic deformation, the hemming process usually is performed on materials with higher formability such as steels. Experimental work on the curved surface-straight edge hemming process based on a fractional factorial design method was conducted by Zhang et al. [143]. The material used in the experiments is AKDQ steel. Through the regression analysis, the output hemming quality indices such as roll-in/out, recoil and spring-back as well as hemming loads can be expressed as functions of the input geometrical and process factors. The regression models can provide information about the significance of the selected input factors and predict output responses under certain circumstances. Hamedon et al. [152] used hemming to join hollow sections made of HSS sheets and compared the tensile and fatigue strength of the joints by RSWed joints of the same materials.

**Table 6** Hemming classification according to surface and edge curvatures [143]

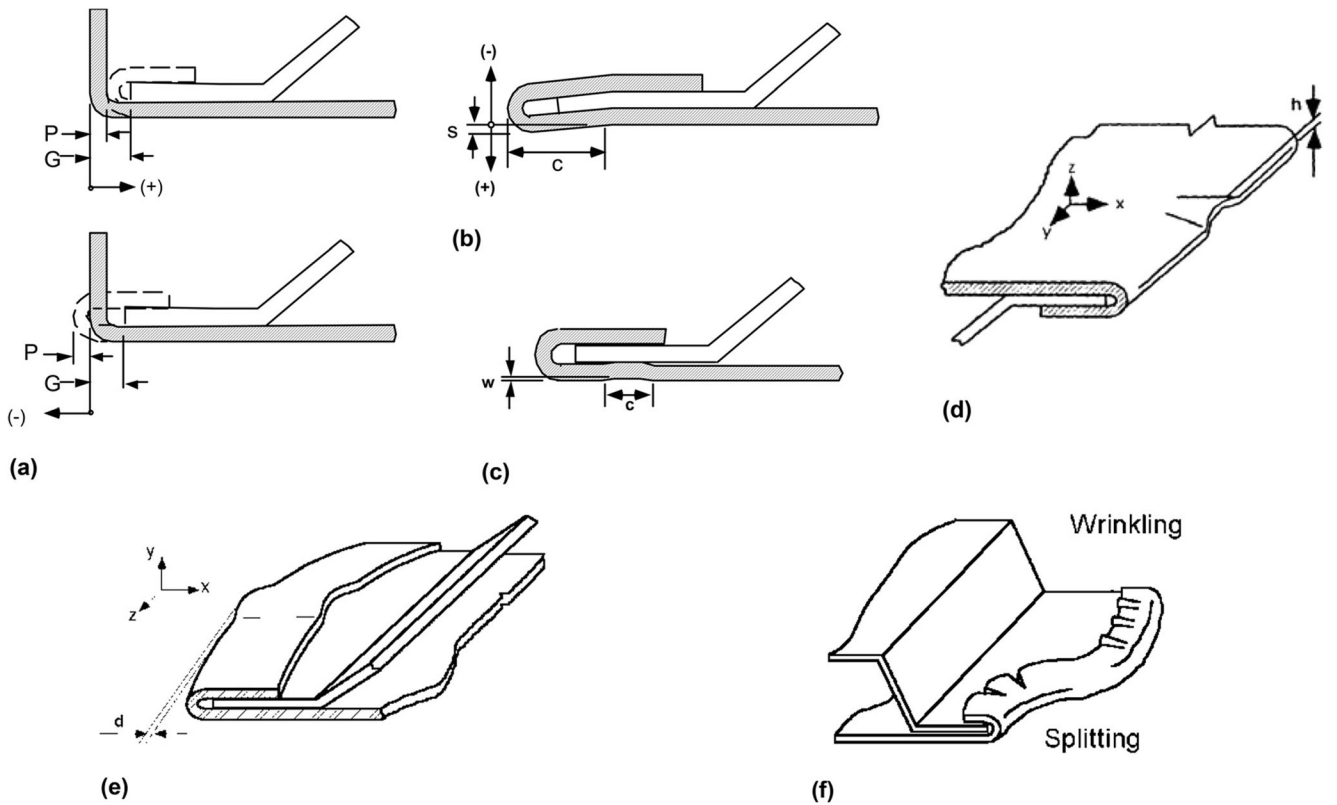|          | I      | II       | III     | IV       | V        | VI       | VII     | VIII     | IX      |
|----------|--------|----------|---------|----------|----------|----------|---------|----------|---------|
| Surface  | Convex | Convex   | Convex  | Straight | Straight | Straight | Concave | Concave  | Concave |
| Edge     | Convex | Straight | Concave | Convex   | Straight | Concave  | Convex  | Straight | Concave |

Fig. 36 The most common hemming defects: **a** roll-in or out, **b** recoil, **c** warp, **d** wind, **e** hem-out, **f** wrinkling and splitting

For the RSW joints, the failure occurred at the upper sheet around the welded spot, whereas for the hemming method, the flange portion that joined the inner and outer sheets was opened and deformed during the tensile test and the sheet separated and came out. There was no crack or fracture occurred on the hemmed sheet. The load-stroke curves are illustrated in Fig. 38. Although the maximum load of the RSWed joints almost doubles the hemming process, it failed earlier and hemming process shows superior elongation. Also, the maximum load for hemming increased as the strength of the steel sheet increased. The fatigue strength of RSW was

superior to hemming at higher cyclic loads, while by decreasing the cyclic load, the fatigue strength of two processes get closer and almost the same.

Materials such as aluminum and magnesium have lower formability compared to steel and are difficult to hem due to their susceptibility to strain localization during the hemming process. This phenomenon produces cracking on the hemmed edge [153]. Since an entirely flat hem requires materials with excellent formability because of the sharp hem radius, so for the materials with lower formability, rope hems with larger hem radii are used to avoid strain localization and cracking which results in exceeding the forming limits [144]. Schematic of a rope hem is illustrated in Fig. 39. Although its higher forming limit, rope hems negatively influence the appearance of the product. Therefore, special techniques must be considered to hem the low formability materials. Muderrisoglu et al. [154] conducted an experimental study on flat surface curved edge hemming using aluminum alloy AA1050. They studied the effect of flange height and flange radius on the hemming process, and it was observed that the flange height has a more significant impact on deformation load than the flange radius. The results showed that cracks were found on the outer surface over the bending area. Lin et al. [155] performed a computational DoEs study for aluminum alloy AA6111-T4 hemming. They found that pre-hemming die angle and the bending die radius significantly

**Table 7** Categorization of hemming defects

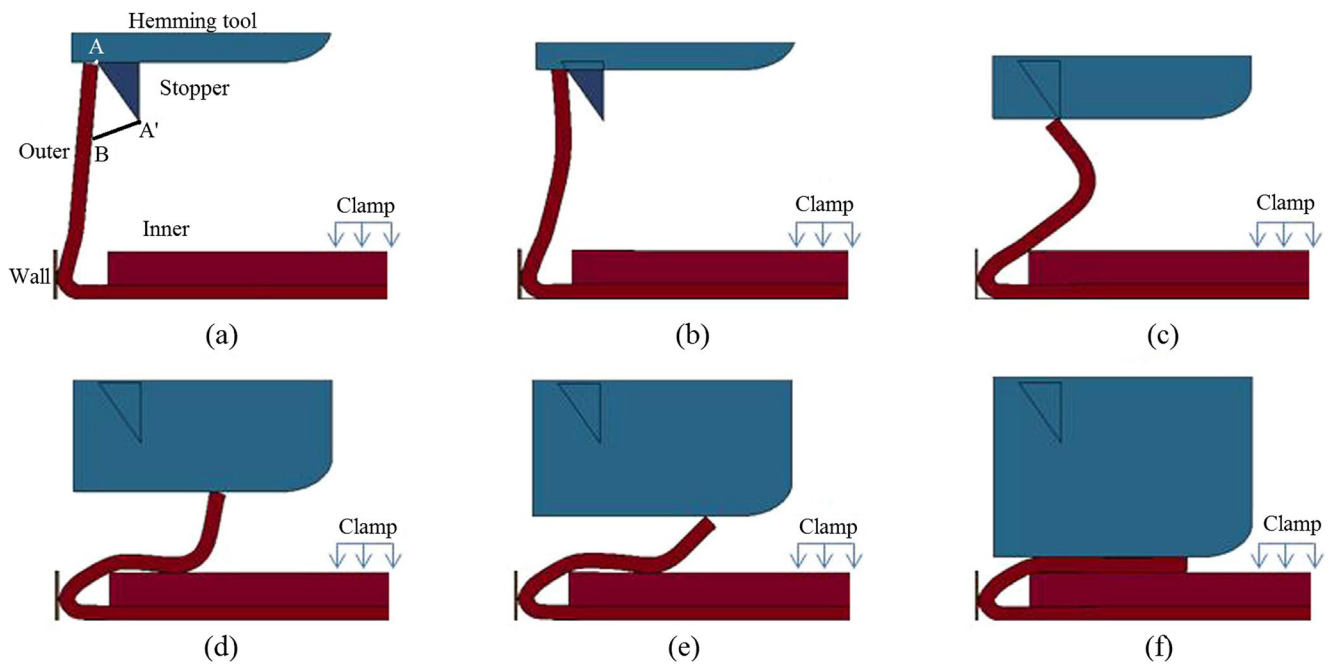| Hemming Defects | Dimensional inaccuracy | Roll-in (creep) |
| --- | --- | --- |
| | | Roll-out (grow) |
| | Fitting defects | Inappropriate clearance |
| | | Level mismatch |
| | Surface defects | Recoil |
| | | Warp |
| | | Wind |
| | | Hem-out |
| | Other defects | Wrinkling |
| | | Splitting |
| | | Spring-back |

Fig. 37 The operational sequence of the hemming with angled stopper: **a** initial state, **b** the edge of flange is constrained by stopper, **c** flange touches the inner panel when the edge is almost released from the stopper, **d** and **e** flange unfolded, **f** finished hem [148]

impact the maximum surface strain. Golovashchenko [156] presented a new method for hemming of aluminum alloy AA6111-T4. It was obtained that flat hem union for aluminum alloy by redistributing the plastic strain of the bending operation through a larger area before the hemming. The flanged parts must have a sharp bending radius to reduce damage to the parts. An additional axial compression step which increases process time and tooling cost.

## 5.4 Process variants

Roller hemming is a variant of classical hemming process. In this method a roller is guided by a robot along the hemmed
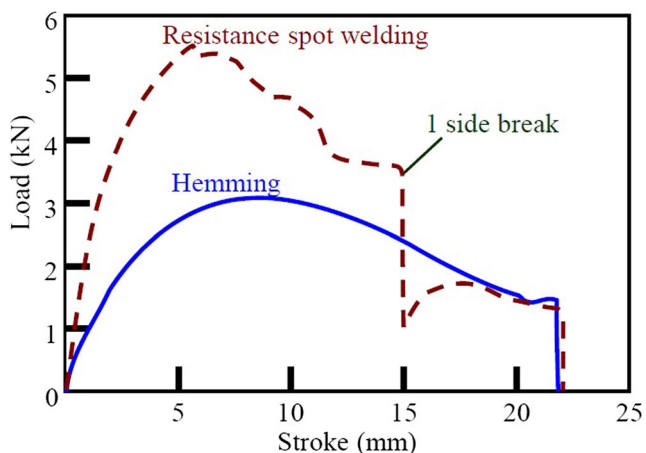


Fig. 38 Load-stroke curves of tensile test for hollow section joints using RSW and hemming for JSC890YN [152]

line, progressively bending the flanged height along the part [157]. In this way, no conventional die is required, and the final shape of the part only depends on the trajectory assigned to the tool [158]. The process is schematically illustrated in Fig. 40.

Roller hemming presents a non-plane strain deformation pattern with a component of strain in the direction of the hemline different from the plane strain bending created with the conventional hemming [153]. Figure 41 shows strain states in the roller hemming process. The main advantages are its low cost, the reduction of delivery time in industrialization, the use of only one tool from prototype to serial production [159], and its high flexibility [158]. Disadvantages are the arduous robot programming of the process [153].

Thuillier et al. [159] conducted the FE simulation of the roller hemming process of an aluminum-magnesium alloy to define roll-in/out. Three different constitutive models were identified to study the influence of mixed hardening and anisotropy on roll-in. Hu et al. [157] presented a numerical simulation of the roller hemming process. The mechanical behavior of the steel panel was described by a combined isotropic and non-linear kinematic hardening rule. Furthermore, roller hemming process simulation was presented for a flat surface straight edge outer panel according to combined hardening and ductile damage criterion [158]. A laser-assisted roller hemming of magnesium alloys was conducted by Levinson et al. [160]. The laser was used to locally warm up the workpiece to successfully perform the hemming process.

Since aluminum alloys exhibit little uniform elongation and high strength, EMF (see section 10) is a promising

technique to enhance its formability and performing the hemming process [144]. Regarding this fact, Jimbert et al. [153] utilized EMF to carry out the hemming on AA6016-T4. Electromagnetic hemming has some advantages over the conventional hemming. First, electromagnetic hemming eliminates the pre-hemming stage and could hem the pre-bent parts from 90° to 180° in one step. Second, due to the high strain rate of the process, the material formability increases and therefore it is a proper way to hem low formability materials. Jimbert et al. [153] also performed a numerical simulation of the electromagnetic hemming process, which confirmed the reduction of the maximum strain in electromagnetic hemming.

Hemming process in a warm state was also performed on the magnesium alloys by Carsley and Kim [161]. A temperature range that enables 90° flanging followed by 180° bending of AZ3113-O was determined. The surface condition of bent samples was examined for evidence of cracking, and the microstructure was scanned in cross-section for indication of unusual bending strain. The hemming process variants and the limitations they enabled to overcome are summarized in Table 8.

# 6 Rolling

Joining by rolling uses the mechanical contact between the rolling elements of a tool and an inner part of a tubular assembly to expand both parts being joined (Fig. 42) [6]. Cylindrical rollers are driven by a conical mandrel (cone) and are
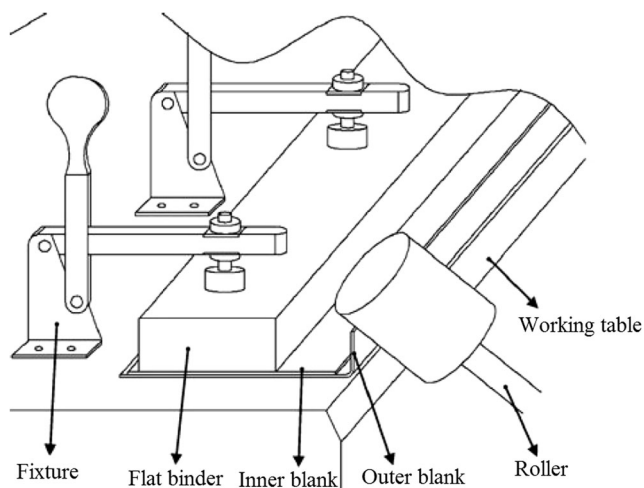


**Fig. 40** Schematics of the roller hemming process [157]

positioned by a cage. By an infeed of the cone, the rollers are moved in the radial direction towards the tube [163]. The internal tube is expanded by the rolling tool, which runs with a defined rolling oversize through the tube. When there is an appropriate external component with a little clearance positioned outside of the internal tube, the outer part will be elastically deformed by the inner tube. This case is seen with the result that the plastic deformation of the inner tube in combination with the elastic recovery of the external component leads to a high bearing pressure, thereby a force-fit joint is created [162]. Using an outer part with a higher yield stress than the inner part gives a more upper strength joint.

The stability of the joint mainly depends on the diameter of the roller body and the material of the joining partners. The joining diameter and the wall thickness of the inner and outer parts also have a significant influence [162]. This method is also used for joining of an aluminum tube and an insert by external rolling using burnishing tools [163]. They used the grooved inserts for experiments as well as the cylindrical ones as indicated in Fig. 43 and the grooved inserts presented higher joint resistant.

The primary application of the joining by rolling is for the manufacturing of hollow and light-weight camshafts. A rolled-in camshaft is indicated in Fig. 44, and a comparison between the weight of the forged camshafts and rolled-in camshafts is presented in Fig. 45. Furthermore rolling is used for joining tubes in the boiler and apparatus engineering. Water and steam tubes are joined to the bottom of heat exchangers for the use in power plants. Today joining by expansion is usually done by hydroforming (section 7) and EMF (Sect. 10) processes because of simple setup and lower cost.

# 7 Die-less hydroforming

One alternative for joining by rolling is joining by die-less hydroforming. Conventional hydroforming process uses a fluid under high pressure to form tubes, profiles, single, and double sheets into a die cavity [164]. Figure 46 indicates the process principles of die-less hydroforming. In die-less hydroforming, to initiate the joining process, a joining tool, so-called hydro-probe is positioned inside the inner part axially underneath the other joining partner. In a gap between hydro-probe and tube, a pressurized working media is applied. If the pressure which acts locally in the joining area exceeds the tube's yield strength because of a limitation in the axial direction by sealing, plastic deformation of the tube occurs

**Fig. 41** Strain state of different sections during roller hemming [157]
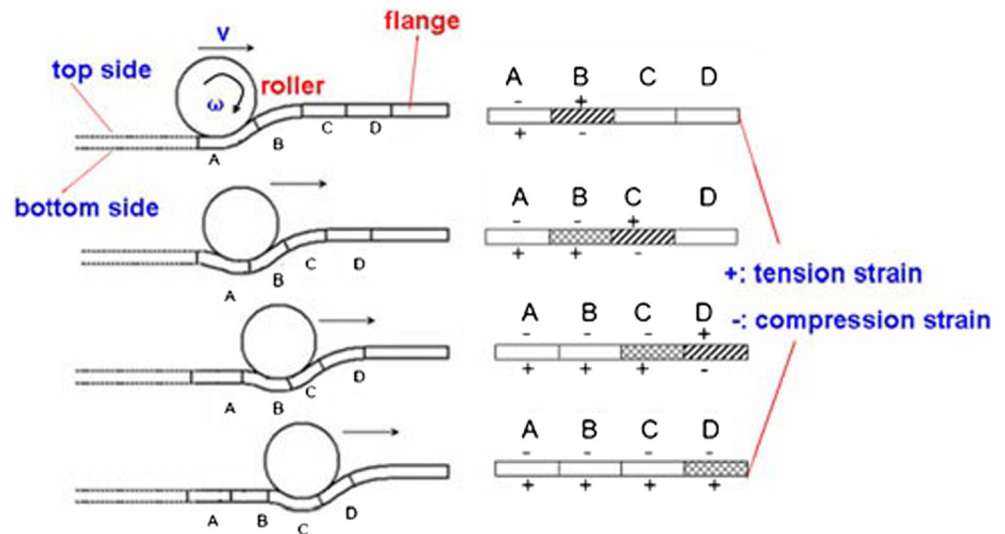


[165]. The force which determines the forming of the tube leads to an elasto-plastic deformation of the tube and an ideally elastic deformation of the external joining partner [163].

Manufacturing of camshafts, intermediate shafts or cylindrical liners, and light-weight frame-structures is done by die-less hydroforming. Furthermore, this technology is potentially suitable to join extruded profiles to casted or machined nodes [165] and for manufacturing heat exchangers [166].

Marre et al. [165] developed an analytical model to calculate the interference pressure between a tube and a ring joined by die-less hydroforming. They introduced four significant strains related to the interference diameter and calculated the interference pressure by Eq. (1), where $p_i$, $k_f$, $E$, $\nu$, and $Q$ are the internal pressure, yield stress, Young's modulus, Poison's ratio, and the ratio of inner and outer diameters of joining partners, respectively, and indices I and O are related to internal and external parts, respectively. They also verified the

analytically calculated interference pressure with FE simulations as depicted in Fig. 47. However, there can be seen a minor deviation between the two calculated interference pressures due to the simplifications.

$$
p = \frac{\dfrac{p_i - k_{f,I}\, ln\dfrac{1}{Q_I}}{E_O} + \left(\dfrac{1+Q_O^2}{1-Q_O^2} + \upsilon_O\right) - \dfrac{k_{f,I}}{E_I}}{\dfrac{1}{E_O}\left(\dfrac{1+Q_O^2}{1-Q_O^2} + \upsilon_O\right) + \dfrac{0.5}{E_I}\left(\dfrac{(r_{I,a}+r_{I,i})}{r_{I,a}-r_{I,i}} - \upsilon_I\right)}
\tag{1}
$$

In addition to joining by tube expansion, other types of joints could be manufactured using die-less hydroforming. Groche and Tibari [167] utilized hydroforming to angularly join hollow workpieces in one die without any welding (Fig. 48). The process involves three phases. During phase I,

**Table 8** Hemming process variants

| Process variant | Schematic | Limitation(s) enabled to overcome |
|---|---|---|
| Roller hemming |  | low cost, the reduction of delivery time in industrialization, the use of only one tool from prototype to serial production |
| Electromagnetic hemming |  | Overcomes the low formability of materials by using a high strain rate forming process via EMF technique |

**Fig. 42** Process principles of joining by rolling [162]
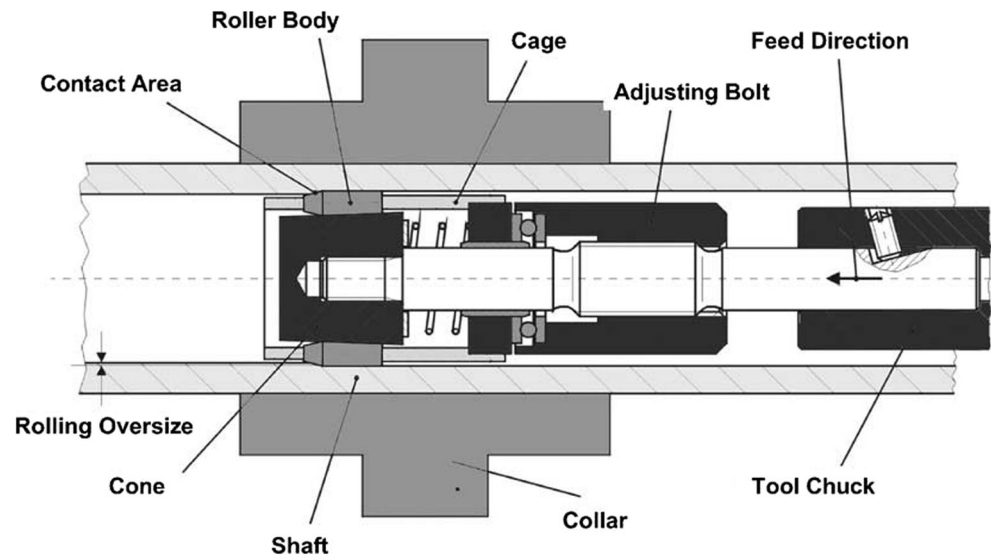
the internal fluid pressure forms an asymmetrically shaped dome into the female component. Then, phase II commences and a counter punch compresses the accumulated dome material and results in a radial flow of the dome material, and subsequently, the female part expands radially until it touches the die cavity. If then the counter punch continues to flatten the dome, the female component resists the material flow of the male component. Consequently, the flattened dome is set under radial and tangential compressive stresses, while the female component faces radial compressive and tensile tangential stresses. Figure 49 shows the stress-strain profiles for a force-fit joint in this case. After unloading, phase III commences when the elastic recovery of a female component creates a force-fit joint between the male and female parts. Since joining and forming were performed simultaneously, the production chain and costly equipment can be reduced.

Merklein et al. [164] combined the tube and double sheet hydroforming processes into one single process to manufacture complex shaped parts; it is almost impossible to build such parts in one step using any other manufacturing technique. Integrated process chain is illustrated in Fig. 50. First, the lower sheet and the tube are placed into the tool; then, the upper sheet is positioned onto the tube and onto guiding elements. During the device closing operation, the sheets are pre-formed by the tube into the die cavity in the junction area between the tube and double sheet. Then the tube is upset with an axial force by the docking cylinder (Fig. 50b). The hydroforming fluid flows through a channel in the docking cylinder and forms the two blanks and the tube against the die cavity. At the end of the forming process, the clinching punches, which were retracted inapposite holes in the blank holder, are actively moved and join the two sheets in six points in the flange (Fig. 50c). Due to the hydroforming operation, a joining by hydroforming between the tube and the double sheet is also realized. Finally, the component can be taken out of the press and finished by additional welding and cutting operations in the adjacent laser station (Fig. 50d). The manufactured part is illustrated in Fig. 51. Wang et al. [168] used hydroforming to make bimetallic corrosion resistant alloy (CRA)-lined pipes. The CRA-lined pipe has a liner pipe
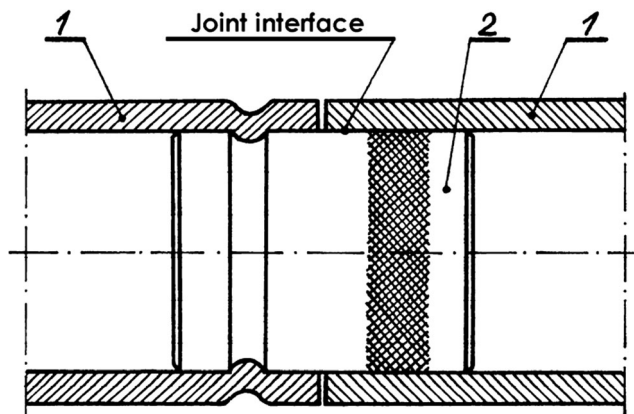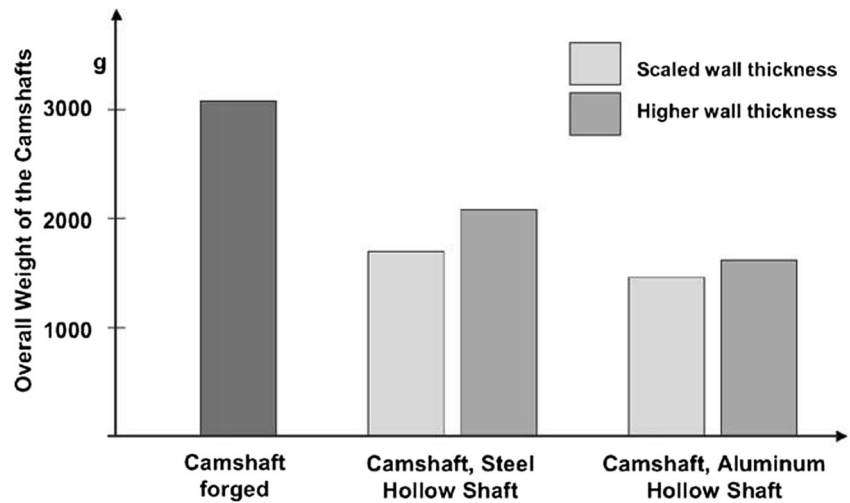


**Fig. 43** Tubular joining by rolling: 1 tube; 2 smooth, grooved, or patterned insert



**Fig. 44** Rolled-in camshafts [162]

**Fig. 45** Weight comparison of forged and rolled-in camshafts [162]

made of corrosion-resistant-alloy (CRA) and an outer pipe made of low-cost steel and has been utilized in oil production, nuclear power plants and refining industry increasingly. First, the carbon steel outer pipe and the CRA liner pipe should be produced by seamless or welded manufacturing processes. The contact area of the two tubes (the outside of the liner and the inside of the outer pipe) has been treated by alkaline cleaning, and then sour cleaning. The two tubes are joined together hydraulically using a nearly complicated setup. The O-rings and the self-energizing seal rings made of rubber are installed on two ends to assure the sealing between two tubes. A core tube is placed inside the liner pipe, and a liquid medium (water is used in this case) is pressed into the cavity between the core tube and the liner pipe (called expanding

cavity). By increasing hydraulic pressure in the expansion cavity, the CRA liner pipe is hydraulically expanded at ambient temperature until it touches the inside wall of the outer carbon steel pipe. And the operation is then followed by a combined expansion of both the liner and the outer pipe. During expanding process of the pipe assembly, the simultaneous pressure in seal cavity is always higher than that in expansion cavity to maintain the condition of the self-energizing seal. When the hydraulic pressure in the expanding cavity is up to the required value, it is held for a few minutes, and then it is released. At this point, the process is finished, and a bi-metal pipe is manufactured.
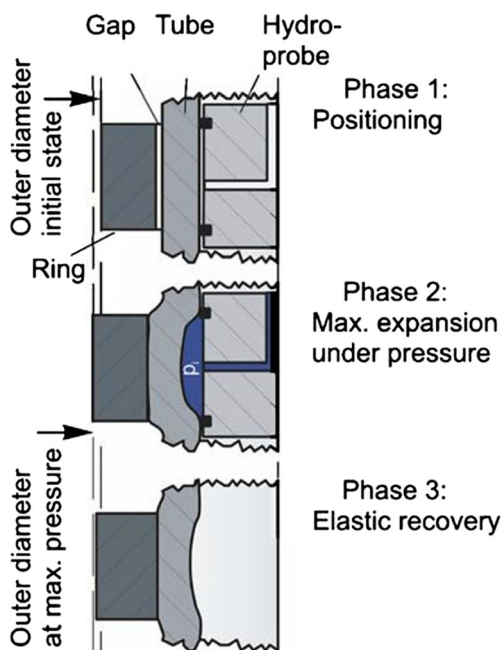
## 8 Joining by incremental forming

Incremental forming is an innovative and highly flexible sheet metal forming technology for small batch production and prototyping that does not require any adapted dies or punches to form a complex shape [169]. Incremental forming can be
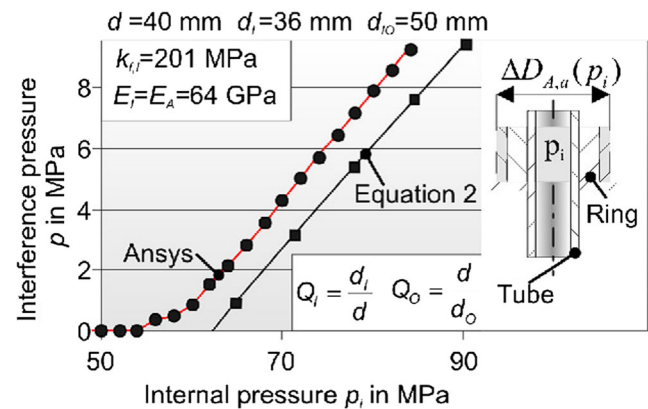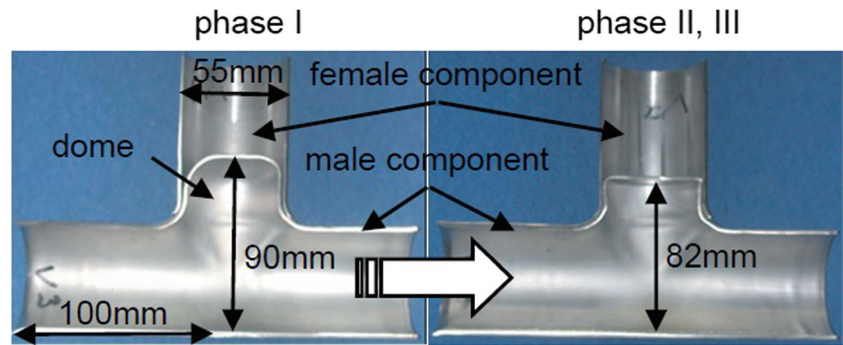


**Fig. 46** Process principles of joining by die-less hydroforming [163]



**Fig. 47** Calculation of interference pressure by FE simulation and Eq. (1) [165]

**Fig. 48** Angular joining by hydroforming; process phases and product [167]



categorized into several techniques, such as flow forming, spinning, single-point incremental forming (SPIF), two-point incremental forming (TPIF), and rotary swaging. Some incremental forming technologies can also be applied to join materials. Joining by incremental forming has four major benefits: (1) Assembly can be carried out without additional joining elements; (2) an enormous freedom of material selection is given since incremental forming processes can lead to high formability [170]; (3) short clock cycles; and (4) possibility to vary the temperature increase of the workpiece by changing the process duration [8].

An application for joining by incremental forming is manufacturing multi-layered (composite) hollow frames or tubes. In many cases, the inner and outer surfaces of hollow sections are exposed to different environments, and different characteristics are required inside and outside. In these instances, various bimetallic or clad tubes are used in the various industries. Utilizing the tube spinning process, a method for cold-bonding of cylinders, so-called spin-bonding was proposed [171]. Figure 52 shows the schematic of the process. Initially, the surface preparation was done on the workpieces; then, the two tubes to be joined were positioned relative to each other. The roller moved on the outer workpiece along the mandrel and thickness of both workpieces reduced, and a force-fit between two workpieces was created under the influence of the heat and pressure. Effect of the process parameters, including temperature, feed rate, roller attack angle, and thickness reduction, was investigated. It is stated that the main difference between spin-bonding and roll-bonding is the strain history of these processes.

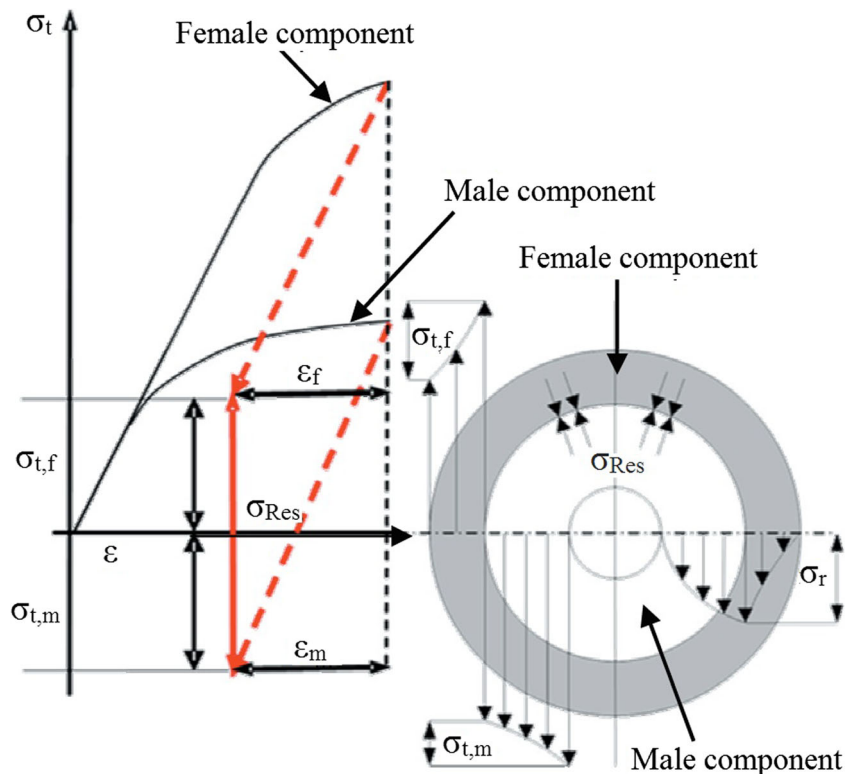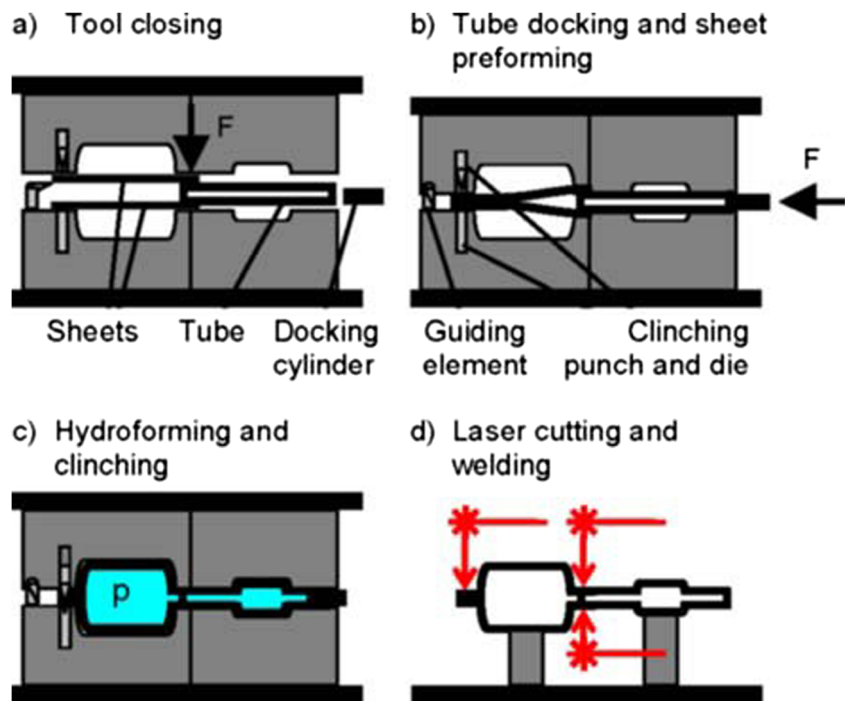**Fig. 49** Stress-strain profile for fluid-based force-fits [167]

**Fig. 50** Integrated process chain for combined tube and double sheet hydroforming [164]



a) **Tool closing**

Sheets    Tube    Docking cylinder

b) **Tube docking and sheet preforming**

Guiding element    Clinching punch and die

c) **Hydroforming and clinching**

d) **Laser cutting and welding**

Incremental forming processes also seem to be particularly attractive for the assembly of smart and structural components by enclosing the functional elements with a plastically deformable material. For example, Groche and Turk [8] used metal spinning to manufacture tube parts with integrated ring magnets (Fig. 53). The integration of the two magnets takes place in three steps. In the first step, an aluminum tube is formed into a preform upon a two-part mandrel. After this, the first ring magnet is positioned on the mandrel, and the undercut is formed. Now, the mandrel can be removed and the outer side of the tube with the second ring magnet is formed by the spinning roller. The rings are fixed into the tube part, and the mandrel can be removed. Figure 53 schematically shows the sectional view of the part design (left) and produced cartridge by metal spinning (right).
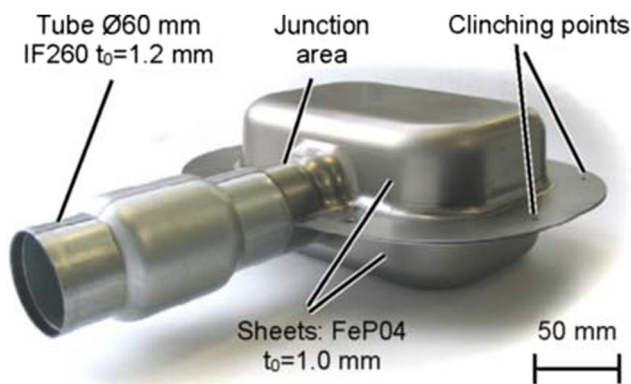


Tube Ø60 mm
IF260 $t_0$=1.2 mm

Junction area

Clinching points

Sheets: FeP04
$t_0$=1.0 mm

50 mm

**Fig. 51** Tube double-sheet component [164]

Rotary swaging is an incremental forming process for the reduction of the cross-section of bars, tubes, and wires. Sets of two, three, four, or in individual cases up to eight dies perform several simultaneous radial movements. During every inward movement of the dies, a small area of the workpiece is deformed. Depending on the kind of relative movement between the workpiece and die, rotary swaging is categorized into infeed and hitch-feed swaging methods [172]. Mainly compressive stresses inside the workpieces lead to plastic deformation during conventional swaging processes [8]. It is widely used in automobile and aviation industries due to its high-cost effectiveness and considerable material saving [173]. Rotary swaging was also used as a joining method to manufacture smart structures. A tube made of aluminum alloy AA6060 and piezoceramic ring were the mating parts [8]. Rotary swaging dies loaded them and supported by an inner mandrel. A groove inside the swaging dies led to a stronger reduction of the tube diameter in areas where the piezoceramic ring was not located. Furthermore, numerical simulations were carried out to prove the relevance of the joining mechanisms.

Joining by rotary swaging was utilized as a joining by plastic deformation method for connecting tube/tube parts [173]. Figure 54 shows the schematics of the process. Two tubes of copper were positioned coaxially and then by rotary swaging dies, the thickness of tubes reduced and an interference pressure between the parts obtained. Both simulation and experimental methods have been used to investigate the joining mechanisms and the deformation process as the joining strength of parts.

**Fig. 52** Schematics of the spin-bonding process [171]
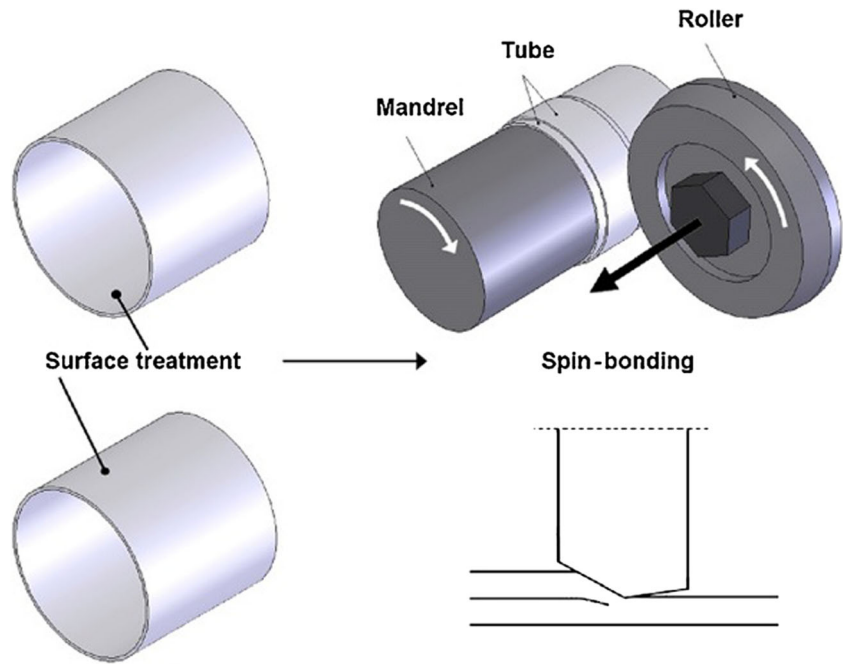


## 9 Joining by hydraulic and mechanical crimping

In crimping process, the tubular component is lowered into the casing to a predetermined depth, and then segmental dies or elastomers are pushed into the housing by mechanical or hydraulic rams, resulting in forming the crimp. The housing is deformed to fill grooves, which were machined on the inner part formerly [146]. Hydraulic and mechanical crimping is almost the same processes with minor difference between process tools and driving force. In mechanical crimping, segmental tools so-called crimping dies are used to apply forming pressure to the outer joining part as depicted in Fig. 55, while in hydraulic crimping, elastomers are used to apply forming pressure, and utterly elastic deformation of elastomers causes plastic deformation of the outer part (Fig. 56). In these processes, a force-fit is
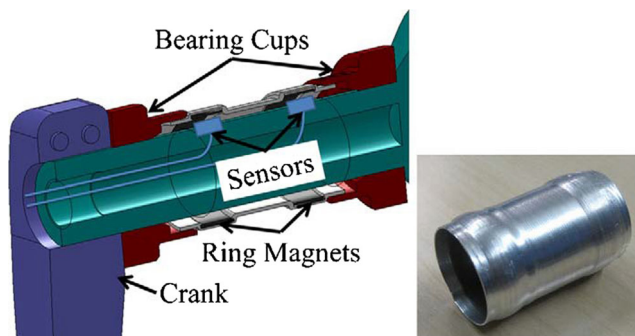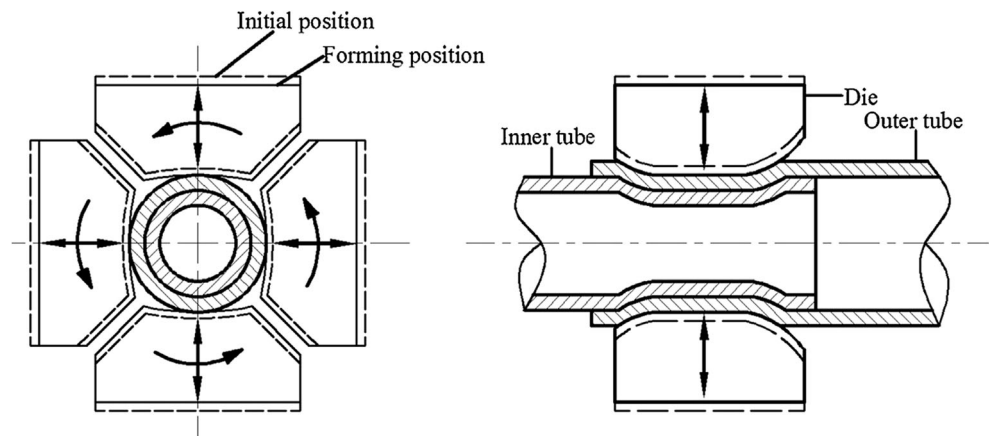
created between joining partners. A principal application of the crimping methods is to join metal casings to rubber hoses [175] and in the field of electrical engineering for assembling composite insulators [176]. The main advantage is the easy installation, small manufacturing time and manufacturing leakage-proof connections [175].

Cho and Song [174] used the crimping process for joining metal fitting to a rubber hose for automotive power steering applications. Figure 55 illustrates schematics of the process. First nipple and sleeve are metal-fitted by jaw 1. Then, the rubber hose is inserted between nipple and sleeve and is crimped to the metal fitting by jaw 2. After unloading, the metal fitting and rubber hose show the spring-back and stress relaxation, respectively. It is proved that stress relaxation negatively influences the strength of the force-fit joint and it is suggested that the shape and dimension of nipple grooves, sleeve concaves, and rubber materials to be determined carefully such that unexpected oil leakage may not be triggered by the stress relaxation. Pavloušková et al. [177] found that the crimped hoses typically fail by fracture running through the ribs. This observation evokes that clamp insert is responsible for the failure of the fitting assembly by providing the force for opening the crack. Cracks initiate at the bottom of the ribs, suggesting that the cause of cracking is the stress concentration during deformation of the material. Furthermore, evaluation of crack in transverse direction revealed that they were formed during crimping of the sleeve when the material at the sleeve's inner surface was subjected to heavy plastic flow.

Shirgaokar et al. [178] focused on the crimping of a rod to a tube using flexible tools. First, the rod is press-fitted into the tube to a predetermined depth and then a



**Fig. 53** Sectional view of a part design with integrated ring magnets (left); produced cartridge by metal spinning (right) [8]

hydraulically pressurized rubber crimper pushes the casing into grooves machined on the rod, forming the assembly. Pull-out forces in the range of 9–15 kN were found for the construction. The design of the crimping processes for assembling tubular parts rely mainly on the experimental trial and error methods, which prove to be very expensive and time-consuming [178]. So, it is advantageous to use FE simulation to predict the process and determine the optimum process parameters, but the numerical analysis of the process is not so simple because this process exhibits the highly non-linear behavior. Cho et al. [175], the FE analysis of the method was presented by fully reflecting material, geometry, and boundary nonlinearities. Shirgaokar et al. [176] discuss the application of FEM in the evaluation of a hydraulic crimping process to enhance the performance of the assembly by determining the optimum process and geometrical parameters. Shirgaokar et al. [178] conducted FE simulations to optimize the process parameters. According to the simulation results, it was proved that the combination of minimum flow stress, minimum force-fit, and maximum friction yields to the maximum pull-out force values. Pavloušková et al. [177] stated that high and excessive degrees of material strengthening during the cold formation leads to failure of the fitting, because of formation of deeper and more stress-concentrating cracks at the bottom of the ribs.

# 10 Electromagnetic forming

EMF is an impulse, high speed, contactless forming technology, which utilizes substantial electromagnetic fields to form electrically conductive materials. First, a high-voltage energy (about 3–30 kV) is charged in a capacitor or bank of capacitors. This charged energy is sufficient to form the material. By discharging the energy suddenly, all the stored energy is released, leading to an electrical discharge current running through a coil which generates an intense transient magnetic field around it. This magnetic field can be induced in any electrically conductive material adjacent to the coil and induces transient eddy current. The two currents running in the opposite direction create a large magnitude magnetic repulsion force between the coil and the workpiece. This magnetic repulsion launches the workpiece at very high speeds, and desired shapes can be obtained on the workpiece [179]. Depending on the arrangement and the geometry of the coil and workpiece, different applications of EMF are achieved: compression and expansion of tubular components or hollow profiles as well as forming of initially flat or three-dimensional preformed sheet metals (see Fig. 57) [181].

In addition to the tube forming and sheet forming in different geometries, the process can be utilized to achieve assembly and joining purposes. Joining by EMF can be
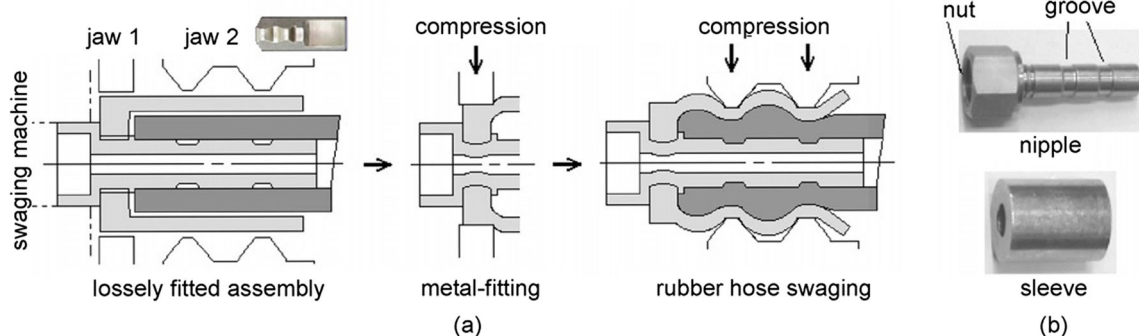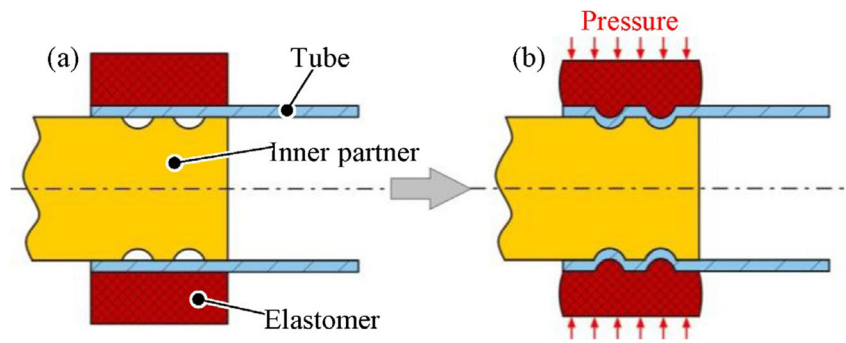


**Fig. 55** **a** Schematic view of the mechanical crimping process. **b** Sleeve and nipple to be joined [174]

applied for connecting tubes as well as sheet metals [181]. Both tube compression and expansion processes are available by this forming technology and all joint mechanisms introduced in Sect. 2 including force-fit, form-fit, and metallurgical joints can be produced. In the case of connections including at least one sheet metal partner, force fit joining is not possible [181], while the main joining mechanism in tube joining by expansion or compression is a force-fit, form-fit joints also can be produced in this category. One of the most common applications of tube expansion/compression by EMF is crimping of shafts, cables, and building frame-structures [6].

In comparison to other conventional joining techniques like mechanical crimping, electromagnetic crimping features very homogenous bond characteristics. These results from a uniform forming pressure distribution [182]. One other application is in the aerospace industry. For example, in Boeing 777 and other recent Boeing aircraft models, this technology is used for manufacturing torque tubes [183].

## 10.1 Force-fit joining

For manufacturing force-fit joints by electromagnetic expansion/compression, the workpieces should be positioned coaxially, and magnetic pressure is applied to their overlap area in the radial direction. In tube compression, the magnetic pressure is applied to the outer surface of the outer part and in tube expansion on the inner surface of the inner portion. The main advantage of force-fit joints created by EMF is the combination of high strength and simplicity of the process. High-velocity forming typically develops a natural force-fit that resists motion, and by forming onto undulating surfaces, joints that have the strength of the weaker joining partner in torsion and tension can be manufactured [183]. This process can be utilized to join any electrically conductive material to any other materials such as steels [15] and even rubber materials like polyurethane [184].

The impact velocity has a significant effect on the joint strength. The impact velocity is under the influence of
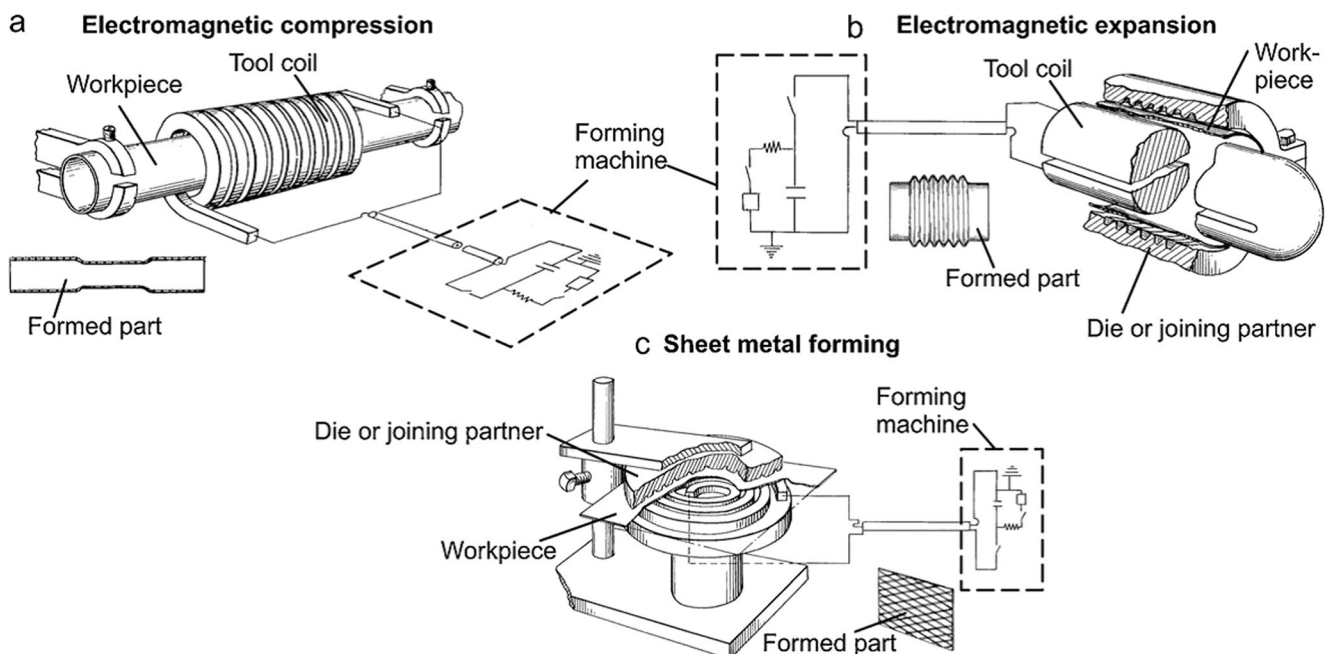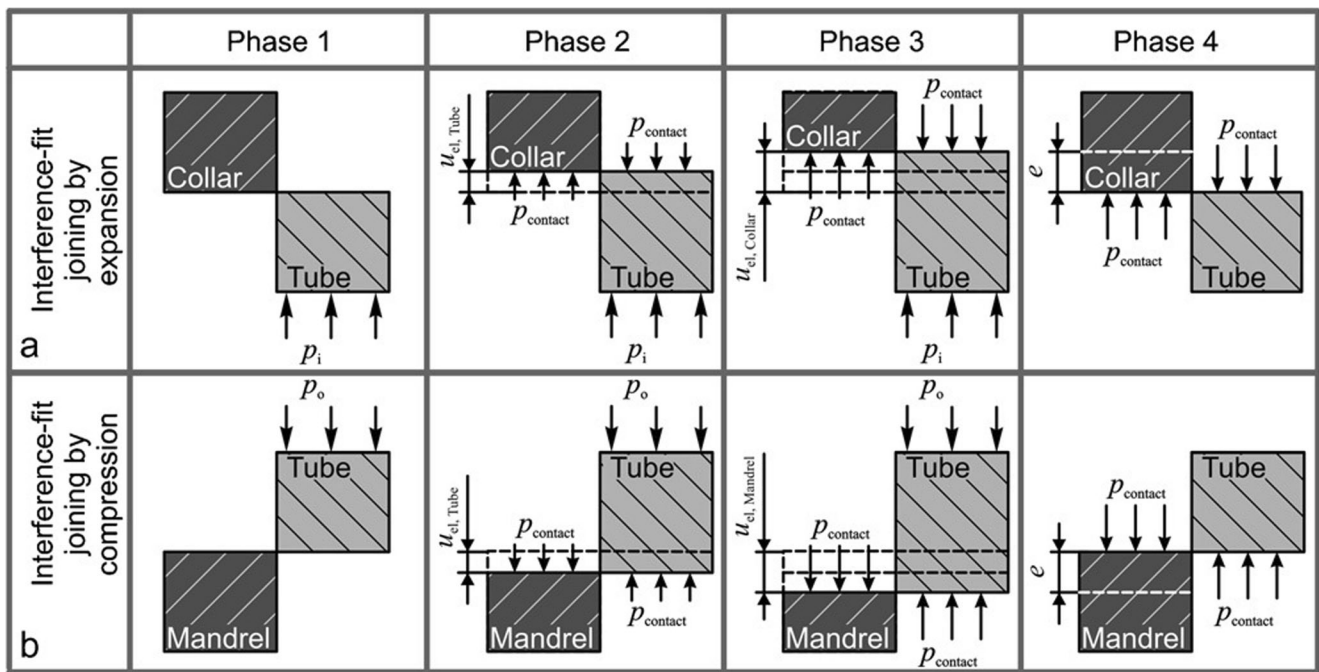


**Fig. 57** Different setups for electromagnetic forming/joining process [180]

$u_{el}$: displacement related to elastic strain; $e$: interference

**Fig. 58** Process principles of electromagnetic force-fit joining by expansion or compression [181]

discharge energy and the initial gap between the joining partners. An optimum initial gap leads to the higher speed of the workpiece as a result to increase the impact energy, and the much stronger joint can be produced. However, this is valid only for metallic workpieces, as Hwang et al. [184] report that initial gap between aluminum and polyurethane workpieces negatively influences the joint strength. Salamati et al. [14] reported the same observations in joining aluminum and CFRP tubes by the electromagnetic compression process.

Considering joining a tube and a collar by electromagnetic expansion (Fig. 58a), once the magnetic pressure applied, both the workpieces deform radially (Fig. 58, phase 2). Thus, the inner joining partner (tube) initially deforms elastically and on final levels of the process deforms plastically. The other joining partner, the collar should necessarily deform elastically (Fig. 58, phase 3), the plastic deformation of this part negatively influences the joint quality and strength. When the energy completely discharges, the elastic recovery of the workpieces initiates, and if the plastically deformed workpiece (tube in this case) avoid the elastic recovery of the outer part, a force-fit creates between the workpieces. Electromagnetic compression (Fig. 58b) is the other way around. In fact, in this case, the pressure is applied to the outer surface of the outer part (e.g., tube), so that the outer parts should deform elastic-plastically, while the inner part (e.g., mandrel) should necessarily deform elastically. Three main factors are influencing the strength of the force-fit joint:

- The interference stress;
- Friction coefficient;
- The contact area between two parts.

Strength and stiffness of the mandrel play a significant role in the force-fit stresses. Kleiner et al. [185] and Barreiro et al. [186] investigated the effect of yield strength and stiffness of the mandrel on joints made by tube compression. As shown in Fig. 59, using a mandrel material of both higher strength ($R_e$) and stiffness results in higher pull-out loads, so it will be favorable to use a mandrel of higher strength and stiffness than the tube material (Fig. 59). To investigate the effect of mandrel material's stiffness on joint strength, the parameter $Q = D_i / D_a$ was introduced [187], where $D_i$ and $D_o$ are the inner and outer diameters of the mandrel, respectively. It is evident that $Q = 0$ corresponds to a rigid solid mandrel with high stiffness and $Q = 1$ corresponds to an infinitely thin-walled mandrel with very little stiffness. When $Q$ is very small (near zero or zero), the interference stresses is low due to the high stiffness and quasi-rigid conditions of the mandrel, and thus joint strength is little too. Increasing $Q$ to a certain point leads to a significant increase in joint strength, but the excessive increase in $Q$ leads to a considerable decrease in joint strength. The reason is that due to the very low wall thickness and stiffness, the mandrel deformation is elastic-plastic and plastic deformation negatively influences the joint force. A critical inner mandrel diameter $d_M$ was found concerning the transferable loads [182]. If $d_M$ be smaller than its threshold value, a supplementary

**Fig. 59** Pull-out loads for different mandrel materials [186]
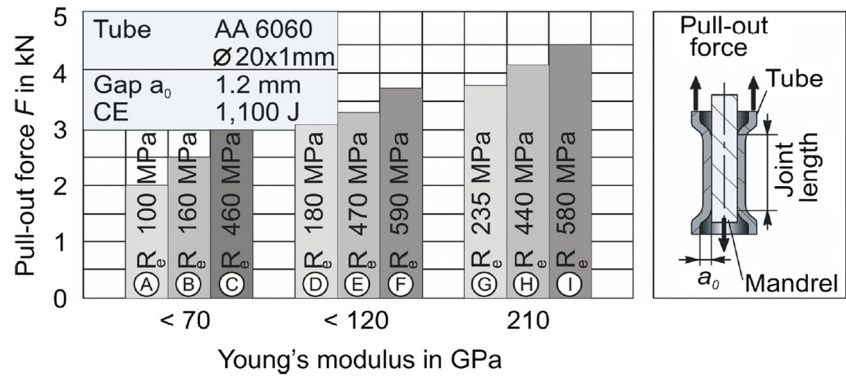
force-fit is generated yielding to an increase in the joint strength, while $d_M$ exceeding its threshold value leads to a reduction of the transferable load. Hollow mandrels have the opportunity to reduce the mass of a connection, but a hollow mandrel can deform easily during the joining process as depicted in Fig. 60a. To solve this problem Weddeling et al. [189] introduced a steel support into the hole of the inner hollow mandrel. Figure 60b indicates that the plastic deformation of the mandrel is reduced significantly when using support.

## 10.2 Form-fit joining

If the abovementioned geometrical elements (threads, grooves, or knurls) become as large as the macro scale, the joint mechanism changes to form-fit. In a form-fit joint, an undercut is created by forming one or more of the joining partners onto the geometrical elements on the other part. Thus the better filling of geometrical elements leads to stronger joints. The minimum pressure required to initiate plastic deformation of a tube into a groove was analytically calculated based on assumptions of typical plastic material behavior and plane strain:

$$p_{\min} = \sigma_y \left[ 3 \cdot \left( \frac{s}{w} \right)^2 + \frac{s}{R} \right] \tag{2}$$

where $\sigma_y$ is the yield strength of the tube, $s$ is the wall thickness of the tube, $w$ is the groove width, and $R$ is the inside radius of the tube [190]. However, it is proved that

the values calculated for the minimum pressure from this analytical approach do not fully correlate with the experimental data [191]. They are smaller than the values that could be derived from the experimental results for the magnetic pressure at which the plastic deformation begins. It can be assumed that this results from the simplifications of the analytical model. Therefore, the results of this model should be considered as the lower limit of the required forming pressure. It has to be noted that the joint manufactured by the minimum necessary energy to fill the groove, never can be of sufficient pull-out strength. Figure 61 schematically shows the joints manufactured by the minimum necessary energy to fill the groove and with a higher discharge energy. It is evident that the joint produced by minimum energy has no sufficient strength.

The effect of groove geometry on joint strength can be divided into three categories as illustrated in Fig. 62: (1) effect of groove radius; (2) effect of groove depth; and (3) effect of groove width. These parameters all have two different effects, there is an optimum value for each parameter and exceeding these optimum values negatively influences the joint strength. Increasing the groove radius leads to reduced thinning on the groove profile but simultaneously results in joint separation quickly. Increasing the groove depth makes the separation more difficult but excessive increase in depth leads to substantial thinning of the outer part and joint strength decreases, and finally increasing the groove width increases the contact area which in turn increases the frictional force but increasing the groove width over a certain point causes wrinkling of the workpiece.

**Fig. 60** Joining of connections with hollow mandrels **a** without support **b** with support [188]
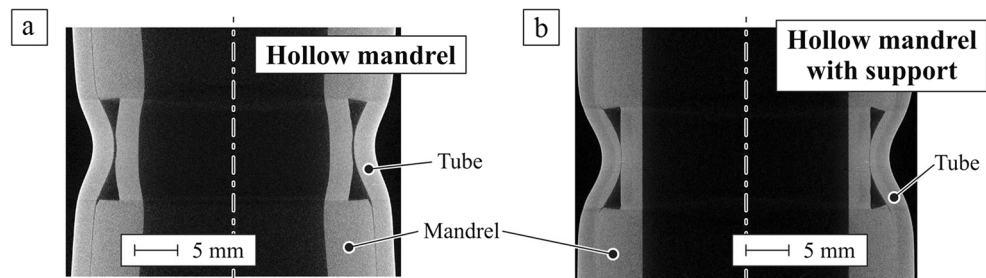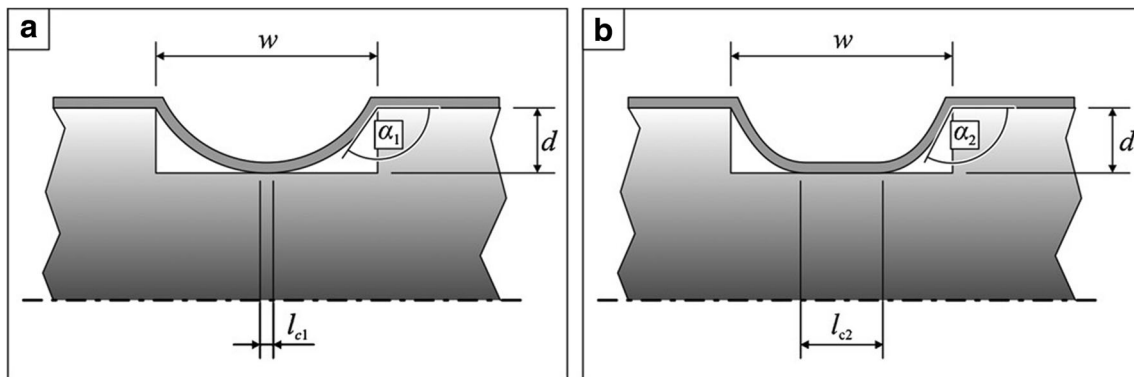
**Fig. 61** **a** Joint manufactured with the minimal necessary discharge energy to fill the groove. **b** Joint produced with a higher discharge energy [191]

Increasing the groove depth and decreasing its width leads to more deformation of the tube and thus higher stiffness and lower angle $\alpha$. The angle $\alpha$ decreases with increasing the discharge energy, and a force-fit can be created in addition to the form-fit [191]. Furthermore, the shape of the groove (i.e., rectangular, circular and triangular) also influences the joint strength. Rectangular grooves showed the highest strength and triangular grooves resulted in the weakest joints [191]. It is because of greater interference stresses in rectangular grooves. For both circular and rectangular grooves, narrower and deeper grooves lead to higher joint strength [192], but until a critical point. Weddeling et al. [182] introduced an analytical joint strength prediction method for joints with the circular grooves. However, the model can be adaptable to the two other form-fit elements (rectangular and triangular). The parameters considered by the model are the geometrical characteristics of the joining zone, such as groove dimensions and shapes and the material properties of the joining partners.

The surface conditions of the joining partners also have an essential influence on joint quality. The joint force, which is the ability to resist external loading, is expressed as $F_{joint} = F_{friction} + F_{groove}$ [15], where $F_{friction}$ is a frictional force arising from contact pressure, and $F_{groove}$ is the restraining force caused by the groove. Since the frictional force resulting from the residual hoop stress is not sufficient to support heavy external loading,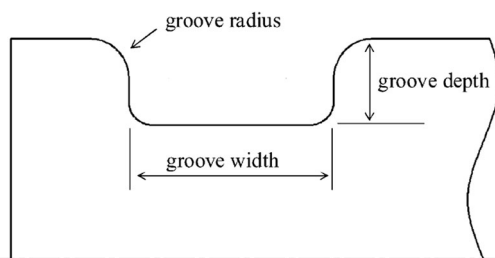 the restraining force must be maximized to make a strong joint. The effect of different machining and shot peening processes on the surface conditions of the workpieces and the joint strength are investigated by Hammers et al. [193]. It is stated that increasing the surface roughness and surface hardening of the parts lead to increased joint strength. Furthermore, Eguia et al. [183] reported that knurled mandrel leads to increased torsion strength. Form-fit joints can be created with sheet metal joining too. Jimbert et al. [194] used an innovative electromagnetically assisted hemming (EM hemming) process for hemming of aluminum alloys. As mentioned in Sect. 5 aluminum is sensitive to hemming because of its poor formability, but by using high strain rate of the EMF process, it was successfully joined to a steel component. Jimbert et al. [195] conducted a two-step electromagnetic flanging and hemming process and influence of the relative positioning of the workpiece and tool coil and the discharge energy are investigated. Jimbert et al. [153] investigated the EM hemming process, numerically and experimentally. Figure 63 shows the experimental setup. First sheet metals were bent mechanically and then were positioned on the EMF machine until the hemming process been conducted. Figure 64 compares the sheets hemmed by EM hemming (right) and conventional hemming (left). Bending radius and cracking on the bending area in EM hemming is considerably lower than the conventional hemming. Discharge energy and coil height have a significant effect on EM hemming process [144]. Zajkani and Salamati [34] introduced electromagnetically assisted clinching (EM clinching) process to join low ductility materials by the clinching. Details are given in Sect. 3. EMF process was used for riveting titanium alloys [196]. The process is schematically illustrated in Fig. 65. The magnetic field produced in the flat coil accelerates an armature, which carries the die to upset the rivet. EM riveting has advantages, such as uniform deformation of the rivet shaft and stable quality of the riveting among the conventional riveting. EM riveting can effectively avoid the damage of composite material in case of joining titanium alloy and composite hybrid structure and deform the difficult to deformation materials, such as titanium alloys.
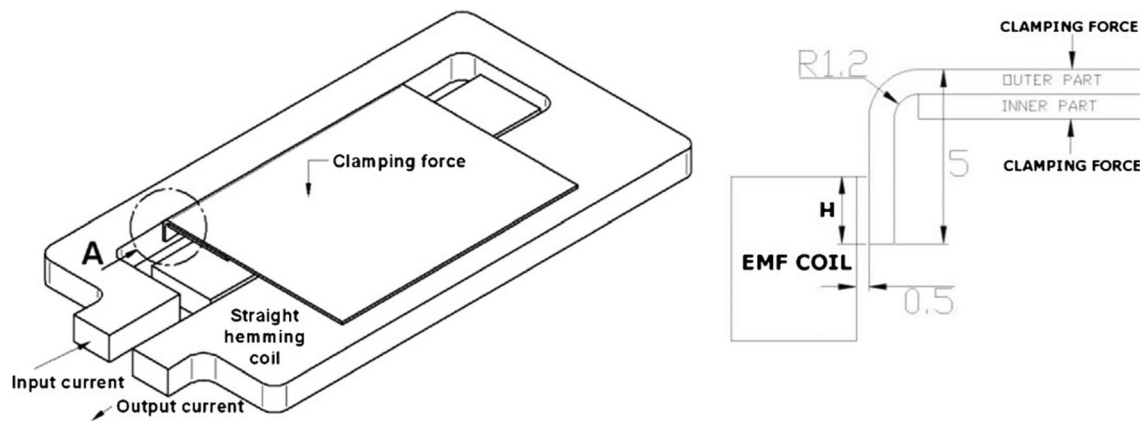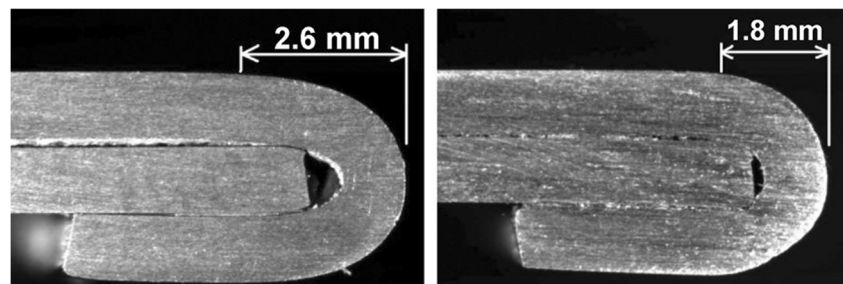


**Fig. 62** The geometric design parameters of the groove for form-fit joints [15]

**Fig. 63** EMF straight hemming experimental set-up (left) and detailed view of the main geometrical parameters (distances in millimeters) (right) [153]

## 10.3 Optimizations

Numerical simulation of EMF process is more complicated than other procedures. There are three ways to FE analysis of the process. First is a loosely coupled scheme that is used in some works such as Oliveira et al. [197]. In this method, the equations governed electromagnetic parts of the problem are assumed to be independent of the structural part of it. The other way is a fully coupled scheme that was used by Stiemer et al. [198]. In this method, electromagnetic and structural-mechanical simulations are iteratively and sequentially performed, and changing the workpiece geometry as a function of time is considered in solving governing equations in the electromagnetic part. Finally, the last method that is simpler than the former methods was used by some researchers such as Correia et al. [179], Uhlmann and Jurgasch [199], and Imbert et al. [200]. In this process, analysis is divided into two different sections: electromagnetic analysis and mechanical analysis, and the pressure resulted from the electromagnetic analysis is applied to the workpiece as a mechanical force. FE simulations were done to predict the effect of some critical parameters on joint strength in tube compression process by the third method. It is concluded that by increasing the discharge energy, the magnetic field density and magnetic pressure both increase and lead to stronger joint and interference stresses at the tube and mandrel surface lead to increase the joint strength [201].

Metallurgical joints can also be manufactured by EMF process that will be discussed in part C of this work.

## 11 Joining shaft-hub connections by lateral extrusion

Joining by lateral extrusion of a shaft-hub connection can be classified into joining by cold forging processes. In this joining by forming technology, shaft deforms elastic-plastically while the hub deforms elastically and resultantly a force-fit joint is generated (Fig. 66). Two important factors influencing the connection strength of such components are the tribological conditions within the contact area of both parts on the one hand and the usage of a suitable internal hub profile [202] on the other hand. The punch force, roundness deviation and cavity filling were determined to have the most effect on an appropriate internal hub profile [203]. The smaller profile eccentricity leads to the lower punch force, but more sophisticated internal hubs result in further increase in the connection strength. Utilizing this process is advantageous for manufacturing shaft-hub connections because there is no need for tight tolerances to ensure a proper connection and by determining optimum process parameters, high-strength torsional loads can be transmitted by such components.

Joining by indentation is a variant of the process in which there is a metallurgical bond on the contact surface. The transition from the force-fit mechanism to the metallurgical one

**Fig. 64** Conventionally, hemmed sample on the left and EMF hemmed sample on the right [153]

**Fig. 65** Schematic of electromagnetic riveting rationale.1 transformer; 2 current-rectifying silicon stack; 3 current limiting resistance; 4 capacitor bank; 5 discharge switch; 6 recoilmass; 7 flatcoil; 8 driver plate; 9 amplifier; 10 rivet; 11 plate stack;12 supporting base [196]
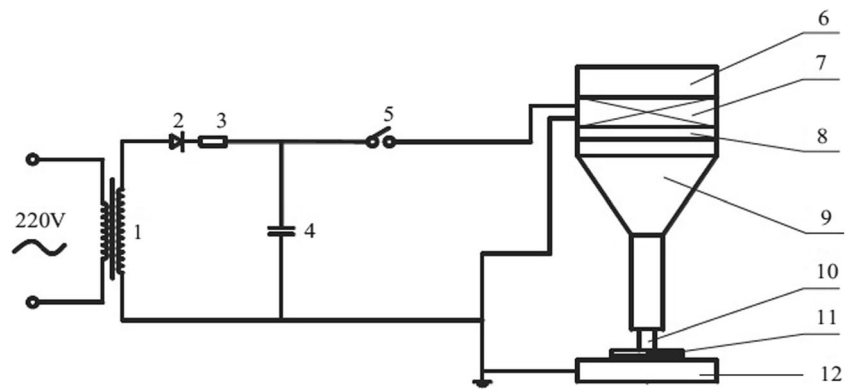
depends on the surface quality of the workpieces, material, compression force [204], and more generally to the severity of the plastic deformation. This process will be discussed in part B of this review article.

## 12 Other mechanical joining methods

There are some processes which could not be classified represented in the sections mentioned above. Such works are innovative or hybrid processes developed by hybridization of two or more conventional method which are briefly explained here.

### 12.1 Adhesive-embossing hybrid bonding method

Huang et al. [205] used a novel process for manufacturing a hybrid joint consisted of adhesive bonding and joining by plastic deformation to join aluminum and CFRP sheets. This process is called "adhesive-embossing hybrid bonding method." In this process, the adhesively bonded specimens were embossed with a hydraulic servo press. In the case of embossing under a warm state, the specimens were heated by an induction coil unit the target temperature, by using a thermocouple-based sensor-feedback system, because as stated by Yanagimoto and Ikeuchi [206], preheating to a specific temperature, increases the formability of thermosetting CFRPs. Furthermore, experimental parameters were
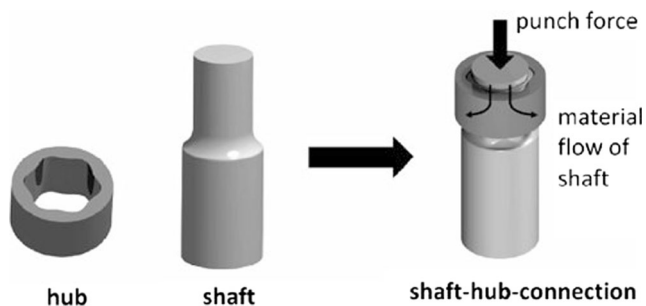
investigated systematically to improve the joining quality. Tensile strength, failure modes, and the negative effects of the process on the properties of the CFRP laminate were studied. As indicated in Fig. 67, the adhesive–embossing hybrid bonding method is superior in terms of tensile shear load and slip displacement among the four joining methods. The tensile shear load of mechanically bonded joints is typically larger than that of adhesively bonded joints, as demonstrated by Di Franco et al. [107]. However, in this case, adhesive bonding is advantageous, because the bonded specimen is very thin and thus, the adhered materials become much weaker owing to the stress concentration on the mechanical joints. After the tensile shear test, the failure modes for both rivet joining and adhesive-rivet hybrid joining were the shear-out failure and gentle ply drop-off failure, while the failure modes for adhesive bonding and adhesive–embossing hybrid bonding were mainly interfacial debonding and cohesive failure.

### 12.2 Tube end forming

Joining sheet panels to tubular profiles is necessary for a broad range of engineering applications. These parts are joined by mechanical fasteners or fusion welding and sometimes adhesive bonding. Alves et al. [207] offered a new joining by
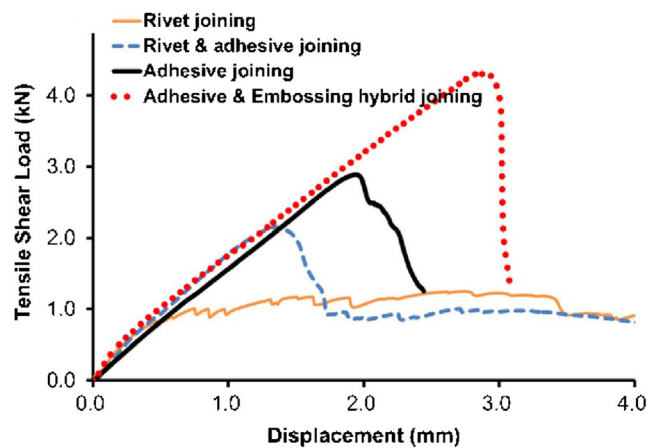

**Fig. 66** Joining of a shaft-hub connection by lateral extrusion [202]


**Fig. 67** Comparison of load-displacement curves for adhesive-embossing hybrid process and some other joining techniques [205]
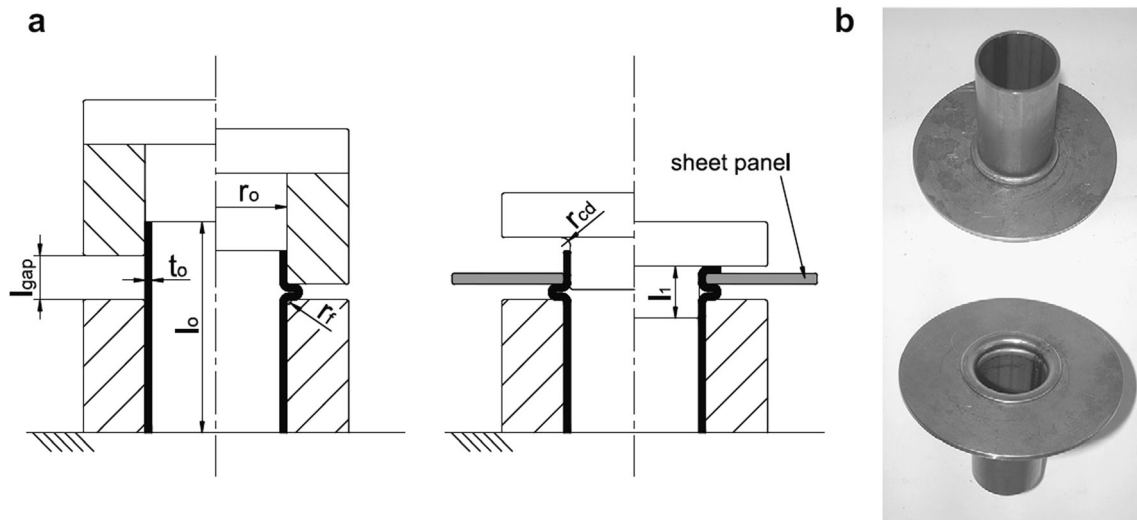
**Fig. 68** Joining sheet panels to thin-walled tubular profiles by tube end forming. **a** Schematic representation of the process. **b** Picture showing an application (circular sheet joined to a tube) [207]

plastic deformation process for manufacturing such parts. It is a two-stage tube end forming process that is schematically illustrated in Fig. 68a, and the manufactured part is shown in Fig. 68b. The process involves compression beading and external inversion. Compression beading is performed by forcing the upper tube end against the bottom tube end while leaving a gap opening between the dies that support/hold the tube. As compression progresses, the tube collapses under local buckling and gives rise to an axisymmetric bead at the gap opening (Fig. 68a, left). The sheet panel is then placed on top of the bead and joining is accomplished by compressing the upper free end of the tube with an appropriate external inversion punch until achieving the required clamp geometry (Fig. 68a, right). Furthermore, experimental observations complemented by FE modeling allowed to systemize the main parameters and to understand their influence in the overall process feasibility window. In another work, Alves and Martins [208] introduced a developed version of the above

process that is capable of fixing sheet panels to tubular profiles with a single ram stroke, to meet the demand of industry for shortening the production time and increasing the manufacturing rate. Schematic of the process, so-called "single-stroke joining by tube forming" is illustrated in Fig. 69. As seen fixing is accomplished by a sequence of two different modes of deformation that are commonly found in tube end forming processes: flaring and compression beading.

### 12.3 Sheet joining by tab bending and sheet-bulk compression

Pragana et al. [209] proposed a new joining by forming technique to connect two deformable sheets in a lap joint configuration. This technique combines partial cutting and bending with mechanical interlocking by sheet-bulk compression of tabs from the two sheets partially placed over one another (Fig. 70). In this process first, the tabs are cut from the sheets

**Fig. 69** Schematic representation of single-stroke mechanical joining of sheet panels to tubular profiles by tube forming [208]
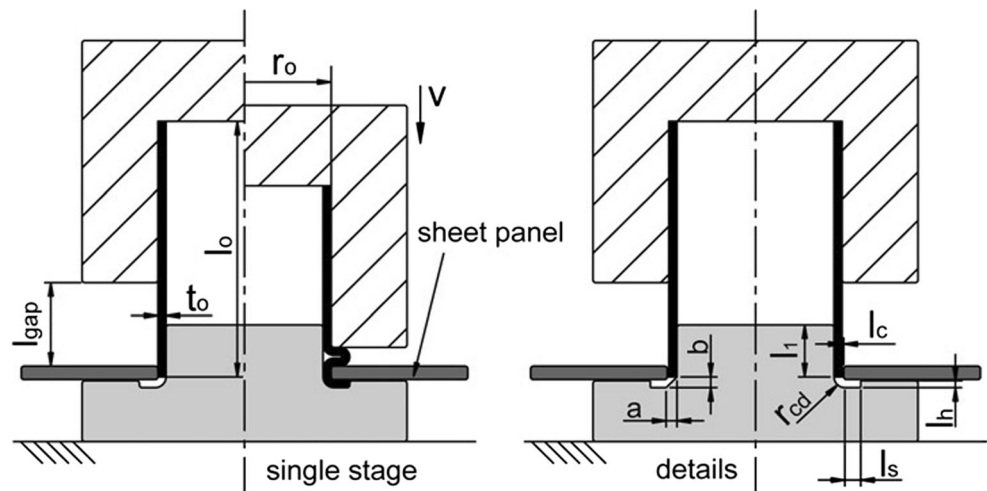
**Fig. 70** The sheet joining by tab bending and sheet-bulk compression: **a** partial cutting, **b** bending, **c** mechanical interlocking by sheet-bulk compression, and **d** photograph with a cross section detail of the joint [209]
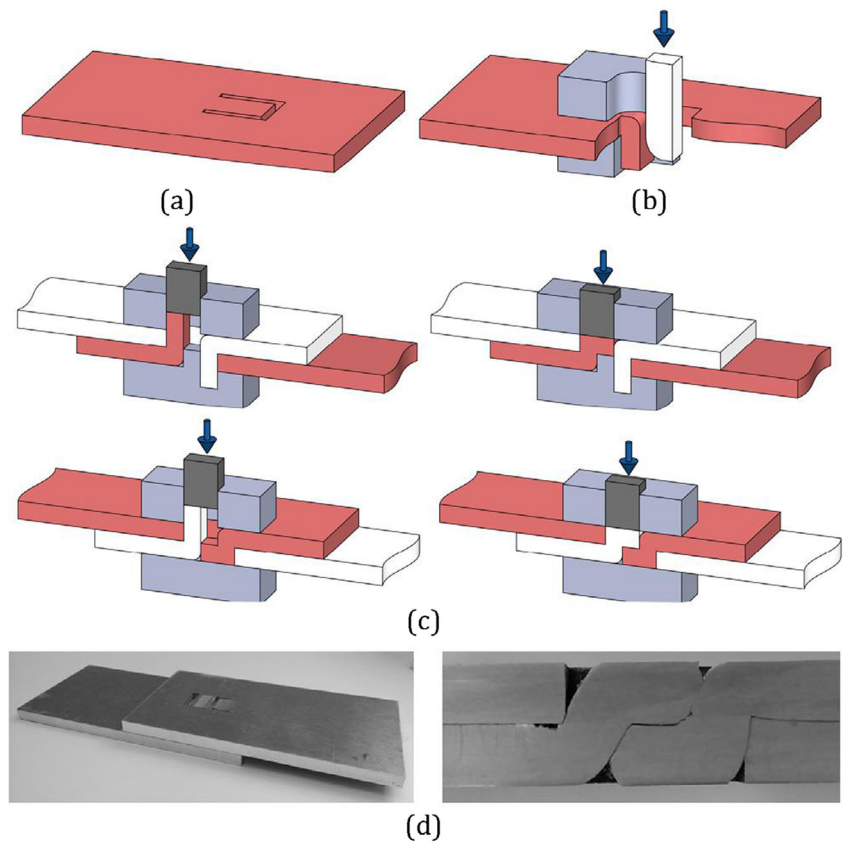


(a)   (b)

(c)

(d)

**Table 9** The most important applications for joining by mechanical forming technologies

| Joining technique | Applications | Similar methods | Relative strength[a] |
|---|---|---|---|
| Clinching | Automotive (especially for body-in-white applications); electronics; construction; lightweight manufacturing; aerospace; home appliances; heating and ventilating; dissimilar joining. it is mostly suitable for non-critical joints. | SPR, RSW | Lower |
| SPR | The most important application is on the automotive industry to join hoods, fenders, doors, deck-lids, lift-gates, body-in-white, seat structures, door modules, moon-roof structures and other hardware. It is a promising technique for automated vehicle construction [210]. | Clinching, RSW | Relatively higher |
| Hemming | It is generally used for manufacturing automotive body panels | Stud welding | Relatively lower but with a better-look design |
| Rolling | Joining tubular parts used for automotive body and chassis; camshafts; frame-structures; heating and ventilating; lightweight manufacturing. | EMF joining, die-less hydroforming, crimping | Relatively comparable but with a more complicated setup |
| Die-less hydroforming | Joining tubular parts used for automotive body and chassis; frame-structure; automotive parts such as tie bar, engine mount bracket, sheet/tube sub-frame, and cooling tubes; heating and ventilating; lightweight manufacturing. | EMF joining, crimping, rolling | Relatively comparable |
| Incremental forming | Multi-layered tubular and hollow frames; tube/tube and tube/mandrel connections; tubular connections with a; smart structures; automotive; aerospace. | EMF joining, crimping, rolling, die-less hydroforming | Relatively comparable |
| Hydraulic/mechanical crimping | Joining tubular parts used for automotive body and chassis; frame-structures; heating and ventilating; lightweight manufacturing. | EMF joining, rolling, die-less hydroforming | Relatively comparable |
| EMF | Joining tubular parts used for automotive body and chassis; frame-structures; heating and ventilating; lightweight manufacturing. | Crimping, rolling, die-less hydroforming | Relatively comparable |
| Lateral extrusion | Joining shaft-hub connections | – | – |

[a] Compared to similar joining techniques

by means of wire electro-discharge machining, waterjet cutting, laser cutting, and so on (Fig. 70a). Then, the two sheets are partially placed on each other as shown in Fig. 70b. A toolset is used to bend the tabs of each metallic sheet as shown in Fig. 70c. Finally, a lap joint with a cross-section illustrated in Fig. 70d can be manufactured. In the work of Pragana et al. [209] lap joints of AA 5754-H111 with 2.5 and 5.0 mm, thicknesses are manufactured. The joints manufactured by this new joining by forming method showed a superior shear strength compared to a joint manufactured by conventional tab bending process (almost twice). The morphology of the cracked surfaces reveals triggering of the cracks by shear followed by opening in tension due to the bending.

Finally, it should be mentioned that the various joining by forming methods are advanced technologies suitable for high-performance applications and high-end products. Using such technologies most of the limitations involved in conventional joining methods could be overcome, and a highly reliable, high quality, and a better-look (from an esthetic point of view) product can be manufactured. As a brief conclusion on the applications of the methods reviewed in this study, the most important applications of each one in the industry are summarized in Table 9. It should be noted that there is no limitation for fields of applications for joining by forming and numerous innovative and productive applications are available. Here, only the most important applications are listed.

# 13 Conclusions

Joining by plastic deformation technologies are reliable tools for joining processes in high-performance applications. Higher efficiency compared to conventional joining techniques and high capability in joining dissimilar materials are the most important advantages. Since the governing joining mechanism in mechanical joining by forming techniques, studied in this part A of the paper is either form-fit, force-fit, or a combination of these mechanisms, rather than metallurgical bonding, obtaining the efficiency of 100% (or higher) is nearly impossible, however they still retain their position as a powerful tool for joining. It is important that utilization of optimized tooling and processing parameters, would lead to significant improvements in joint mechanical behavior. Thus, realization and optimization of these parameters would result in a stronger and more reliable joint. However, there are several areas for further studies and advancement in this technological field, including the implementation of technologies on low-formability materials, improvement in mechanical behavior, the combination of different techniques in order to develop hybrid techniques, improvements in simulation techniques, and standardization of the various techniques. Future trends will be discussed in more detail in the final part of the review article (part C).

# References

1. Baldan A (2004) Adhesively-bonded joints in metallic alloys, polymers and composite materials: mechanical and environmental durability performance. J Mater Sci 39:4729–4797
2. Hart-Smith LJ (1999) A peel-type durability test coupon to assess interfaces in bonded, co-bonded, and co-cured composite structures. Int J Adhes Adhes 19(2–3):181–191
3. Crumple zones are well designed. [Online]. Available: http://www.suburbanautobody.com/Blog/entryid/15
4. Lambiase F, Ko DC (2016) Feasibility of mechanical clinching for joining aluminum AA6082-T6 and carbon fiber reinforced polymer sheets. Mater Des 107:341–352
5. Homberg W, Marré M, Beerwald C, Kleiner M (2006) Joining by forming of lightweight frame structures. Adv Mater Res 10:89–100
6. Mori K, Bay N, Fratini L, Micari F, Tekkaya AE (2013) Joining by plastic deformation. CIRP Ann Manuf Technol 62(2):673–694
7. Groche P, Wohletz S, Brenneis M, Pabst C, Resch F (2014) Joining by forming—a review on joint mechanisms, applications and future trends. J Mater Process Technol 214(10):1972–1994
8. Groche P, Turk M (2011) Smart structures assembly through incremental forming. CIRP Ann Manuf Technol 60:21–24
9. Mori K, Abe Y (2018) A review on mechanical joining of aluminium and high strength steel sheets by plastic deformation. Int J Light Mater Manuf 1(1):1–11
10. Godwin EW, Matthews FL (1980) A review of the strength of joints in fibre-reinforced plastics: Part 1. Mechanically fastened joints. Composites 11:155–160
11. Hart-Smith LJ (1980) Mechanically fastened joints for advanced composites—phenomenological considerations and simple analyses. Fibrous Composites in Structural Design 543–574
12. Kelly G (2004) Joining of carbon fibre reinforced plastics for automotive applications. Royal Institute of Technology Stockholm, Sweden
13. International Impulse Forming Group (2016) Joining by high velocity forming. [Online]. Available: http://i2fg.org/impulse-forming/joining-by-high-velocity-forming/
14. Salamati M, Soltanpour M, Fazli A and Zajkani A (2017) Parametric study on the electromagnetic force-fit joining of carbon fiber reinforced plastic and aluminum tubes. Procedia Eng 12th Int Conf Technol Plast ICTP 2017 207:986–991
15. Park YB, Kim HY, Oh SI (2005) Design of axial/torque joint made by electromagnetic forming. Thin-Walled Struct 43:826–844
16. Lambiase F, Di Ilio A (2013) Optimization of the clinching tools by means of integrated FE modeling and artificial intelligence techniques. Procedia CIRP 12:163–168
17. Lambiase F, Di Ilio A, Paoletti A (2015) Joining aluminium alloys with reduced ductility by mechanical clinching. Int J Adv Manuf Technol 77:1295–1304
18. Carboni M, Beretta S, Monno M (2006) Fatigue behaviour of tensile-shear loaded clinched joints. Eng Fract Mech 73:178–190
19. Pedreschi RF, Sinha BP (2008) An experimental study of cold formed steel trusses using mechanical clinching. Constr Build Mater 22:921–931
20. Abe Y, Mori K, Kato T (2012) Joining of high strength steel and aluminium alloy sheets by mechanical clinching with dies for control of metal flow. J Mater Process Technol 212:884–889
21. Su ZM, Lin PC, Lai WJ, Pan J (2015) Fatigue analyses of self-piercing rivets and clinch joints in lap-shear specimens of aluminum sheets. Int J Fatigue 72:53–65

22. Lambiase F, Di Ilio A (2015) Mechanical clinching of metal-polymer joints. J Mater Process Technol 215:12–19

23. Hamel V, Roelandt JM, Gacel JN, Schmit F (2000) Finite element modeling of clinch forming with automatic remeshing. Comput Struct 77:185–200

24. Neugebauer R, Kraus C, Dietrich S (2008) Advances in mechanical joining of magnesium. CIRP Ann Manuf Technol 57:283–286

25. Lambiase F (2013) Influence of process parameters in mechanical clinching with extensible dies. Int J Adv Manuf Technol 66:2123–2131

26. Lambiase F (2015) Joinability of different thermoplastic polymers with aluminium AA6082 sheets by mechanical clinching. Int J Adv Manuf Technol 80:1995–2006

27. Mucha J (2011) The analysis of rectangular clinching joint in the shearing test. Maint Reliab 3:45–50

28. Abe Y, Saito T, Nakagawa K, Mori K (2018) Rectangular shear clinching for joining of ultra-high strength steel sheets. Procedia Manuf 15:1354–1359

29. Lambiase F, Durante M, Di Ilio A (2016) Fast joining of aluminum sheets with glass fiber reinforced polymer (GFRP) by mechanical clinching. J Mater Process Technol 236:241–251

30. Mucha J (2011) The analysis of lock forming mechanism in the clinching joint. Mater Des 32:4943–4954

31. Lambiase F (2015) Mechanical behaviour of polymer-metal hybrid joints produced by clinching using different tools. Mater Des 87:606–618

32. Lambiase F, Di Ilio A (2014) An experimental study on clinched joints realized with different dies. Thin-Walled Struct 85:71–80

33. Ismail MIS, Buang AS (2018) Precision joining of steel-aluminum hybrid structure by clinching process. J Adv Manuf Technol 12(1):25–36

34. Zajkani A and Salamati M (2016) Numerical and experimental investigation of joining aluminium and carbon fiber reinforced composites by electromagnetic forming process. In: Proceedings of 7th International Conference on High Speed Forming—ICHSF-2016, pp 59–68

35. Krztoń H, Mucha J, Witkowski W (2016) The application of laboratory X-ray micro-diffraction to study the effects of clinching process in steel sheets. Acta Phys Pol A 130(4):985–987

36. He X, Zhang Y, Xing B, Gu F, Ball A (2015) Mechanical properties of extensible die clinched joints in titanium sheet materials. Mater Des 71:26–35

37. Neugebauer R, Mauermann R, Dietrich S, Kraus C (2007) A new technology for the joining by forming of magnesium alloys. Prod Eng Res Dev 1:65–70

38. Xing B, He X, Wang Y, Yang H, Deng C (2015) Study of mechanical properties for copper alloy H62 sheets joined by self-piercing riveting and clinching. J Mater Process Technol 216:28–36

39. Lee CJ, Kim JY, Lee SK, Ko DC, Kim BM (2010) Parametric study on mechanical clinching process for joining aluminum alloy and high-strength steel sheets. J Mech Sci Technol 24:123–126

40. Varis JP (2003) The suitability of clinching as a joining method for high-strength structural steel. J Mater Process Technol 132:242–249

41. Abe Y, Kishimoto M, Kato T, Mori K (2009) Joining of hot-dip coated steel sheets by mechanical clinching. Int J Mater Form 2(1):291–294

42. Zhou Y, Lan F, and Chen J (2010) Influence of tooling geometric parameters on clinching joint properties for steel-aluminum hybrid car-body structures. In: Computer Science and Information Technology (ICCSIT), 2010 3rd IEEE International Conference on, Volume 5, pp 441–445

43. Kaščák L, Spišák E, Kubik R, Mucha J (2016) FEM analysis of clinching tool load in a joint of dual-phase steels. Strength Mater. 48(4):533–539

44. Kaščák L, Mucha J, Spišák E, Kubik R (2017) Wear study of mechanical clinching dies during joining of advanced high-strength steel sheets. Strength Mater 49(5):726–737

45. Lüder S, Härtel S, Binotsch C, Awiszus B (2014) Influence of the moisture content on flat-clinch connection of wood materials and aluminium. J Mater Process Technol 214:2069–2074

46. Lee CJ, Lee JM, Ryu HY, Lee KH, Kim BM, Ko DC (2014) Design of hole-clinching process for joining of dissimilar materials—Al6061-T4 alloy with DP780 steel, hot-pressed 22MnB5 steel , and carbon fiber reinforced plastic. J Mater Process Technol 214:2169–2178

47. Lee SH, Lee CJ, Lee KH, Lee JM, Kim BM, Ko DC (2014) Influence of tool shape on hole clinching for carbon fiber-reinforced plastic and SPRC440. Adv Mech Eng 6:1–12

48. Busse S, Merklein M, Roll K, Ruther M, Zürn M (2010) Development of a mechanical joining process for automotive body-in-white production. Int J Mater Form 3(1):1059–1062

49. Meschut G, Matzke M, Hoerhold R, Olfermann T (2014) Hybrid technologies for joining ultra-high-strength boron steels with aluminum alloys for lightweight car body structures. Procedia CIRP 23:19–23

50. Han D, Hörhold R, Wiesenmayer S, Merklein M, Meschut G (2018) Investigation of the influence of tool-sided parameters on deformation and occurring tool loads in shear-clinching processes. Procedia Manuf 15:1346–1353

51. Hörhold R, Müller M, Merklein M, Meschut G (2016) Mechanical properties of an innovative shear-clinching technology for ultra-high-strength steel and aluminium in lightweight car body structures. Weld World 60(3):613–620

52. Abibe AB, Amancio-Filho ST, Dos Santos JF, Hage E (2011) Development and analysis of a new joining method for polymer-metal hybrid structures. J Thermoplast Compos Mater 24:233–249

53. Abibe AB, Amancio-filho ST, Santos JF, Hage E Jr (2013) Mechanical and failure behaviour of hybrid polymer-metal staked joints. Mater Des 46:338–347

54. Neugebauer R, Mauermann R, Grützner R (2008) Hydrojoining. Int J Mater Form 1(1):1303–1306

55. Chen C, Zhao S, Cui M, Han X, Fan S (2016) Mechanical properties of the two-steps clinched joint with a clinch-rivet. J Mater Process Technol 237:361–370

56. Mucha J, Witkowski W (2014) The clinching joints strength analysis in the aspects of changes in the forming technology and load conditions. Thin Walled Struct 82:55–66

57. Kaščák L, Spišák E, Mucha J (2013) Clinchrivet as an alternative method to resistance spot welding. Acta Mech Autom 7(2):79–82

58. Mucha J, Kaščák L and Spišák E (2013) The experimental analysis of forming and strength of clinch riveting sheet metal joint made of different materials. Adv Mech Eng 5:1–11

59. Zhang Y, Shan H, Li Y, Guo J, Luo Z, Ma CY (2017) Joining aluminum alloy 5052 sheets via novel hybrid resistance spot clinching process. Mater Des 118:36–43

60. Zhang Y, Wang C, Shan H, Li Y, Luo Z (2018) High-toughness joining of aluminum alloy 5754 and DQSK steel using hybrid clinching–welding process. J Mater Process Technol 259:33–44

61. Wang X, Li C, Ma Y, Shen Z, Sun X, Sha C, Gao S, Li L, Liu H (2016) An experimental study on micro clinching of metal foils with cutting by laser shock forming. Materials (Basel) 9(7):571

62. Wang X, Li X, Li C, Shen Z, Ma Y, Liu H (2018) Laser shock micro clinching of Al/Cu. J Mater Process Technol 258(April):200–210

63. Osten J, Söllig P, Reich M, Kalich J, Füssel U, Kessler O (2014) Softening of high-strength steel for laser assisted clinching. Adv Mater Res 966–967:617–627

64. Lambiase F (2015) Clinch joining of heat-treatable aluminum AA6082-T6 alloy under warm conditions. J Mater Process Technol 225:421–432

65. Zhou H, Cui H, Qin QH (2018) Influence of ultrasonic vibration on the plasticity of metals during compression process. J Mater Process Technol 251(May 2018):146–159

66. Heßeln F, Wanner MC (2014) Ultrasonic assisted clinching of aluminium alloy sheets. Adv Mater Res 966–967:641–650

67. Mizushima D, Sato T, Murakami H, Ohtake N (2011) Stirring phenomenon of aluminum sheets by ultrasonic vibrations and its application to clinching. J Solid Mech Mater Eng 5(12):810–824

68. Beyer E, Kalich J, Kotter H (2006) Vorrichtung und Verfahren zum formschlussigen Verbinden von Werkstucken. Patent DE102004062896B4

69. He X (2017) Clinching for sheet materials. Sci Technol Adv Mater 18(1):381–405

70. Reich M, Osten J, Milkereit B, Kalich J, Füssel U, Kessler O (2014) Short-time heat treatment of press hardened steel for laser assisted clinching. Mater Sci Technol 30(11):1287–1296

71. Chen LW, Huang JM, Hsu YC (2015) Investigation of the clinching process combines with hot stamping process for high-strength steel sheets. MATEC Web Conf 21

72. Chen LW, Cai MJ (2018) Development of a hot stamping clinching tool. J Manuf Process 34(June):650–658

73. Lambiase F, Paoletti A, Di Ilio A (2017) Advances in mechanical clinching: employment of a rotating tool. Procedia Eng 183:200–205

74. Lambiase F, Paoletti A (2018) Friction-assisted clinching of aluminum and CFRP sheets. J Manuf Process 31:812–822

75. Lambiase F, Paoletti A (2018) Mechanical behavior of AA5053/polyetheretherketone (PEEK) made by friction assisted joining. Compos Struct 189:70–78

76. Mota NG, Costa CPA (2005) A comparative study between the sheet joining processes by point TOX and spot welding, In Proceedings of the Annual Congress of the Brazilian Society for Metallurgy and Materials, pp 2733–2741

77. Mucha J (2011) Joining the car-body sheets using clinching process with various thickness and mechanical property arrangements. Arch Civ Mech Eng XI(1):135–148

78. He X, Zhao L, Yang H, Xing B, Wang Y, Deng C, Gu F, Ball A (2014) Investigations of strength and energy absorption of clinched joints. Comput Mater Sci 94:58–65

79. Lambiase F, Di Ilio A (2016) Damage analysis in mechanical clinching: experimental and numerical study. J Mater Process Technol 230:109–120

80. Oudjene M, Ben-Ayed L (2008) On the parametrical study of clinch joining of metallic sheets using the Taguchi method. Eng Struct 30:1782–1788

81. Roux E, Bouchard PO (2013) Kriging metamodel global optimization of clinching joining processes accounting for ductile damage. J Mater Process Technol 213:1038–1047

82. Wang X, Li X, Shen Z, Ma Y, Liu H (2018) Finite element simulation on investigations, modeling, and multiobjective optimization for clinch joining process design accounting for process parameters and design constraints. Int J Adv Manuf Technol 96(9–12):3481–3501

83. Kaščák L, Spišák E, Kubik R, Mucha J (2017) Finite element calculation of clinching with rigid die of three steel sheets. Strength Mater 49(4):488–499

84. De Paula AA, Aguilar MTP, Pertence AEM, Cetlin PR (2007) Finite element simulations of the clinch joining of metallic sheets. J Mater Process Technol 182:352–357

85. Abe Y, Kato T, Mori K, Nishino S (2014) Mechanical clinching of ultra-high strength steel sheets and strength of joints. J Mater Process Technol 214(10):2112–2118

86. Oudjene M, Ben-ayed L, Delameziere A, Batoz JL (2008) Shape optimization of clinching tools using the response surface methodology with moving least-square. J Mater Process Technol 209:289–296

87. Lee CJ, Kim JY, Lee SK, Ko DC, Kim BM (2010) Design of mechanical clinching tools for joining of aluminium alloy sheets. Mater Des 31:1854–1861

88. Ferreira SLC, Bruns RE, Ferreira HS, Matos GD, David JM, Brand GC, Silva EGP, Reis PS, Souza AS, Santos WNL (2007) Box-Behnken design: an alternative for the optimization of analytical methods. Anal Chim Acta 597:179–186

89. Dean A, Sahraee S, Reinoso J, Rolfes R (2016) Finite deformation model for short fibre reinforced composites: application to hybrid metal-composite clinching joints. Compos Struct 151:162–171

90. Han L, Chrysanthou A (2008) Evaluation of quality and behaviour of self-piercing riveted aluminium to high strength low alloy sheets with different surface coatings. Mater Des 29:458–468

91. Abe Y, Kato T, Mori K (2009) Self-piercing riveting of high tensile strength steel and aluminium alloy sheets using conventional rivet and die. J Mater Process Technol 209:3914–3922

92. He X, Pearson I, Young K (2008) Self-pierce riveting for sheet materials: state of the art. J Mater Process Technol 199:27–36

93. Pickin CG, Young K, Tuersley I (2007) Joining of lightweight sandwich sheets to aluminium using self-pierce riveting. Mater Des 28:2361–2365

94. Han L, Chrysanthou A, Young KW (2007) Mechanical behaviour of self-piercing riveted multi-layer joints under different specimen configurations. Mater Des 28:2024–2033

95. Ioannou J (2009) Mechanical behavior and corrosion of interstitial-free steel to aluminum alloy self-piercing riveted joints. University of Hertfordshire, Hertfordshire

96. Voelkner W (2000) Present and future developments of metal forming: selected examples. J Mater Process Technol 106:236–242

97. Durandet Y, Deam R, Beer A, Song W, Blacket S (2010) Laser assisted self-pierce riveting of AZ31 magnesium alloy strips. Mater Des 31:S13–S16

98. Han L, Chrysanthou A, O'Sullivan JM (2006) Fretting behaviour of self-piercing riveted aluminium alloy joints under different interfacial conditions. Mater Des 27:200–208

99. Barnes TA, Pashby IR (2000) Joining techniques for aluminium spaceframes used in automobiles. Part II—adhesive bonding and mechanical fasteners. J Mater Process Technol 99:72–79

100. Abe Y, Kato T, Mori K (2006) Joinability of aluminium alloy and mild steel sheets by self piercing rivet. J Mater Process Technol 177:417–421

101. Fratini L, Ruisi VF (2009) Self-piercing riveting for aluminium alloys-composites hybrid joints. Int J Adv Manuf Technol 43:61–66

102. Hoang NH, Porcaro R, Langseth M, Hanssen AG (2010) Self-piercing riveting connections using aluminium rivets. Int J Solids Struct 47(3–4):427–439

103. http://www.repairerdrivennews.com/2016/09/02/self-piercing-rivets-get-another-boost-as-stanley-enters-north-american-market/. (2016)

104. Abe Y, Kato T, Mori K (2008) Self-pierce riveting of three high strength steel and aluminium alloy sheets. Int J Mater Form 1(1):1271–1274

105. Meschut G, Gude M, Augenthaler F, Geske V (2014) Evaluation of damage to carbon-fibre composites induced by self-pierce riveting. Procedia CIRP 18:186–191

106. Ueda M, Miyake S, Hasegawa H, Hirano Y (2012) Instantaneous mechanical fastening of quasi-isotropic CFRP laminates by a self-piercing rivet. Compos Struct 94(11):3388–3393

107. Di Franco G, Fratini L, Pasta A (2012) Influence of the distance between rivets in self-piercing riveting bonded joints made of carbon fiber panels and AA2024 blanks. Mater Des 35:342–349

108. Briskham P, Blundell N, Han L, Hewitt R, Young K, Boomer D (2006) Comparison of self-pierce riveting , resistance spot welding and spot friction joining for aluminium automotive sheet. SAE Technical Paper 2006-01-0774

109. Han L, Thornton M, Shergold M (2010) A comparative study between self-piercing riveting and resistance spot welding of aluminium sheets for the automotive industry. Mater Des 31(3): 1457–1467

110. Lennon R, Pedreschi R, Sinha BP (1999) Comparative study of some mechanical connections in cold formed steel. Constr Build Mater 13:109–116

111. Mori K, Abe Y, Kato T (2012) Mechanism of superiority of fatigue strength for aluminium alloy sheets joined by mechanical clinching and self-pierce riveting. J Mater Process Technol 212: 1900–1905

112. Mucha J, Witkowski W (2015) Mechanical behavior and failure of riveting joints in tensile and shear tests. Strength Mater 47(5):755–769

113. Mucha J (2014) The numerical analysis of the effect of the joining process parameters on self-piercing riveting using the solid rivet. Arch Civ Mech Eng 14(3):444–454

114. Mucha J (2015) The failure mechanics analysis of the solid self-piercing riveting joints. Eng Fail Anal 47:77–88

115. Sun X, Stephens EV, Khaleel MA (2007) Fatigue behaviors of self-piercing rivets joining similar and dissimilar sheet metals. Int J Fatigue 29:370–386

116. Li B, Fatemi A (2006) An experimental investigation of deformation and fatigue behavior of coach peel riveted joints. Int J Fatigue 28:9–18

117. Fu M, Mallick PK (2003) Fatigue of self-piercing riveted joints in aluminum alloy 6111. Int J Fatigue 25:183–189

118. Chen YK, Han L, Chrysanthou A, O'Sullivan JM (2003) Fretting wear in self-piercing riveted aluminium alloy sheet. Wear 255: 1463–1470

119. Zhang X, He X, Xing B, Zhao L, Lu Y, Gu F, Ball A (2016) Influence of heat treatment on fatigue performances for self-piercing riveting similar and dissimilar titanium, aluminium and copper alloys. Mater Des 97:108–117

120. Lee MH, Kim HY, Oh SI (2006) Crushing test of double hat-shaped members of dissimilar materials with adhesively bonded and self-piercing riveted joining methods. Thin-Walled Struct 44: 381–386

121. Porcaro R, Langseth M, Hanssen AG, Zhao H, Weyer S, Hooputra H (2008) Crashworthiness of self-piercing riveted connections. Int J Impact Eng 35:1251–1266

122. Han L, Young KW, Chrysanthou A, O'Sullivan JM (2006) The effect of pre-straining on the mechanical behaviour of self-piercing riveted aluminium alloy sheets. Mater Des 27:1108–1113

123. Johnson P, Cullen JD, Sharples L, Shaw A, Al-shamma'a AI (2009) Online visual measurement of self-pierce riveting systems to help determine the quality of the mechanical interlock. Measurement 42(5):661–667

124. Xie Z, Yan W, Yu C, Mu T, Song L (2018) Experimental investigation of cold-formed steel shear walls with self-piercing riveted connections. Thin-Walled Struct 131(May):1–15

125. He X, Gu F, Ball A (2012) Recent development in finite element analysis of self-piercing riveted joints. Int J Adv Manuf Technol 58:643–649

126. Mori K, Kato T, Abe Y, Ravshanbek Y (2006) Plastic joining of ultra high strength steel and aluminium alloy sheets by self piercing rivet. Ann CIRP 55(1):283–286

127. Mucha J (2011) A study of quality parameters and behaviour of self-piercing riveted aluminium sheets with different joining conditions. J Mech Eng 57(4):323–333

128. Porcaro R, Hanssen AG, Langseth M, Aalberg A (2006) Self-piercing riveting process: an experimental and numerical investigation. J Mater Process Technol 171:10–20

129. Cai W, Wang PC, Yang W (2005) Assembly dimensional prediction for self-piercing riveted aluminum panels. Int J Mach Tools Manuf 45:695–704

130. Qu SG, Deng WJ (2008) Finite element simulation of the self-piercing riveting process. In: Proceedings of International Mechanical Engineering Congress and Exposition, pp 1–7

131. Porcaro R, Hanssen AG, Langseth M, Aalberg A (2006) The behaviour of a self-piercing riveted connection under quasi-static loading conditions. Int J Solids Struct 43:5110–5131

132. Westerberg C (2002) Finite element simulation of crash testing of self-piercing rivet joints, peel specimen. MS Dissertation. Lund University, Sweden

133. Carandente M, Dashwood RJ, Masters IG, Han L (2016) Improvements in numerical simulation of the SPR process using a thermo-mechanical finite element analysis. J Mater Process Technol 236:148–161

134. Li Y, Wei Y, Wang Z, Li Z (2013) Friction self-pierce riveting of aluminum alloy AA6061-T6 to magnesium alloy AZ31B. J Manuf Sci Eng 135(6):061007

135. Ma Z, Li Y, Hu Y, Lou W, Lin M (2016) Modeling of friction self-piercing riveting of aluminum to magnesium. J Manuf Sci Eng 138:061007

136. Liu X, Lim YC, Li Y, Tang W, Ma Y, Feng Z, Ni J (2016) Effects of process parameters on friction self-piercing riveting of dissimilar materials. J Mater Process Technol 237:19–30

137. Ma Y, Xian X, Lou M, Li Y, Lin Z (2017) Friction self-piercing riveting (F-SPR) of dissimilar materials. Procedia Eng 207:950–955

138. Mucha J (2013) The effect of material properties and joining process parameters on behavior of self-pierce riveting joints made with the solid rivet. Mater Des 52:932–946

139. Hahn O, Meschut G, Bergau M, Matzke M (2014) Self-pierce riveting and hybrid joining of boron steels in multi-material and multi-sheet joints. Procedia CIRP 18:192–196

140. Li Y, Wei Z, Wang Z, Li Y (2013) Friction self-piercing riveting of aluminum alloy AA6061-T6 to magnesium alloy AZ31B. J Manuf Sci Eng 135(6):7. 061007

141. Livatyali H, Muderrisoglu A, Ahmetoglu MA, Akgerman N, Kinzel GL, Altan T (2000) Improvement of hem quality by optimizing-anging and pre-hemming operations using computer aided die design. J Mater Process Technol 98:41–52

142. Svensson M, Mattiasson K (2002) Three-dimensional simulation of hemming with the explicit FE-method. J Mater Process Technol 128:142–154

143. Zhang G, Hao H, Wu X, Hu SJ (2000) An experimental investigation of curved surface-straight edge hemming. J Manuf Process 2(4):241–246

144. Shang J, Wilkerson L, Hatkevich S (2011) Hemming of aluminum alloy sheets using electromagnetic forming. J Mater Eng Perform 20:1370–1377

145. Zhang G, Hu SJ, Wu X (2003) Numerical analysis and optimization of hemming processes. J Manuf Process 5(1):87–96

146. Altan AE, Tekkaya T (2012) Sheet metal forming, processes and applications. ASM International, Materials Park, Ohio

147. Livatyali H, Larris SJ (2004) Experimental investigation on forming defects in flat surface-convex edge hemming: roll, recoil and warp. J Mater Process Technol 153–154:913–919

148. Wanintradul C, Golovashchenko SF, Gillard AJ, Smith LM (2014) Hemming process with counteraction force to prevent creepage. J Manuf Process 16(3):379–390

149. Svensson M and Mattiasson K (2000) Simulation of hemming of automotive body components with the explicit FE-method. In: European Congress on Computational Methods in Applied Sciences and Engineering, pp 1–12

150. Le Maoût N, Thuillier S, Manach PY (2010) Drawing , flanging and hemming of metallic thin sheets: a multi-step process. Mater Des 31:2725–2736

151. Huang YM (2007) An elasto-plastic finite element analysis of the sheet metal stretch flanging process. Int J Adv Manuf Technol 34:641–648

152. Hamedon Z, Mori K, Abe Y (2014) Hemming for joining high strength steel sheets. Procedia Eng 81:2074–2079

153. Jimbert P, Eguia I, Perez I, Gutierrez MA, Hurtado I (2011) Analysis and comparative study of factors affecting quality in the hemming of 6016T4AA performed by means of electromagnetic forming and process characterization. J Mater Process Technol 211:916–924

154. Muderrisoglu A, Murata M, Ahmetoglu MA, Kinzel G, Altan T (1996) Bending, flanging, and hemming of aluminum sheet-an experimental study. J Mater Process Technol 59:10–17

155. Lin G, Iyer K, Hu SJ, Cai W, Marin SP (2005) A computational design-of-experiments study of hemming processes for automotive aluminium alloys. J Eng Manuf 219:711–722

156. Golovashchenko SF (2005) Sharp flanging and flat hemming of aluminum exterior body panels. J Mater Eng Perform 14:508–515

157. Hu X, Zhao Y, Huang S, Li S, Lin Z (2012) Numerical analysis of the roller hemming process. Int J Adv Manuf Technol 62:543–550

158. Hu X, Lin ZQ, Li SH, Zhao YX (2010) Fracture limit prediction for roller hemming of aluminum alloy sheet. Mater Des 31:1410–1416

159. Thuillier S, Le Maout N, Manach PY, Debois D (2008) Numerical simulation of the roll hemming process. J Mater Process Technol 198:226–233

160. Levinson A, Mishra RK, Doherty RD, Surya RK (2012) Microstructure evolution during roller hemming of AZ31B magnesium sheet. Metall Mater Trans A 43A:3824–3833

161. Carsley J, Kim S (2007) Warm hemming of magnesium sheet. J Mater Eng Perform 16:331–338

162. Hagedorn M, Weinert K (2004) Manufacturing of composite workpieces with rolling tools. J Mater Process Technol 153–154:323–329

163. Przybylski W, Wojciechowski J, Klaus A, Marré M, Kleiner M (2008) Manufacturing of resistant joints by rolling for light tubular structures. Int J Adv Manuf Technol 35:924–934

164. Merklein M, Geiger M, Celeghini M (2005) Combined tube and double sheet hydroforming for the manufacturing of complex parts. CIRP Ann Manuf Technol 54(1):199–204

165. Marre M, Ruhstorfer M, Tekkayya AE, Zaeh MF (2009) Manufacturing of light-weight frame structures by innovative joining by forming processes. Int J Mater Form 2(1):307–310

166. Marre M, Gies S, Maevus F, Tekkaya AE (2010) Joining of light-weight frame structures by die-less hydroforming. Int J Mater Form 3(1):1031–1034

167. Groche P, Tibari K (2006) Fundamentals of angular joining by means of hydroforming. Ann CIRP 55(1):259–262

168. Wang X, Li P, Wang R (2005) Study on hydro-forming technology of manufacturing bimetallic CRA-lined pipe. Int J Mach Tools Manuf 45:373–378

169. Henrard C, Habraken AM, Szekeres A, Duflou JR, He S, Van Bael A, Van Houtte P (2005) Comparison of FEM simulations for the incremental forming process. Adv Mater Res 6–8:533–542

170. Groche P, Fritsche D, Tekkaya AE, Allwood JM, Hirt G, Neugebauer R (2007) Incremental bulk metal forming. Ann CIRP 56(2):635–656

171. Mohebbi MS, Akbarzadeh A (2010) A novel spin-bonding process for manufacturing multilayered clad tubes. J Mater Process Technol 210:510–517

172. Turk M and Groche P (2010) Integration of adaptive components by incremental forming processes. In: SPIE 7643, Active and Passive Smart Structures and Integrated Systems 2010, 76431I

173. Zhang Q, Jin K, Mu D (2014) Tube/tube joining technology by using rotary swaging forming method. J Mater Process Technol 214(10):2085–2094

174. Cho JR, Song JI (2007) Swaging process of power steering hose: its finite element analysis considering the stress relaxation. J Mater Process Technol 187–188:497–501

175. Cho JR, Song JI, Noh KT, Jeon DH (2005) Nonlinear finite element analysis of swaging process for automobile power steering hose. J Mater Process Technol 170:50–57

176. Shirgaokar M, Cho H, Ngaile G, Altan T, Yu JH, Balconi J, Rentfrow R, Worrell WJ (2004) Optimization of mechanical crimping to assemble tubular components. J Mater Process Technol 146:35–43

177. Pavloušková Z, Klakurková L, Man O, Švejcar J (2015) Assessment of the cause of cracking of hydraulic hose clamps. Eng Fail Anal 56:14–19

178. Shirgaokar M, Ngaile G, Altan T, Yu JH, Balconi J, Rentfrow R, Worrell WJ (2004) Hydraulic crimping: application to the assembly of tubular components. J Mater Process Technol 146:44–51

179. Correia JPM, Siddiqui MA, Ahzi S, Belouettar S, Davies R (2008) A simple model to simulate electromagnetic sheet free bulging process. Int J Mech Sci 50(10–11):1466–1475

180. Harvey GW and Brower DF (1958) Metal forming device and method. 2976907

181. Psyk V, Risch D, Kinsey BL, Tekkaya AE, Kleiner M (2011) Electromagnetic forming—a review. J Mater Process Technol 211(5):787–829

182. Weddeling C, Walter V, Haupt P, Tekkaya AE, Schulze V, André K (2015) Joining zone design for electromagnetically crimped connections. J Mater Process Technol 225:240–261

183. Eguia I, Zhang P, Daehn GS (2004) Improved crimp-joining of aluminum tubes onto mandrels with undulating surfaces. In: Proceedings of 1st International Conference on High Speed Forming - ICHSF2004, pp 161–170

184. Hwang WS, Kim NH, Sohn HS, Leeb JS (1992) Electromagnetic joining of aluminum tubes on polyurethane cores. J Mater Process Technol 34:341–348

185. Kleiner M, Marré M, Beerwald C, Homberg W, Löhe D, Barreiro P, Schulze V (2006) Investigation of force-fit joints produced by electromagnetic tube compression. Ann Ger Acad Soc Prod Eng WGP XIII:227–230

186. Barreiro P, Schulze V, Löhe D, Marré M, Beerwald C, Homberg W, Kleiner M (2006) Strength of tubular joints made by electromagnetic compression at quasi-static and cyclic loading. In: Proceedings of 2nd International Conference on High Speed Forming-ICHSF-2006, pp 107–116

187. Bühler H, von Finckenstein E (1968) Fügen durch magnetumformung. Werkstatt und Betr 101(4):209–215

188. Weddeling AE, Woodward C, Marré ST, Nellesen M, Psyk J, Tekkaya V and Tillman W (2010) Development of design principles for form-fit joints in lightweight frame structures. In: Proceedings of the 4th International Conference on High Speed Forming-CHSF2010, pp 137–148

189. Weddeling C, Woodward S, Nellesen J, Psyk V, Marré M, Tekkaya AE, Daehn GS, Tillmann W (2010) Development of design principles for form-fit joints in lightweight frame structures. In: Proceedings of 4th International Conference on High Speed Forming-ICHSF-2010, pp 137–148

190. Buhler E, von Finckenstein H (1971) Bemessung von Sickenverbindungen fur ein Fugen durch Magnetumformung. Werkstatt und Betr 104:45–51

191. Weddeling C, Woodward ST, Marré M, Nellesen J, Psyk V, Tekkaya AE, Tillmann W (2011) Influence of groove characteristics on strength of form-fit joints. J Mater Process Technol 211: 925–935

192. Golovashchenko S (2001) Methodology of design of pulsed electromagnetic joining of tubes. In: Proceedings of the 2nd Global Symposium on Innovation in Material Processing and Manufacturing: Sheet Materials. TMS Annual Meeting, New Orleans

193. Hammers T, Marré M, Rautenberg J, Barreiro P, Schulze V, Löhe D, Brosius A, Tekkaya AE (2008) Influence of Mandrel's surface on the mechanical properties of joints produced by electromagnetic. In: Proceedings of 3rd International Conference on High Speed Forming-ICHSF2008, pp 245–256

194. Jimbert G, Perez P, Eguia I, Daehn I (2007) Straight hemming on aluminum sheet panels using the electromagnetic forming technology: first approach. Key Eng Mater 344:365–372

195. Jimbert P, Eguia I, Gutierrez MA, Gonzalez B, Daehn GS, Zhang Y, Anderson R, Sundberg H, Olsson SO, Brännström P (2008) Flanging and hemming of auto body panels using the electro magnetic forming technology. In: Proceedings of 3rd International Conference on High Speed Forming-ICHSF2008, pp 163–172

196. Deng JH, Tang C, Fu MW, Zhan YR (2014) Effect of discharge voltage on the deformation of Ti grade 1 rivet in electromagnetic riveting. Mater Sci Eng A 591:26–32

197. Oliveira DA, Worswick MJ, Finn M, Newman D (2005) Electromagnetic forming of aluminum alloy sheet: free-form and cavity fill experiments and model. 170(1–2):350–362

198. Stiemer H, Unger M, Svendsen J, Blum B (2006) Algorithmic formulation and numerical implementation of coupled electromagnetic-inelastic continuum models for electromagnetic metal forming. Int J Numer Methods Eng 68:1301–1328

199. Uhlmann D, Jurgasch E (2004) New impulses in the forming of magnesium sheet metals. In: Proceedings of the 1st International Conference on High speed Forming—ICHSF 2004, pp 229–241

200. Imbert JM, Worswick MJ, Golovashchenko S (2006) Contributing factors to the increased formability observed in electromagnetically formed aluminum alloy sheet. In: Proceedings of 2nd International Conference on High Speed Forming-ICHSF-2006, pp 3–12

201. Zohoor M, Ghorbani B (2014) Analytical and numerical investigation of significant parameters on strength of electromagnetically assembled aluminum tube joints. Journal of Modern Processes in Manufacturing and Production 3(1):35–46

202. Tekkaya A, Homberg AE, Brosius W (2015) 60 excellent inventions in metal forming. Springer Vieweg, Berlin

203. Dörr F, Funk M, Liewald M, Binz H, Köstlmeier R (2014) Influence of internal hub profile on joining process of shaft-hub-connection by lateral extrusion. Procedia Eng 81(October):1988–1993

204. Danesh Manesh H, Mashreghi A, Ehteman Haghighi S, Khajeh A (2009) Investigation of cold pressure welding of aluminum powder to internal surface of aluminum tube. Mater Des 30(3):723–726

205. Huang Z, Sugiyama S, Yanagimoto J (2013) Hybrid joining process for carbon fiber reinforced thermosetting plastic and metallic thin sheets by chemical bonding and plastic deformation. J Mater Process Technol 213(11):1864–1874

206. Yanagimoto J, Ikeuchi K (2012) Sheet forming process of carbon fiber reinforced plastics for lightweight parts. CIRP Ann Manuf Technol 61(1):247–250

207. Alves LM, Dias EJ, Martins PAF (2011) Joining sheet panels to thin-walled tubular profiles by tube end forming. J Clean Prod 19(6–7):712–719

208. Alves LM, Martins PAF (2013) Single-stroke mechanical joining of sheet panels to tubular profiles. J Manuf Process 15(1):151–157

209. Pragana JP, Silva CM, Bragança IM, Alves L, Martins PA (2018) A new joining by forming process to produce lap joints in metal sheets. CIRP Ann Manuf Technol 67(1):301–304

210. Chrysanthou A, Sun X (2014) Self-piercing riveting: properties, processes, and applications. Woodhead Publishing, Cambridge